Multifunctional biopolymer-based materials for modulating the activities of chronic wound enzymes

Antonio Francesko

A thesis submitted in fulfilment of the requirements for the degree of

European Doctor of Philosophy

at the

Universitat Politècnica de Catalunya

This work was carried out under the supervision of **Dr. Tzanko Tzanov**

Group of Molecular and Industrial Biotechnology (GBMI)

Department of Chemical Engineering

Universitat Politècnica de Catalunya

Terrassa, 2012

The work carried out during the thesis as well as the financial support of the candidate was provided by:

Becas FPI
Ref beca: BES-2008-003744

GBMI

Group of Molecular and Industrial Biotechnology

FP6-026741

Mojoj porodici...

Abstract

This thesis focuses on the development of active multifunctional dressing materials and nanoparticle formulations with suitable exploitation characteristics for chronic wounds treatment. Chronic wounds – a growing clinical challenge in the aging and/or reduced mobility population – include pressure, venous, arterial and diabetic neuropathic ulcers. Due to the non-healing character of these ulcers their management requires an intensive medical intervention at huge healthcare costs. The prolonged inflammation and elevated concentrations of oxidative and proteolytic enzymes in all chronic wounds, imposes the need for novel functional dressing materials to actively modulate the wound environment at molecular level and stimulate the healing process. Based on an extensive analysis of the current state-of-the-art in chronic wound healing, the proper **dressings should combine both antimicrobial and enzyme inhibitory functions** coupled to optimal hydrophilicity. Such integrated approach would allow for the suppression of the persistent inflammation and stimulation of the synthesis of the dermal tissue components. **Biopolymers** with intrinsic antimicrobial and wound repair properties appear as appropriate matrix materials to be further upgraded with **bioactive molecules** (therapeutics) that couple high reactivity with the ability to address specific targets in the biochemical environment of chronic wounds. Therapeutic devices can be designed in different forms depending on the particular clinical application, i.e. wound type and its characteristics.

During the thesis realisation **biopolymer-based platforms were generated in various designs and functionalised with active agents for controlled inhibition of major chronic wound enzymes**. The capacity of all developed materials to inhibit proteolytic (e.g. collagenase) and oxidative (e.g. myeloperoxidase) enzymes involved in chronic inflammation was evaluated *in vitro*.

In the first approach **sponge-like biopolymer matrices** were produced via freeze-drying technique and controlled chemical cross-linking. These matrices were further impregnated with **natural polyphenolic compounds**. Modulation of the deleterious wound enzyme activities was achieved upon **release of active agent from the platform**. The exploitation characteristics of the sponges, i.e. mechanical properties, biostability, biocompatibility, extent and duration of wound enzymes inhibition, were tuned by: the biopolymer composition, concentration of the cross-linking agent, and the proper selection of the bioactive phenolic compounds.

The second approach aimed at the permanent functionalisation of the biopolymeric platforms with thiol-bearing compounds. In this case the **active agent is expected to act from the platform**, without being released into the wound. The obtained thiolated biopolymers were further processed into **functional nanomaterials of** different design:

- **Nanoscale films/coatings** were built using a layer-by-layer approach for alternate deposition of oppositely charged polyelectrolytes. Naturally occurring glycosaminoglycans were used as counterions to cationic thiolated conjugates.
- **Nanoparticle formulations** were obtained from thiolated conjugates in a one-step sonochemical process.

In both cases the biopolymer thiolation degree was identified as a key factor for the successful fabrication of the multilayered coatings and nanoparticles, as well as to achieve control of the thickness/size of the functional nanomaterials. In addition, tuneable inhibition/adsorption of the deleterious enzymes coupled to fibroblast attachment/proliferation was observed by ruling the biopolymer modification degree.

Keywords: Biopolymers • Polyphenols • Thiol compounds • Functionalisation • Cross-linking • Functional materials • Wound dressings • Myeloperoxidase • Collagenase • Chronic wounds • Enzyme inhibition • Wound healing

Table of Contents

Abstract vii
Table of Contents ix
Abbreviation list xiii
List of Figures xv
List of tables xvii
List of Schemes xviii
Section A: Background and objectives 1
Objective of the thesis 3
Chapter 1: General introduction 5
1.1 Chronic wounds: formation and pathogenesis 7
1.1.1 Skin and its function 7
1.1.2 Acute wounds and healing process 8
1.1.3 Chronic wounds and impaired healing 10
1.1.4 Chronic wound pathogens 11
1.2 Chronic wound management 14
1.3 Biopolymers as dressing materials 16
1.3.1 Chitosan 16
1.3.2 Collagen 18
1.3.3 Glycosaminoglycans 19
1.3.4 Problematic and advanced treatment solutions 20
1.4 Attenuating the enzymatic activities in chronic wounds 21
1.4.1 Active agents to modulate the enzymes activities in chronic wounds – an integrated approach. 22
1.5 Modification/functionalisation of biopolymers 23
1.5.1 Chemically modified chitosan 24
1.5.2 Chemical cross-linking of biopolymers 26
1.5.3 Modification/blending of biopolymers using enzymatic tools 29
1.6 Dressing design 31
1.7 Research objectives 32
SECTION B: Dressing platforms loaded with plant polyphenols 35
Chapter 2: Cross-linked biopolymer sponges 37
2.1 Introduction 39
2.2 Materials and methods 40
2.2.1 Biopolymers 40
2.2.2 Reagents 40
2.2.3 Preparation of biopolymer sponges 40
2.2.4 Determination of the degree of collagen cross-linking with genipin 41
2.2.5 Scanning electron microscopy (SEM) 41
2.2.6 Fourier transform infrared spectroscopy (FTIR) 41
2.2.7 Tensile testing 41
2.2.8 Biostability of the cross-linked biopolymer sponges 41
2.2.9 Swelling behaviour of the biopolymer sponges 42
2.2.10 Extent of collagenase adsorption onto the biopolymer composite sponges 42
2.2.11 Statistical analysis 42
2.3 Results and discussion 43
2.3.1 Genipin cross-linked collagen sponges 43

2.3.2 EDAC cross-linked biopolymer composite sponges 47
2.4 Conclusions 53

Chapter 3: Biopolymer sponges loaded with plant polyphenols 55
3.1 Introduction 57
3.2 Materials and methods 58
3.2.1 Sponges and reagents 58
3.2.2 Active agents - polyphenols 58
3.2.3 Loading of the biopolymer sponges with polyphenols 59
3.2.4 Polyphenols binding onto the biopolymer sponges and release studies 59
3.2.5 Swelling behaviour of the biopolymer dressings 59
3.2.6 Biostability of the biopolymer dressings 60
3.2.7 Collagenase inhibition with polyphenols 60
3.2.8 Myeloperoxidase inhibition assay 60
3.2.9 Cell viability, morphology and distribution 61
3.2.10 Statistical analysis 61
3.3 Results and discussion 62
3.3.1 Collagen sponges loaded with *Hammamelis virginiana* polyphenols 62
3.3.2 Biopolymer composite sponges loaded with green tea polyphenols 65
3.4 Conclusions 71

SECTION C: Thiolated biopolymers and derived functional nanomaterials 73

Chapter 4 : Thiolated biopolymers 75
4.1 Introduction 77
4.2 Materials and methods 78
4.2.1 Biopolymers and reagents 78
4.2.2 Chitosan thiolation 78
4.2.3 Synthesis of thiolated aminocellulose 79
4.2.4 Quantification of the thiol groups immobilised onto biopolymers 80
4.2.5 ζ-potential measurements 80
4.2.6 Enzymes assays 80
4.3 Results and discussion 81
4.3.1 Thiolated chitosan 81
4.3.2 Thiolated aminocellulose 82
4.3.3 Effect of thiolated chitosan on myeloperoxidase and collagenase activities 84
4.4 Conclusions 86

Chapter 5: Functional nanocoatings based on thiolated chitosan 87
5.1 Introduction 89
5.2 Materials and methods 90
5.2.1 Polyelectrolytes and reagents 90
5.2.2 Layer-by-layer assembly of PEM coatings and collagenase adsorption 90
5.2.3 Characterisation of PEM coatings 91
5.2.4 Cell adhesion, proliferation and morphology 91
5.2.5 Statistical analysis 92
5.3 Results and discussion 93
5.3.1 Build-up of polyelectrolyte multilayered coatings 93
5.3.2 XPS analysis 96
5.3.3 Collagenase adsorption on PEM coatings 97
5.3.4 Cell culture studies 99
5.4 Conclusions 101

Chapter 6: Thiolated chitosan nanoparticles 103
6.1 Introduction 105
6.2 Materials and methods 106
6.2.1 Thiolated chitosan and reagents 106

6.2.2 Nano/micro-parcticles preparation 106
6.2.3 Determination of free thiol groups 106
6.2.4 Dynamic light scattering 107
6.2.5 Biostability of nanoparticles 107
6.2.6 Myeloperoxidase inhibition 107
6.3 Results and discussion 108
6.3.1 Sonochemical generation of thiolated chitosan nanoparticles 108
6.3.2 Degree of chitosan thiolation in nanoparticles 109
6.3.3 Particle size and size distribution 111
6.3.4 Biostability of nanoparticles 113
6.3.5 Myeloperoxidase inhibition 114
6.4 Conclusions 115

SECTION D: Final remarks 117

Chapter 7: Conclusions and future plans 119
7.1 Conclusions 121
7.2 Future perspectives 122

Acknowledgments 123

References 125

Abbreviation list

B
BSA: Bovine serum albumin

C
CAT: Catechin
CD: Cyclodextrin
CGC: Chitosan membrane cross-linked with genipin and loaded with collagen particles
CHA: Collagen-hyaluronic acid sponge
CHACS: Collagen-hyaluronic acid-chitosan sponge
CS: Chitosan
CSU: Chondroitin sulphate

D
DAPI: 4,6-diamidina-2-phenylin
DLS: Dynamic light scattering
DMEM: Dulbecco's modified eagle's medium
DMSO: Dimethylsulphoxide
DTBP: Dimethyl 3,3'-dithiobispropionimidate dihydrochloride
DTT: Dithiothreitol

E
ECM: Extracellular matrix
EDA: Ethylendiamine
EDAC: N-(3-Dimethylaminopropyl)-N′-ethylcarbodiimide hydrochloride
EDC: 1-ethyl-3-(3-dimethylaminopropyl) carbodiimide
EDTA: Ethylenediaminetetraacetic acid
EGCG: Epigallocatechin gallate

F
FALGPA: N-(3-[2-Furyl]Acryloyl)-Leu-Gly-Pro-Ala
FBS: Fetal bovine serum
FTIR: Fourier transform infrared spectroscopy
FWHM: Full width at half maximum

G
GA: Gallic acid
GAG: Glycosaminoglycan

H
HA: Hyaluronic acid
HClO: Hypochlorous acid
HRP: Horseradish peroxidase
Hyp: Hydroxyproline

I
IC_{50}: The half maximal inhibitory concentration

M
MMP: Matrix metalloproteinase
MPO: Myeloperoxidase
MTT: 3-dimethylthiazol-2,5-diphenyltetrazolium bromide
Mw: Molecular weight

N
NHS: N-hydroxysuccinimide
NPs: Nano/micro-particles
NPWT: Negative pressure wound therapy

O
OWH: Organic dry fraction of the Hamamelis virginiana polyphenolic extract

P
PA: Polyanion
PB: Phosphate buffer
PBS: Phosphate buffered saline
PC: Polycation
PDGF: Platelet derived growth factor
PDI: The polydispersity index
PEC: Polyelectrolyte complex
PEM: Polyelectrolyte multilayer
pI: Isoelectric point

Q
QCM-D: Quartz crystal microbalance with dissipation

R
RGD: Arginine-Glycine-Aspartic acid recognition sequence
ROS: Reactive oxygen species

S
SEM: Scanning electron microscopy

T
TC: Thiolated chitosan
TCPS: Tissue culture polystyrene surface
TGF-β: Tumour growth factor
TIMP: Tissue inhibitor of matrix metalloproteinase

U
UV: Ultraviolet

X
XPS: X-ray photoelectron spectroscopy

List of Figures

Figure 1.1 Histology of the human skin (taken from: http://www.lab.anhb.uwa.edu.au)..... 7
Figure 1.2 Phases and physiological process in acute wound healing (taken from: http://www.fastbleep.com)..... 10
Figure 1.3 The enzymatic cycles of myeloperoxidase (adapted from [18]..... 13
Figure 1.4 Chitosan structure..... 17
Figure 1.5 Structure of hyaluronic acid..... 19

Figure 2.1 SEM images of collagen sponges. (A) Uncross-linked, cross-linked with (B) 0.25 mM, (C) 0.50 mM, (D) 0.75 and (E) 1.00 mM genipin.. 44
Figure 2.2 Representative stress-strain curves of uncross-linked and collagen sponges cross-linked with different concentrations of genipin. 45
Figure 2.3 Swelling capacity of uncross-linked and collagen sponges cross-linked with various genipin concentrations 46
Figure 2.4 Percentage of collagen degradation from the uncross-linked and sponges cross-linked with various genipin concentrations..... 47
Figure 2.5 Representative FTIR A) spectra of a) collagen, and EDAC cross-linked biopolymer matrices: b) collagen, c) CHA830, d) CHACS. B) normalised spectra of CHA6 (dot line), CHA830 (dashed line), CHA2000 (solid line)..... 48
Figure 2.6 A) Linear elastic (Young's) modulus and B) failure strain for the cross-linked, hydrated (PBS, pH 7.4) biopolymer composite sponges. Statistical differences are related to the collagen sponge and represented as **p<0.01 and ***p<0.001..... 49
Figure 2.7 A) Binding extent of collagenase onto the cross-linked collagen-based matrices and B) collagen proteolysis by 10 μg/mL (light grey bars) and 60 μg/mL (dark grey bars) collagenase from the cross-linked collagen-based matrices. Statistical differences are related to the collagen sponge and represented as **p<0.01 and ***p<0.001..... 50
Figure 2.8 Swelling of the cross-linked biopolymer matrices after 24 h incubation in PBS (pH 7.4). Statistical differences are related to the collagen sponge and represented as **p<0.01 and ***p<0.001 51

Figure 3.1 Percentage of collagen degradation from the collagen sponges cross-linked with 1.00 mM genipin and further loaded with different polyphenols concentration (0.5, 1 and 2 mg/mL) 62
Figure 3.2 The percentages of collagenase activity inhibition with polyphenols at different concentrations 63
Figure 3.3 Time-course inhibition of MPO by *Hamamelis virginiana* polyphenols released from the collagen-based sponges (A), and polyphenols release from the sponges within 6 h (B) and 96 h (C). Collagen sponges were cross-linked with 1 mM of genipin and further loaded with various polyphenols concentrations: 0.5 mg/mL (□), 1 mg/mL (○) and 2 mg/mL (Δ). 64
Figure 3.4 Toxicity effects of uncross-linked, collagen cross-linked with 1 mM of genipin and cross-linked collagen sponges loaded with different polyphenols concentration (0.5, 1 and 2 mg/mL) on fibroblasts measured by MTT colorimetric assay at 24 h. 65
Figure 3.5 A) Collagen proteolysis in cross-linked biopolymers matrices without and loaded with polyphenols by 60 μg/mL collagenase, and B) extent of polyphenols binding onto cross-linked specimens: Collagen (white bars), CHA830 (grey bars) and CHACS (black bars). Statistical differences in the biostability of the non-treated and polyphenols loaded specimens are represented as

**p<0.01 and ***p<0.001, in light grey, dark grey and black if related to Collagen, CHA830 and CHACS, respectively 66
Figure 3.6 Time-course inhibition of MPO by polyphenols: A) EGCG, B) CAT and C) GA released from the cross-linked Collagen (solid line), CHA830 (dot line) and CHACS (dash line). The inset graphs show the polyphenols release patterns from the corresponding biopolymer composite matrices. 67
Figure 3.7 Time-course evaluation of fibroblasts metabolic activity using MTS assay. Statistical differences are represented as * p<0.05, ** p<0.01 and *** p<0.001 68
Figure 3.8 Morphology of the fibroblasts cultured for 3 days onto cross-linked Collagen (A-B), CHA6 (C-D), CHA830 (E-F), CHA2000 (G-H), CHACS (I-J). Scale bars correspond to 100 µm (left-side images) and 10 µm (right-side images). 69
Figure 3.9 Effect of the polyphenols loaded sponges on fibroblasts viability after 3 days in culture. Statistical differences are represented as * p<0.05, ** p<0.01 and *** p<0.001, in black, light grey or dark grey, if related to Collagen, CHA830 or CHACS, respectively. 70

Figure 4.1 Amount of free thiol groups immobilised onto EDA-cellulose prepared using different concentrations of DTBP 83
Figure 4.2 Amount of free thiol groups immobilised onto EDA-cellulose prepared at different pH .. 83
Figure 4.3 Effect of thiolated chitosan conjugates on MPO activity measured with guaiacol as substrate 85

Figure 5.1 ζ-potential of collagenase and the polyelectrolytes used for the QCM-D studies. Polyelectrolytes (0.5 mg/mL) and collagenase (0.1 mg/mL) solutions were prepared in 0.150 M NaCl, pH 5.5 93
Figure 5.2 Build-up assessments of 5½ bi-layers of CS/CSU (light grey), TC10-1/CSU (black) and TC5-2/CSU (dark grey). Signals for normalized a) frequency (Δf/υ) and b) dissipation (ΔD) were obtained during QCM-D monitoring. Labelled arrows indicate polyelectrolyte injection (PC for polycation, PA for polyanion), whereas small arrows without labels indicate rinsing with 0.15M NaCl, pH 5.5. c) Thickness evolution of the obtained PEMs estimated using the Voigt model for three independent experiments 94
Figure 5.3 Build-up assessments of 5½ bi-layers of TC5-2/HA using hyaluronic acid with different Mw: 6 kDa (light grey), 830 kDa (black) and 2000 kDa (dark grey). Signals for normalized a) frequency (Δf/υ) and b) dissipation (ΔD) were obtained during QCM-D monitoring. Labelled arrows indicate polyelectrolyte injection (PC for polycation, PA for polyanion), whereas small arrows without labels indicate rinsing with 0.15M NaCl, pH 5.5. c) Thickness evolution of the obtained PEMs estimated using the Voigt model for three independent experiments. 95
Figure 5.4 S2p spectrum of TC5-2/HA830 multilayer system consisting of 5½ bi-layers adsorbed onto gold surface acquired by XPS. Polyelectrolytes were deposited onto gold from 0.15M NaCl, pH 5.5 solution, using concentrations of 0.5 mg/mL. The S peaks were fit using three S2p doublets with a 2:1 area ratio and a splitting of 1.2 eV. The positions of the S2p3/2 peaks assigned to bound thiolate, unbound thiol and oxidized S species are shown. 97
Figure 5.5 Variation of collagenase adsorption (0.1 mg/mL) onto PEMs with different outermost layer in terms of amount adsorbed by surface area. The results were obtained by extracting the data acquired with QCM-D and calculated using the Voigt model. PEM coatings comprised 10 layers in case of polyanion and 11 in case of polycation outermost layer. For the PEMs terminating with polycation CS was used, whereas for those terminating with polyanion TC5-2 served as a counter polyelectrolyte. Polyelectrolytes were deposited onto gold from 0.15 M NaCl, pH 5.5 solution, using concentrations of 0.5 mg/mL. **p<0.01 and ***p<0.001 98

Figure 5.6 Morphology of L929 cells cultured for 24 h and 7 d on (A-B) CSU-terminated; (C-D) HA830-terminated, (E-F) TC terminated (TC5-2/CSU system, (G-H) TC terminated (TC/HA830 system) and (I-J) TCPS (scale bar=100 μm) . Insets show fluorescence microscopy images of DAPI and phalloidin staining 99
Figure 5.7 Morphology of L929 cells cultured for 7 d on (A) $(TC\text{-}CS)_5$; (B) $(TC\text{-}HA)_5$, (C) $(TC\text{-}CS)_5$-TC and (D) $(TC\text{-}HA)_5$-TC (scale bar=20 μm). 100

Figure 6.1 Efficiency of oil encapsulation by chitosan and thiolated chitosans NPs 109
Figure 6.2 Optical microscopy images of NPs obtained under sonication A) chitosan NPs, and B) thiolated chitosan (TC5-1) NPs 109
Figure 6.3 Amount of free thiol groups in thiolated chitosan conjugates and the corresponding NPs formulations obtained at indicated pH values of the aqueous phase during the sonication process. .. 110
Figure 6.4 Comparison of the mean particle sizes of chitosan NPs and NPs obtained from thiolated chitosan conjugates after one week (grey bars) and three months (black bars) storage 112
Figure 6.5 Comparison of the Gaussian particles size distributions between the NPs formulations obtained at various pH values: pH 3 (solid line), pH 4.5 (dashed line) and pH 6 (dot line) 113
Figure 6.6 Degradation of TC NPs by lysozyme 114
Figure 6.7 Inhibition of MPO activity by with thiolated chitosan nanoparticles 114

List of tables

Table 2.1 Denomination and the cross-linking degree of the genipin treated collagen sponges 43
Table 2.2 Mechanical properties of the genipin cross-linked collagen sponges 44

Table 3.1 IC_{50} values for collagenase inhibition by single unit polyphenols 66
Table 3.2 IC_{50} values for MPO inhibition by single unit polyphenols 67

Table 4.1 Denomination of the thiolated chitosan conjugates 79

Table 4.2 ζ-potential of some thiolated chitosan solutions (0.5 mg/mL) prepared in 0.15 M NaCl, pH 5.5… 81

Table 4.3 Total sulphur content, percentage of free thiol groups, and disulphide content in the obtained thiolated chitosan conjugates 82

Table 4.4 Amount of free thiol groups immobilised onto aminocellulose prepared using the same reaction conditions for three independent experiments 84

Table 5.1 Au and S content (%) for various multilayered systems deposited onto gold covered microscopy slides 96

Table 6.1 Estimated percentage of disulphide bonds in the NPs formulations obtained from different thiolated chitosan conjugates at indicated pH values of the aqueous phase 110

Table 6.2 Mean particle size of chitosan and thiolated chitosan NPs obtained at various pH values 111

List of Schemes

Scheme 1.1 Summary of the work carried out during the thesis development 33

Scheme 2.1 Cross-linking of the biopolymers with EDAC..... 47

Scheme 3.1 Structure of polyphenolic units from Camellia sinesis: A) EGCG, B) CAT and C) GA.. 58

Scheme 4.1 Schematic representation of aminocellulose structure..... 78
Scheme 4.2 Proposed structure of the obtained thiolated chitosan..... 81
Scheme 4.3 Synthetic pathway for thiolation of the aminocellulose conjugate 82

Scheme 6.1 Sonochemical preparation of biopolymer NPs 108

Section A

Background and objectives

Objective of the thesis

Since chronic wounds most often occur in a setting of combined risk factors of age, repeated ischemia - reperfusion injury, oxidative stress and bacterial colonisation, it could not be expected that a therapy directed at only one of these factors would be efficient. Even though many active and passive approaches have been investigated there is not yet a valid and unique approach to heal chronic wounds. Hence there is a need to provide an, as much as possible, general strategy combining previously developed knowledge, and based on understanding of chronic wound pathogenesis.

Despite different underlying mechanisms of formation, the common feature of virtually all chronic wounds is the **prolonged inflammation**. Continuous influx of inflammatory cells into the wound site where they undergo apoptosis leads to the accumulation of their secondary metabolites. The elevated levels of the released oxidative and proteolytic enzymes appear to degrade the dermal tissue components, growth factors and receptors essential for healing. Therefore, it is believed that chronic wound repair would be stimulated after the **partial inhibition of the deleterious neutrophil-derived proteolytic and oxidative enzymes**, besides providing the infection-free and moist environment.

Under these circumstances, recent progress in dermal tissue management is directed towards physiological repair at molecular level using **functional dressing materials**. An efficient chronic wound dressing should comprise an intrinsically antimicrobial platform/carrier upgraded with active agents to address the local biochemical environment and stimulate the wound healing process. The use of biopolymer platforms to support the formation of the new extracellular matrix in the wound further loaded with bioactive molecules able to reduce the excessive enzyme levels appears to be an integrated approach for efficient chronic wound management. **This thesis aims on the development of various multifunctional dressings/formulations based on the biopolymer-therapeutic combinations for modulation of the enzymatic activities related to the prolonged inflammation in chronic wounds.**

Chapter 1

General introduction

1.1 Chronic wounds: formation and pathogenesis

1.1.1 Skin and its function

Skin is the largest organ in the human body with several important functions, including body's regulation of water and electrolyte balance, thermoregulation, and function as a protective barrier. It is well-known that skin is composed of epidermis, dermis and hypodermis (Figure 1.1). The outer epidermis forms a protective barrier, being responsible for keeping water in the body and preventing pathogens from entering in addition to helping the skin to regulate body temperature. This layer is a stratified scaly epithelium composed of proliferating basal and differentiated suprabasal keratinocytes. The stratum corneum is the outermost part of epidermis with specific barrier properties. It consists of non-viable cells and is very firm but pliable and wrinkled. The underlying layer, the dermis, is largely composed of a very dense fibre network – extracellular matrix (ECM), dominating the mechanical behaviour of the total skin, and therefore providing structural support to the organ. This gel-like matrix, secreted locally by the cells that it surrounds, is composed of a variety of polysaccharides and proteins: collagen fibrils, microfibrils, and elastic fibres, embedded in proteoglycans. An intricate network of these macromolecules assembled in close association with the surface of the cell that produced them provides the unique structure of the ECM, exhibiting high tensile strength combined with the substantial elasticity and compressibility. The deepest skin layer, the hypodermis or subcutaneous adipose tissue, is composed of loose fatty connective tissue. Finally, all skin layers contain blood vessels, lymph vessels, nerve endings, sweat glands and hair follicles.

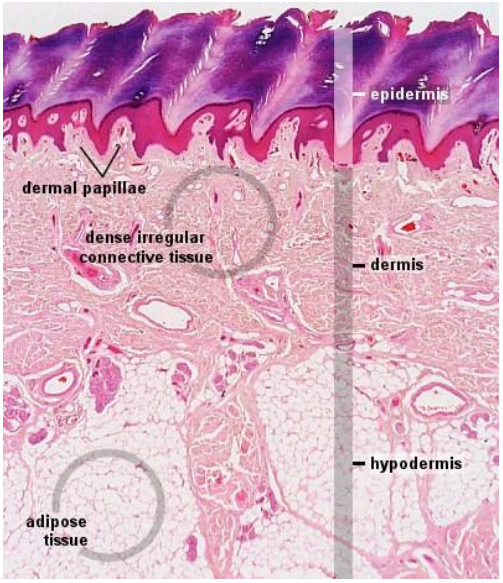

Figure 1. 1 Histology of the human skin (taken from: http://www.lab.anhb.uwa.edu.au)

1.1.2 Acute wounds and healing process

According to the Wound Healing Society (www.woundheal.org), a wound is the result of disruption of normal anatomic structure and function of a tissue. A dermal wound is defined as a break in the integrity of the skin, raised due to external or internal noxious stimulus, and leads to an inadequate performance of the skin functions. It is therefore vital to restore the skin integrity and consequently functions as soon as possible. A completely healed wound implies that the affected part of the skin has returned to its normal anatomical structure and function, and similar appearance within a reasonable period of time [2]. The primary causes of acute wounds include mechanical injuries due to external factors such as abrasions and tears due to a frictional contact between the skin and hard surfaces. These also include penetrating wounds caused by knives and firearm shots, surgical incisions, etc. Burns and chemical injuries arise from a variety of sources such as radiation, electricity, corrosive chemicals and thermal sources. For burns, the temperature of the source and the exposure time defines the degree of a thermal burn. Another classification of wounds is based on the number of skin layers and area of skin affected. Based on this it is possible to distinguish between an epidermal or a superficial wound and an injury involving both the epidermis and dermis that in addition affects the blood vessels and is referred to as partial thickness wound. Full thickness skin wounds occur when the underlying subcutaneous fat or deeper tissues are damaged in addition to the epidermis and dermal layers [3]. Epidermal and partial thickness wounds can regenerate by the body's self-healing capacity for re-epithelisation. Conversely, in the full-thickness wounds regenerative elements that reside in dermis are completely destroyed such that epithelisation is possible only on the wound edges. Such wounds need skin grafting to prevent extensive scar formation, using allo- or autografts, or tissue engineered skin substitutes. Unfortunately, even after successful treatment full-thickness wounds almost exclusively result in an impaired mobility and cosmetic deformities of the affected part of the skin [4]. The basis of the tissue engineering consists in the development of temporary, or in some cases, permanent biological substitutes for failing tissues and/or organs. In particular, skin engineering involves seeding of cells onto porous biodegradable polymer scaffold that serves as a starting platform for dermal tissue recovery. However, skin grafting is not in the scope of this thesis and therefore is not discussed in detail.

Normal wound healing involves a complex series of orchestrated events leading to the repair of injured tissues. These dynamic events occur as a sequential cascade of processes requiring the coordinated completion of a variety of cellular activities correlating with the appearance of different cell types in the wound during various stages of the healing process [5]. All acute wounds heal in a very orderly and efficient manner characterised by several distinct in nature, but overlapping phases: haemostasis, inflammation, cell migration and proliferation, and maturation or remodelling phase. After injury the bleeding flush out bacteria and antigens from the injury site, also causing the aggregation of the platelets accumulated in the wound. The platelets form a haemostatic plug due to

conversion of fibrinogen to fibrin in order to prevent an excessive loss of blood. Thus, haemostasis contributes to successful wound healing playing a protective role to the underlying layers of opened skin. In addition, platelets release growth factors such as tumour growth factor (TGF-β), platelet derived growth factor (PDGF) and adhesive proteins to activate cells in the surrounding area. During the inflammatory phase neutrophils arrive at the site of the injury, releasing a variety of highly active antimicrobial substances such as, proteases and reactive oxygen species, important for wound cleaning and the prevention of infections [6]. Moreover, phagocytes enter the wound and engulf dead cells (necrotic tissue). Hard necrotic tissue is liquefied by enzymatic (protease) action to produce a yellowish coloured mass characterised with bad odour referred as slough. The inflammatory phase occurs almost simultaneously with haemostasis and lasts for about 3 days in normal healing process. However, if the action of these active compounds released in wound is prolonged or they are found in counts higher than normal levels, the process is harmful for healthy cells – the common situation found in chronic wounds (discussed in sections 1.1.3 and 1.1.4) [7]. Thus, multiple processes for digestion of matrix elements and cell debris occur [8]. Moreover, cytokines released by circulating basophiles and other leukocyte subsets are also considered to be involved in tissue repair. The migration phase involves the movement of keratinocytes and fibroblasts to the injured area to replace damaged and lost tissue. These cells regenerate from the margins, rapidly growing over the wound and cause epithelial thickening. Accompanied proliferative phase is characterised by the in-growth of capillaries and lymphatic vessels into the wound and collagen synthesis by fibroblasts giving the skin strength and form. The newly formed granulation tissue and ECM consist of glycosaminoglycans (GAGs), proteoglycans, collagen (type III), thrombospondin, fibronectin and vitronectin to promote angiogenesis. During angiogenesis the fibroblasts transform into myofibroblasts that bring the margins of the wound together in order to reduce its size. The final phase of wound healing is the transformation of granulation tissue into a scar. The scar formation is characterised by a decreased inflammation and reduction of the capillaries size. Myofibroblasts further undergo apoptosis and a new collagenous matrix replaces the provisional one [7, 9]. The described cascade occurs in normal wound healing, with a reestablishment of the equilibrium between scar formation and scar remodelling, the longest part of the healing (up to two years) marking the end of the wound healing process (Figure 1.2).

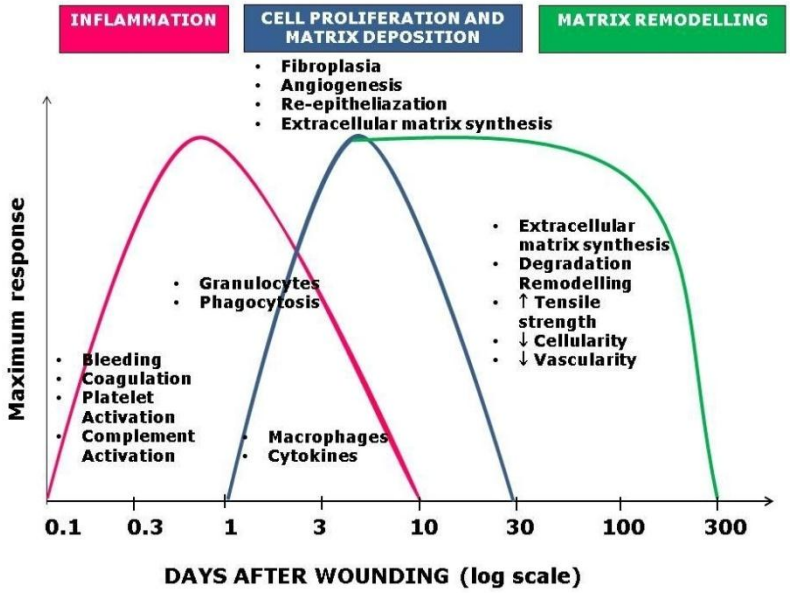

Figure 1. 2 Phases and physiological process in acute wound healing (taken from: http://www.fastbleep.com)

1.1.3 Chronic wounds and impaired healing

In contrast to acute wounds, abnormal response to an injury leads to formation of non-healing wounds, referred as chronic. Chronic wounds can affect any anatomical region as a result from various causes and thereby are classified as chronic venous leg ulcers, arterial ulcers, neuropathic ulcers, pressure ulcers (decubitus), vasculitis and serious burns. Except for burns, all the conditions leading to chronic ulceration are more prevalent in the population with low mobility and elderly population in general. In addition, the increased occurrence and longevity of these ulcers are further compounded by the detrimental effects ageing has on the skin and the wound healing process. Due to their non-healing nature, intensive and costly medical treatment is required for the successful management. Furthermore, as elderly individuals become the fastest-growing segment of the population, the chronic wounds occurrence will have an even more pronounced economic impact in the future.

Chronic wound formation

A chronic wound arises after disruption of the acute wound healing process at one or more of its phases, impairing the reestablishment of anatomical and functional integrity of the affected tissue in a physiologically appropriate length of time. In such cases the healing process is stuck in one of its phases. Various factors can cause the failure of the normal healing process. For example, foreign bodies introduced deep into the wound at time of injury can trigger chronic inflammatory responses,

sometimes leading to macrophages granuloma or abscess formation. On the other hand, inadequate management of already infected wounds can lead to inflammation of cells and loss of their function. Poor nutritional status of a patient and aged skin also reduce the ability to fight infection. Moreover, underlying diseases such as diabetes and anaemia compromise the circulation resulting in poor delivery of blood cells and oxygen to the wound.

The disruption of the acute healing process is usually expressed in its inflammatory phase. The caused prolonged inflammation leads to fibrosis, an excessive matrix deposition and loss of tissue function [10]. As growth factors, cytokines and specific enzymes play important roles in this phase of the healing process, their altered expression during the prolonged inflammation could account for the impaired healing in chronic wounds. In addition, oxidative damage caused by free radicals contributes to the non-healing nature of these ulcers. Healing is also impeded by the accumulation of necrotic tissue or slough at the wound site. Moreover, the initiation of chronic wounds is accelerated in situations of bacterial infection, common in such environment. Indeed, the prolonged treatment times makes chronic ulcers prone to infections and most of them are colonised with several bacterial species like: *Staphylococcus aureus*, *Pseudomonas aeruginosa* and *Peptostreptococcus* [11]. The polymicrobial synergy and bacteria metabolites accumulated in the site delay the wound healing [12] which, in many cases, is additionally impaired by acquired bacteria resistance against medication (e.g. antibiotics). Hence, chronic ulcers have both biological and physiological reasons for not healing.

1.1.4 Chronic wound pathogens

Despite the different underlying aetiology, most chronic wounds show a similar behaviour and progress. This uniformity is due to consistent components of the multifactorial pathogenesis of most chronic wounds: impaired oxygen supply (hypoxia) to local tissue, repeated friction of the local tissue, severe bacterial colonisation of an acute wound, reperfusion injury and cellular as well as systemic changes of ageing [10]. Likewise, the specific biological markers characterise all chronic wounds. Accordingly, key biomolecules significantly differentiate the environment of acute and chronic wounds. In acute wounds there is a balance between production and degradation of molecules (e.g. collagen); in chronic wounds this balance is disturbed in favour of degradation.

Chronic ulcer fluids contain elevated level of neutrophils and neutrophil-derived enzymes compared with acute wound fluids [13]. During the healing process these most abundant white blood cells leave the vasculature and migrate towards the inflammation site. However, the continuous influx of neutrophils during the prolonged inflammation in chronic wounds cause the accumulation of these cells on the site, where they undergo apoptosis and release their constituents such as oxidative enzyme myeloperoxidase (MPO). Under physiological conditions MPO catalyses the generation of

hypochlorous acid (HClO), the most powerful reactive oxygen species (ROS) in human body, creating oxidative stress and impairing the healing of the wounds. The cytotoxicity of this reaction allows the killing of bacteria in the first line of defence. However, the HClO reacts with most biological molecules, including natural protease inhibitors. In healing wounds the production and activity of proteolytic enzymes, such as matrix metalloproteinases (MMPs) and serine proteases (e.g. elastase), are tightly regulated by counteraction of their natural inhibitors [14]. During granulation tissue formation levels of MMPs have been shown to be decreased compared to levels found in chronic wounds. In normal levels, these proteases play a role in cellular migration through extracellular matrix. In chronic wounds the generation of HClO induces disturbed ratio proteases/inhibitors [15], so that most of the enzymes are uninhibited [16]. In increased levels these proteases have detrimental effect on wound healing by uncontrolled digestion of the extracellular matrix and the growth factors [17].

Myeloperoxidase

Myeloperoxidase (EC 1.11.2.2), a versatile heme-containing protein is the key enzyme in human neutrophils and monocytes. In contrast to other peroxidases, MPO also shows chlorinating activity. When neutrophils become activated during phagocytosis, they undergo the respiratory burst process, generating antimicrobial ROS such as superoxide radical and hydrogen peroxide (H_2O_2). MPO catalyses the conversion of the produced H_2O_2 and halides (mainly Cl^-) into corresponding hypohalous acid, e.g. HClO, 50 times more potent in killing bacteria than hydrogen peroxide. In addition, the products of the MPO/H_2O_2/Cl^- system are believed to play a role in killing other microorganisms like fungi, parasites, protozoa and viruses. MPO also directly chlorinates phagocytosed bacteria, completing the importance of this enzyme in the innate immune system. The enzyme is further thought to be involved in terminating the respiratory burst process, since the individuals deficient in MPO display prolonged respiratory burst (source: http://emedicine.medscape.com).

In the presence of H_2O_2, the MPO native form is oxidised by a two-electron equivalent to the redox intermediate – compound I (Figure 1.3). Being a strong oxidant, compound I mediates both one- and two-electron oxidation reactions. Depending on the substrate availability, MPO follows either the halogenation or the peroxidase cycle. The halogenation cycle is a direct two-electron reduction of compound I to the native form of the enzyme. In the peroxidase cycle, this compound is reduced in a two-step one-electron sequential reaction (via formation of compound II). Many inorganic and organic substrates have been found to act as electron donors for these intermediates. The principal reaction catalysed by MPO under physiological conditions is the oxidation of Cl^- to the corresponding HClO due to high concentrations of Cl^- *in vivo* [18].

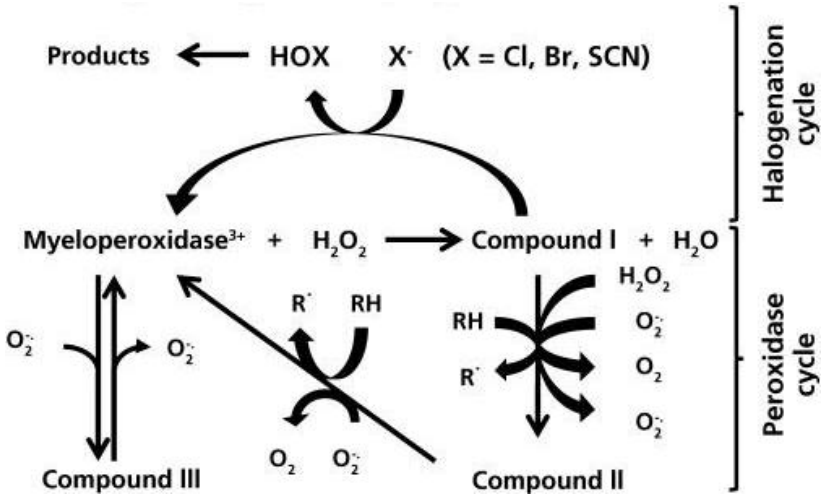

Figure 1. 3 The enzymatic cycles of myeloperoxidase (adapted from [18]

Matrix metalloproteinases - collagenases

Matrix metalloproteinases belong to the family of structurally related Zn^{2+}- and Ca^{2+}-dependent endopeptidases, all involved in the cleavage of the ECM constituents. To date, numerous MMPs have been identified and these enzymes are loosely classified based on their substrate specificity into collagenases, gelatinases, stromelysins, matrilysins, membrane-type MMPs, and seven others not classified in those categories. In normal physiology, MMPs are required for various processes such as tissue remodelling, embryonic development, angiogenesis, cell adhesion and proliferation, and wound healing [19]. During these processes synthesis/activation levels of MMPs are tightly regulated by cytokines, growth factors, other enzymes and tissue inhibitors of metalloproteinases (TIMPs). There are a total of four TIMPs (TIMP-1, -2, -3, and -4) and these four protein inhibitors are able to control the proteolytic activity of all MMPs [20]. The diversity of MMPs and their expression implies that these enzymes perform many functions during e.g. wound healing, acting on a variety of substrates at the wound site [21, 22].

Despite their physiological importance, misregulation of MMPs activities leads to the progression of various pathologies such as arthritis, multiple sclerosis, periodontal disease, and cancer. Overexpression of MMPs during the chronic inflammatory diseases has verified the importance of MMPs as a therapeutic target. Because of the role of MMPs in these pathologies, MMP inhibitors have emerged as an important area of drug development research [20].

1.2 Chronic wound management

Effective treatment of chronic wounds depends on understanding a number of different factors such as the underlying mechanism of wound formation, the type of wound, the healing process and general condition of a patient in terms of health (e.g. diabetes, aged patient, etc.). First, in order to inspect a wound correctly for the proper treatment choice, it is indispensible to remove the necrotic tissue and foreign material from the areas around the wound. The removal of the dead tissue is known as wound debridement and could be carried out using several methods. Surgical removal using scalpel and scissors is the most effective and precise, however, can only be undertaken by highly skilled and trained practitioners. Wound irrigation, on the other hand, implies rehydration of necrotic tissue using e.g. hydrogel dressings and further its autolytic digestion by the enzymes accumulated in the wound site [23]. Here the outcome depends on many individual factors in the treated patient, and thus, little control over the process is granted. The more efficient alternative is the enzymatic removal of the necrotic tissue after liquefying using bacterial or animal derived collagenases [24]. Despite being more controllable than the autolytic digestion, the biggest disadvantage of all enzymatic methods still remains the long duration compared to the surgical debridement. Besides to assure establishing of the proper diagnosis of the wound, another objective of debridement is to provide a favourable environment at the surface of the wound in which healing could take place in combination with proper treatment strategy [25].

Depending on the type and cause of the chronic wound, and its position on the body, the **management** can involve one or the combination of the conventional treatment options: topical application of antibiotics and/or antiseptics, multiple dressing changes per day and, recently, treatments involving the application of local mechanical stresses or energy to a wound: negative pressure wound therapy (NPWT) and mist ultrasound therapy.

Epicutaneous application of **antimicrobial agents** is, thus far, the most effective way to treat wound infections. However, the biggest concern is the overdoses due to the accumulation of immunoreactive compounds at the wound site [26].

Negative pressure wound therapy involves the controlled application of sub-atmospheric pressure to the local wound environment, using a sealed wound dressing connected to a vacuum pump. Studies suggested that NPWT assists in wound healing by providing a moist environment, stimulating circulation to the wound bed, decreasing bacterial colonisation and increasing the rate of granulation tissue formation [27]. On the negative side, NPWT is a costly treatment and there is not still an

overall plan of care for the patients suffering different kind of ulcers, especially chronic wounds. Although a consistent evidence of the benefit of NPWT in the treatment of diabetes-associated chronic leg ulcers together with safety of the treatment was found [28], its effectiveness compared to conventional/advances dressing treatments is still disputable [29, 30]. Moreover, the evaluation on "mixed wounds" was of poor quality and therefore requires better quality research to be conducted.

A novel technology using non-contact, kilohertz-range **ultrasound therapy** is gaining popularity in chronic wound management. Energy from the ultrasound wave is absorbed by individual bioentities, proteins and cells, resulting in their conformational changes and initiating signal-transduction pathways with direct implications for wound healing. The key effect of the mechanical energy realised by the cells is that of cavitation – the production and vibration of micron-sized bubbles [31] within inter- and intracellular fluids. The movement and compression of the microbubbles cause changes in the cellular membrane potentials and cellular activities of the tissues subjected to ultrasound. Mist ultrasound has been shown to increase the healing rate in recalcitrant diabetic foot ulcers [32] and other lower extremity wounds [33], however, it is rather cost-ineffective compared to standard wound care.

Regarding **wound dressings**, in most cases a combination of dressings that feature different functional properties, including antibacterial, occlusive, absorbent and adherence, is necessary in order to achieve efficient wound healing in a reasonable time. Besides the classification on their function, wound dressings can be categorised according to the type of material employed for their production (synthetic or naturally occurring polymers) and the dressing design (film, sponge, (hydro)gel) [34]. The design of wound dressings is dominated nowadays by the hydrocolloids applied to a carrier – usually polyurethane foam or film. Hydrocolloids are useful for clean, granulating, epidermal wounds, with low to medium exudate, and inefficient on infected and exuding wounds. Over recent years, many new dressings, but few new dressing types appeared on the market. Currently, polyurethane foams are promoted as an alternative to hydrocolloids, but no significant improvement was recorded in the healing rate of chronic ulcers. The healing concept of most dressings relies on maintaining of a moisture environment, without any active component involved. Regardless of the wound dressing constituents and design, a major focus of chronic wound care in recent years has been the development of new advanced dressings able to promote chronic wound healing, combining as many as possible functional properties in one [25]. However, despite the advances in understanding of molecular aspects of chronic wound pathogenesis, the development of functional dressings and tissue-engineered skin substitutes, and a range of other therapeutic options, chronic ulceration remains a significant problem in society.

1.3 Biopolymers as dressing materials

The modern industries necessarily need to exploit renewable resources in a sustainable manner, promoting bio-based, environmentally friendly and beneficial technologies in order to keep competitive market position. The highly demanding market calls for constant improvement in quality of products as well as competitive technologies for their generation. In last decades naturally derived polymers, due to their intrinsically beneficial properties for a broad spectrum of applications, are gaining importance as raw materials in many industrial sectors. Biodegradable and biocompatible materials that do not cause immune response in organism, able to integrate with a particular cell type/tissue are required for medical and pharmaceutical uses.

A primary factor for dermal repair is the availability of suitable biomaterials to support and evoke regeneration of the skin. The biomaterials used in skin repair should display intrinsic biocompatibility and biodegradability at the ideal rate corresponding to the rate of new tissue formation [35]. Moreover, these materials and their degradation products should not be toxic, immunogenic and carcinogenic. Polysaccharides and proteins, being natural components of all living structures, are fascinating candidate materials for fabrication of wound dressings. Carbohydrate moieties of the polysaccharides interact with integral components of many extracellular matrix glycoproteins and cell adhesion molecules in the skin. Chitin and its deacetylated derivative chitosan, due to their molecular and supramolecular structure, and intrinsic antimicrobial and wound healing properties have been identified as suitable bioplatforms that can be further improved by targeted functionalisation for skin repair. Among proteins collagen and its partial hydrolysate gelatine showed potential for wound dressings and drug delivery systems being a major natural constituent of connective tissue and a major structural protein of any organ. The collagen-based materials are meant to provide a structural support for the various cells involved in dermal tissue regeneration.

1.3.1 Chitosan

Chitin, a polysaccharide composed of ß-(1-4)-linked N-acetyl-D-glucosamine residues, is a structural material in the exoskeletons or the cuticles of many invertebrates and in the cell walls of green algae, some fungi, and yeasts. It is one of the most abundant organic materials obtained through biosynthesis. Chitin exhibits structural similarity to cellulose, differing only in the replacement of C-2 hydroxyl groups by acetamide residues. Depending on the polysaccharide source and isolation conditions, chitin could have a different degree of acetylation. Chitin is insoluble in water, diluted acid/base solutions and in most of the organic solvents. It is usually dissolved in concentrated acids as well as in hexafluoroisopropanole or hexafluoroacetone.

Chitosan is produced by chitin deacetylation with concentrated alkali solutions at elevated temperatures. The degree of chitin deacetylation can be controlled by the temperature of the process.

Moreover, since the length of chitin molecule in nature largely varies, the molecular weights of chitosan ranging from oligosaccharides to well above 1000 kDa are available. For instance, 5000-8000 N-acetyl-D-glucosamine residues are found in the crab chitin, while the one from yeast contains only up to 100 residues [36]. The rigid D-glucosamine structures of chitosan (Figure 1.4), characterised with high crystallinity and hydrogen bonding capacity between its macromolecules, define the poor solubility of chitosan in common organic solvents and complete insolubility in aqueous solutions above pH 7. Reducing the molecular weight and lowering the crystallinity by random deacetylation improves its solubility in dilute acids below pH 5 where the free amino groups are protonated. Chitosan displays interesting physicochemical properties, including both its solid-state structure and the dissolved state conformation [37]. In solid state, relatively rigid crystals are formed due to the regularly arranged hydroxyl and amino groups, while in solution hydrogen bonding drives the formation of microfibrils, depending on chitosan concentration [38]. Furthermore, chitosan is a biopolymer easy to develop in various designs, i.e. films, sponges, scaffolds, and hydrogels, a fact essential for the preparation of a great diversity of wound dressings and tissue engineering materials.

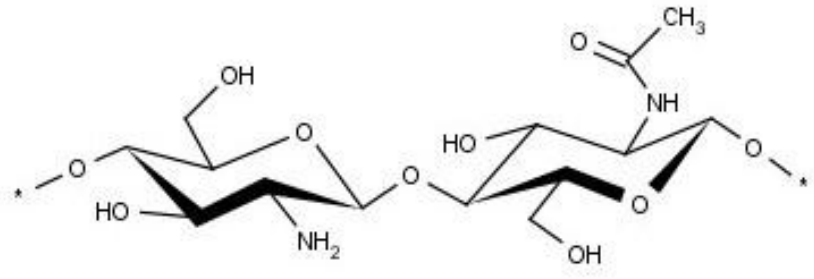

Figure 1. 4 Chitosan structure

The unique biological properties of chitosan including biocompatibility, biodegradability, nontoxicity, antibacterial and haemostatic properties assure the biochemical significance of this biopolymer in skin repair processes. The haemostatic activity of chitosan is crucial for early treatment of open wounds [39], especially in large injuries subjected to heavy bleeding [40]. Many haemostatic products on the market consist, fully or partially, of chitosan. Moreover, a rapid closure of full-thickness cutaneous wounds was demonstrated using poly-N-acetyl glucosamine membranes, attributing the effect to the fast growing of new blood vessels (angiogenesis) in the injured tissue [41]. On the other hand, chitosan has indirect role in wound healing supporting the regeneration of the extracellular matrix, and promotes physiologically ordered dermal regeneration during skin reconstruction regulating the deposition and faster arrangement of thin collagen fibres [42]. However, chitosan surfaces are hostile environments for fibroblasts viability and proliferation [43, 44].

Therefore, chitosan that shares structural similarities with GAGs from skin, attracted much attention as material for dermal regeneration, as these should closely match properties of the targeted tissue

[45]. On the other hand, these materials and their degradation products are still not sufficiently characterised for their inflammatory response cytotoxicity induced effects.

1.3.2 Collagen

Collagen is the major structural protein in any organ and the principal constituent of the connective tissue. The collagen fundamental structural unit, the right-handed triple helix, consists of three coiled polypeptide chains. A repeated sequence of three amino acids together with the unique conformation accounts for the collagen great tensile strength in biological tissues. Every third amino acid is glycine, a small amino acid that easily fits inside the helix. Many of the remaining positions in the chain are filled by two large amino acids: proline and hydroxyproline. Due to their conformational rigidity, these amino acids are difficult to accommodate in typical globular proteins, however, both fit into the triple-helical structure. Polypeptide chains are held together by hydrogen bonds that link the peptide amine bonds of glycine residues to peptide carbonyl groups in an adjacent polypeptide.

Collagen fibrils are formed by the packing of many three-stranded collagen molecules. The molecules packing is stabilised by covalent aldol cross-links between lysine or hydroxylysine residues at the C-terminus of one collagen molecule and the N-terminus of an adjacent one. A highly organised meshwork of collagen fibres strengthen ligaments and tendons, and support the skin and internal organs providing the structure to our bodies, protecting and supporting the softer tissues and connecting them with the skeleton.
So far, 29 types of collagen have been identified and described. However, over 90 % of all collagen in the body are of type I, II, III, and IV. The most abundant type of collagen in the skin is type I. Type III is also found in the skin in the early stages of wound repair, later being replaced by type I.

The resemblance to human tissue has been exploited to produce biomaterials of all designs for medical purposes for more than a quarter of a century [46]. Biomaterials made of collagen are biocompatible and nontoxic to tissues, and have well-documented structural, physical, chemical, biological and immunological properties [47]. Mechanical biological and, to some extent, immunologic properties of collagen-based materials can be influenced by modification of matrix properties (porosity, density) or by different chemical treatment affecting its degradation rate [48, 49]. Furthermore, the collagen matrix can be medicated, thus serving as a reservoir for drug delivery. The use of collagen matrices for delivery of different antibiotics have been discussed extensively [50]. The collagens from biomaterials may be derived from bovine, porcine and, lately, human sources. Although expensive, the human collagen, derived from donor cadavers, placentas and aborted fetuses, may minimise the possibility of immune reactions of collagen degradation products.

Previously, this protein was thought to be used only as a structural support. However, it is evident that collagen and the derived fragments control many cellular functions during dermal regeneration. Collagen plays a significant role in the wound healing process from the induction of clotting to the formation and appearance of the final scar [51]. It stimulates formation of fibroblasts and accelerates the migration of endothelial cells upon contact with damaged tissue [52]. Thus, collagen is a natural substrate for cellular attachment, growth and differentiation in its native state.

1.3.3 Glycosaminoglycans

Glycosaminoglycans or mucopolysaccharides are long unbranched polysaccharides consisting of a repeating disaccharide unit. GAGs form an important component of connective tissues where their chains are covalently linked to a protein to form proteoglycans. As highly hydrophilic structures GAGs possess especially high affinity for physiological fluids that originates from the high density of negative charges binding a cloud of cations, most notably Na^+, which are osmotically active and, thus, promote swelling [53]. GAGs in nature include heparin and heparan sulphate as anticoagulants, keratan and dermatan sulphate, and the most abundant chondroitin sulphates and hyaluronans.

Chondroitin sulphate is composed of a chain of alternating monosaccharides N-acetylgalactosamine and glucuronic acid. This GAG is an important structural component of cartilage and provides much of its resistance to compression [54]. Materials made from chondroitin sulphate are biocompatible and non-immunogenic. In addition, it has been suggested that these biomaterials act as surrogate extracellular matrices, serving as repositories for cytokines and growth factors during wound healing [55]. They may also provide structural frameworks for fibroblasts and epithelial regeneration.

The only GAG that is exclusively non-sulphated is **hyaluronic acid** (HA), a copolymer of D-glucuronic acid and N-acetyl-D-glucosamine (Figure 1.5), and is an intracellular component of connective tissues such as the synovial fluid of joints, vitreous fluid of the eye, the scaffolding within cartilage and the umbilical cord, and an important part of the ECM.

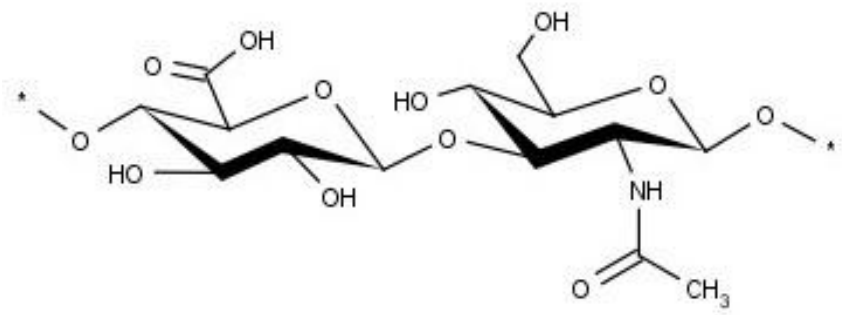

Figure 1. 5 Structure of hyaluronic acid

Perhaps the most important property of HA is its crucial effect in the formation of new blood vessels (angiogenesis): whereas high molecular weight HA inhibits angiogenesis, HA oligosaccharide units are proangiogenic [56, 57]. Conversely, HA macromolecules have greater ability to inhibit the expression of some MMPs [58]. Furthermore, HA plays an important role in cell differentiation and growth [59], influencing the processes of morphogenesis, inflammation and wound repair. Like that soluble HA has been used in several clinical applications including wound healing. However, the poor mechanical properties, rapid degradation and clearance in vivo of soluble HA are limiting factors for the more widespread use of HA in direct clinical applications [60].

The processed biomaterials based on HA are naturally biocompatible, biodegradable and lack immunogenicity. Cross-linked hyaluronic acid hydrogel films have been produced for use as polymeric drug delivery platforms with improved exploitation characteristics [61]. Furthermore, the biological properties of HA have been also combined with other biomaterials for the production of tissue engineering scaffolds or membranes [62, 63]. Hyaluronic acid-modified liposomes as bioadhesive carriers for topical delivery of growth factors to wound site have been developed [64]. An open ended study of hyaluronic acid based dressing found them to be effective for managing acute wounds particularly in terms of its safety and efficacy [65].

1.3.4 Problematic and advanced treatment solutions

Despite all biopolymer-based materials promote wound repair to a certain extent, these materials exploit only the intrinsic properties of the biopolymer matrix itself without further upgrading them with active functions to interact with the chronic wound pathogens at the molecular level. Moreover, the use of biopolymers in wound management has not yet been clearly translated into a platform for widespread clinical use, as the existing studies only offer evidences for beneficial properties of the biopolymers as dressing matrices and not as active agents. **The multifactorial nature of virtually all chronic wounds requires an intervention at molecular level with the biochemical events governing the ECM breakdown and impaired healing.** Such effect is expected in case of **controlled application of active agents, e.g. antimicrobials and enzyme inhibitors.**

1.4 Attenuating the enzymatic activities in chronic wounds

The recent discovery of elevated levels of oxidative and proteolytic enzymes in conditions characterised with prolonged inflammation, such as chronic wounds, gave new insights for their treatment. The effect of biopolymers *per se*, e.g. chitosan and its derivatives on the MMPs activities has been the subject of a limited number of scientific reports [66]. It has been found that especially oligosaccharides of chitosan display inhibitory effect on gelatinase (MMP-2) expression and its transcriptional activity. Both zymogen and active MMP-2 were inhibited with 3 - 5 kDa chitosan and this effect was attributed to their chelating ability on Zn^{2+} [67]. At the same time partially hydrolysed chitosan was found to be potent inhibitor of gene and protein expression of other gelatinase (MMP-9) according to the same inhibitory mechanism [68]. High molecular weight chitosan (500 kDa) showed elevated binding-specificity for MMP-2 and also displayed inhibitory activity by non-competitive inhibition. Atomic force microscopy revealed complex formation between the chitosan and the enzyme [69]. On the other hand, collagenases, a group of MMPs that specifically recognise and cleave collagen include MMP1, MMP8 and MMP13. Collagen produced in various designs was investigated as a competing enzyme substrate, with a goal to distract MMPs from the cleavage of the ECM [70, 71]. Up to a certain extent this can positively influence the imbalance between proteinase activities and inhibitors and thus, the coordination of the breakdown/regeneration of the ECM. Further, the addition of HA macromolecules to the collagen-based dressings suppress the expression of some MMPs [58].

However, the intrinsic biodegradability of the biopolymers may compromise their use in the physiological fluids with elevated and persistent enzymatic activity. This is especially emphasized due to the requirement for low frequency of dressing changes during the management of chronic wounds [72]. Moreover, little control over attenuation of the chronic wound enzyme activities by application of biopolymers *per se* can be guaranteed. Both oxidative and proteolytic enzymes play a role in controlled proteolysis of the ECM in the inflammatory phase of healing. Thus, the total inhibition of these enzymes is also not desirable for the regeneration of the ECM and wound progression towards closure.

In one attempt, an active dressing specifically targeted towards reducing local levels of MMPs in non-healing wounds was developed using bovine collagen and oxidised regenerated cellulose. When placed in the woundbed, the dressing chemically binds MMPs. The concept is based on bringing the active levels of these enzymes back down into the ranges found in healing wounds to allow healing to progress [70]. The mechanism of action has been postulated as the collagen moiety acting as a "sacrificial" substrate for the proteases, whereas the oxidised cellulose with its multiple negative charges dislodges the positively charged metal ions common to this family of enzymes. Although this composite represented a breakthrough in the dressings meant specifically for chronic wound treatment, the concept considers only attenuation of the activities of some proteases at the wound site.

This concept could be further complemented by addressing other common factors influencing non-healing nature of chronic wounds of various aetiologies.

1.4.1 Active agents to modulate the enzymes activities in chronic wounds – an integrated approach

Abnormal redox state and impaired antioxidant defence in the inflammatory stage of chronic wounds calls for the use of redox drugs. Matrix metalloproteinases are a group of metalloenzymes, where the catalytic Zn^{2+} in the active centre is coordinated by a redox-sensitive cysteine residue. Displacement (e.g. upon oxidation) of the cysteine ligand coordinating the metal ion leads to the activation of the enzyme [73] – a mechanism termed **"cysteine switch"**. The MMP activation/inhibition could be, therefore, redox-regulated by e.g. **thiol compounds** affecting the sulfhydryl/disulphide state of the switch [74]. Another, rather non-specific regulation of MMPs activity could be achieved through metal chelation. Since thiols combine both metal chelating and redox functions [75], thiol-functionalised biopolymers could be expected to control the activities of these enzymes via a combination of these two mechanisms. To this end, thiolated conjugates have been patented as MMP inhibitors, however, the application is limited to thiol-compound release from a platform. Moreover, the release mechanism is either complicated [76], or realised in a non-controllable way [77].

On the other hand, MPO is an oxidative enzyme able to produce HClO, overwhelming the natural shield of protease inhibitors, enabling accumulation of these enzymes in the chronic wound site. Furthermore, through HClO generation MPO is directly involved in the regulation of MMPs activity [78]. The prevention of MPO-derived HClO accumulation can be envisaged at two levels by: i) using competitive amounts of peroxidase substrates to avoid the pathway of the enzyme chlorination activity and subsequently HClO production, and ii) application of HClO scavengers. Thiol-containing molecules were reported to interfere with $MPO/H_2O_2/Cl^-$ system and consequently inhibit HClO production [79]. Thus, **the use of thiol-bearing compounds would be an integrated approach for attenuation of both oxidative and proteolytic enzyme activities.**

Similar effects on both enzymes are expected using **polyphenolic antioxidants**. Plants polyphenolic extracts, which structures vary from simple molecules to highly polymerised compounds are well-known for their antioxidant capacity and scavenging activity over both free radical and non-radical reactive species [80], metal-chelating capability [81] and inhibitory activity over radical-generating enzymes [82]. The degree of polymerisation and the chemical nature of the repetitive units constitute important structural features related to their physicochemical and biological properties. Plant polyphenols have been also reported to have anti-inflammatory [83], antimicrobial [84], immunomodulatory [85] and wound healing promoting properties [86]. All of these benefits indicate that plant polyphenols could be employed for the chronic wound management. Some polyphenolic

extracts are widely used in the therapy of skin diseases, skin damages such as burns, and as protective component in cosmetic formulations [87, 88]. Various polyphenolic extracts are reported as efficient inhibitors of both MPO [89] and MMPs [90]. Indeed, their propensity to bind proteins presumably accounts for the fact that polyphenols inhibited virtually every enzyme tested with in vitro [91]. Moreover, by functionalisation of the biopolymer carrier with microbicidal polyphenols synergistic enzyme inhibition and antibacterial activity is expected.

The use of biopolymeric materials with intrinsic antimicrobial properties, further upgraded with bioactive compounds that specifically interfere with biochemical environment of chronic wounds could be an integrated strategy for their efficient management. Moreover, controllable enzymatic inhibition could be expected by tuning the degree of biopolymer functionalisation (e.g. biopolymer thiolation, dosed biopolymer impregnation with polyphenols). This would be a step forward towards the regulation of the optimal enzyme/inhibitors ratio necessary for healing.

1.5 Modification/functionalisation of biopolymers

Biopolymers have been used as materials in dermal wound regeneration due to their beneficial skin repair properties. However, despite the fact that these natural macromolecules appear to be efficient to a different extend in the tissue repair process, the currently marketed products exploit only the intrinsic properties of the biopolymers without further upgrading them with active functions to react at molecular level with chronic wound pathogens. Moreover, biopolymers attracted much attention as materials for recovery of damaged skin because the materials degradation and the new tissue formation should be parallel processes. The situation with chronic wounds is more complicated due to very low stability of these materials in contact with the fluids containing elevated levels of enzymes that hydrolyse biopolymers. For example, chitosan is a substrate of lysozyme [92] and chitosan-based materials are readily digested by this enzyme [93], whereas collagen is a natural substrate of several MMPs.

Regarding targeted functionalisation, chitosan bears two types of reactive groups that can be modified - the free amino groups on the deacetylated units and the hydroxyl groups on the C3 and C6 carbons on both acetylated and deacetylated units. This allows its functionalisation with a variety of (bio)active molecules or the use of cross-linking reagents for blending with other biopolymers. The cationic nature of chitosan facilitates the preparation of various materials in combination with anionic GAGs forming polyelectrolyte complexes (PEC). This property of chitosan was exploited in this work for the development of polyelectrolyte multilayered (PEM) assemblies combining the biopolymer and its thiolated derivatives and GAGs for modulation of collagenase and MPO activities (Chapter 5).

Being a protein, collagen has much more complex structure allowing for many functionalisation approaches. One of the most used protein modifications is targeting controlled biodegradation through mentioned cross-linking reactions between the protein molecules itself or for combining with other materials.

1.5.1 Chemically modified chitosan

Chemical modification of biopolymers to improve their biofunctionality (e.g. biocompatibility, biodegradability, antibacterial activity and wound healing promotion) tends to preserve the original physicochemical and biochemical properties of the polymers, while widening their biomedical applications potential. However, except for the chemically cross-linked biomaterials, the use of chemically modified biopolymer derivatives specifically evaluated *in vitro* or *in vivo* for dermal tissue regeneration has been sparsely reported.

Major functionalisation of chitosan include: (i) substitution, introducing small functional groups to chitosan backbone and (ii) depolymerisation by chemical, physical or enzymatic treatments. Moreover, further chemical modifications of the functionalised chitosan can be performed in order to extend the range of their applications [94].

Introducing small functional groups to the chitosan structure, such as carboxymethyl groups, can drastically increase the solubility of chitosan at neutral and alkaline pHs, a major drawback for the processing of this biopolymer, without affecting its cationic character. N-carboxyalkylation of chitosan involves the introduction of acidic (anionic) groups onto the polymer backbone. Besides good solubility, carboxymethylated chitosan promotes significantly the proliferation of normal skin fibroblasts, but inhibits the proliferation of keloid (scar) fibroblasts; reduces the ratio of collagens I/III in keloid fibroblasts by inhibiting the secretion of collagen type I, while not affecting the secretion of collagens I and III in normal skin fibroblasts [95, 96]. Increase of the antimicrobial activity is also observed with this derivative, which either renders unavailable the essential transition metal ions for bacteria by complexation, or disturbs the cell membrane binding to the negatively charged bacterial surface [97]. Finally, carboxymethyl chitosan can be used in the development of different protein drug delivery systems as porous, pH-sensitive, cross-linked hydrogels for wound healing applications [98, 99].

N-acylation involves reaction between chitosan and an acid anhydride or acyl halide. The reaction proceeds through an addition/elimination type mechanism, where the amide functionality of the N-amino groups is restored. Several N-acyl derivatives comprising aliphatic side chains have been prepared. For example, a series of water-soluble N-saturated fatty acyl derivatives of chitosan have been synthesised through reactions with propionic, butyric, pentanoic, hexanoic, and octanoic

anhydride, and the longer chain acid anhydrides decanoic, lauric, myristic, palmitic, and stearic anhydride [100]. Studies also showed that N-acylated chitosans with different degree of substitution prepared exhibited different antibacterial activity *in vitro* [101].

N-sulphation of chitosan is another example of introducing anionic charge to the polymer backbone with various methods involving combinations of sulphating agents and reaction media used to date [102]. Sulphated chitosan is analogue to the natural blood anticoagulant heparin [103, 104], a highly sulphated glucosaminoglycan used for treatment of various conditions in medicine.

Phosphate groups, due to their ion-exchange properties, are appropriate functionalities for specific binding of biologically active species. Phosphate carriers in solution are exchangers of ionically bound cations (e.g., Na^{+}, Ca^{2+}) with cationic residues of biomolecules. Phosphorylation of porous chitosan matrices can be used to immobilize signalling biomolecules and growth factors [105]. The ionic binding character coupled with the mild conditions for immobilisation leads to minor conformational changes in the immobilised biomolecules with subsequent high retention of activity. Phosphorylation of chitosan can be achieved by various chemical methods. The products of these reactions are normally water-soluble phosphorylated chitosans with high degree of substitution. Furthermore, chitosan phosphorylation has been reported as a way to improve viability, attachment and proliferation of cells onto chitosan-based surfaces [106]. Both phosphorylation and sulphation increase the biopolymer anti-inflammatory properties [107].

The derivatisation of the primary amino groups of chitosan with coupling reagents bearing thiol functions leads to the formation of thiolated chitosans. Sulfhydryl bearing agents such as cysteine and thioglycolic acid can be covalently attached via amide bond formation between the carboxylic acid group of the thiolating agent and the primary amino group of chitosan mediated by a water-soluble carbodiimide [108]. In another approach, a one-step method using 2-iminothiolane HCl (Traut's reagent) for preparation of highly thiolated chitosan was described [109]. Thiolated polymer conjugates display a series of interesting functions such as mucoadhesive [110], permeation-enhancing [111] and in situ gelling properties within a wide pH range [112], in addition to be biodegradable. Further studies in the direction of the use as novel scaffold materials were performed with L-929 mouse fibroblasts seeded onto chitosan–thioglycolic acid sheets. The thiolated chitosan provided a porous scaffold structure for cell anchorage, proliferation and 3D tissue formation [113]. Water insoluble thiolated polysaccharides (e.g. chitin/chitosan) with antioxidant properties against ROS present in early stages of chronic wounds are patented [114]. The thiolated polysaccharides were also able to complex Fe^{3+} essential for the bio-cycle of some bacteria found in chronic wound environment.

Quaternary ammonium functionalities could be introduced to chitosan either by direct alkylation of the N-amino functional groups, or via covalent attachment of quaternary ammonium substituents to

the N-amino groups. These processes are referred to as quaternisation. The simplest synthetic approach to give chitosan quaternary ammonium functionality is via conversion of the N-amino groups into N-trimethylammonium halide salts. Different degree of quaternisation of amino groups in chitosan can be achieved with methyl iodide in alkaline solution of N-methyl pyrrolidinone [115]. The major advantage of these derivatives over the parent chitosan is the permanent positive charge of the macromolecules, resulting in increased antimicrobial activity [116, 117]. Alkylchitosans quaternised by methylation [118] increased their free radical scavenging activity making them potentially useful in inflammatory diseases such as chronic wounds [119], characterised with elevated levels of ROS.

Other interesting biomedical applications using biochemically modified chitosan have also been reported. The hydrogel showed strong tissue-adhesion properties, significant induction of wound contraction and acceleration of wound closure and healing properties, hence suitable as biological adhesive in surgical applications. Ethylene diamine tetraacetic acid (EDTA) grafted onto chitosan increased its antibacterial activity by complexing magnesium that under normal circumstances stabilizes the outer membrane of gram-negative bacteria [120]. Grafting of cyclodextrins (CDs), cyclic oligosaccharides built from six to eight D-glucose units that are formed during the enzymatic degradation of starch and related compounds, onto chitosan may lead to a molecular carrier that possess the cumulative effects of inclusion, size specificity and transport properties of CDs together with controlled release ability of the polymeric matrix. There are different methods used to graft CD on chitosan and the inclusion ability, sorption and controlled release properties of the products [121]. For example, chitosan-based systems bearing cyclodextrin cavities have been proposed as a matrix for controlled drug release [122]. Due to the presence of the hydrophobic-cyclodextrin rings these systems provide slow release of the entrapped hydrophobic drug.

1.5.2 Chemical cross-linking of biopolymers

Due to their intrinsic biodegradability, biopolymers are digested by enzymes in body fluids. The biodegradability of biomaterials is even more pronounced in contact with chronic wound fluids, containing elevated counts of digestive enzymes. Therefore, for the exploitation of biopolymers as clinical materials this deterioration must be avoided, preferably beyond the material application time. The aim is to prolong the original structural and mechanical integrity of the biomaterial and to neutralise the antigenic properties attributed to their hydrolysis products [46]. Methods typically include creating new additional chemical bonds between the biopolymer molecules and within the same molecule, i.e. inter- and intra-molecular cross-links, respectively. These supplementary links reinforce the material to give a strong but usually less viable material. Both physical and chemical methods for the biopolymers cross-linking are available. The chemical ways are employed to stabilise

the material using the bifunctional cross-linking agent to form irreversible or reversible chemical bonds between the functional groups of biopolymers at two different sites. A drawback of using cross-linking agents is the potential cytotoxic effect resulting from a reversal of the cross-links or unremoved reagent after the treatment. Physical methods include drying, heating or exposure to ultraviolet (UV) or gamma radiation. Unlike chemical cross-linking, these methods do not use potentially toxic chemicals. However, the efficiency of the physical cross-linking is usually lower than using chemical reagents. Accordingly, the exploitation properties of the obtained materials are not comparable with the covalently cross-linked biopolymers.

The more exploited functional group of chitosan is $–NH_2$ and most of the chitosan chemical cross-linkers are homobifunctional reagents. On the other hand, due to the presence of other functional groups, collagen cross-linkers include a variety of homo- and hetero-bifunctional chemicals. Due to their reactivity with amino groups (and in less extent with hydroxyl moieties) in aqueous media under mild reaction conditions, the most exploited cross-linkers of both collagen and chitosan are dialdehydes, such as glyoxal and glutaraldehyde. Their use, however, was lately avoided due to toxicity concerns [123]. Other reagents that have been used for cross-linking chitosan include tripolyphosphate, ethylene glycol, diglycidyl ether and diisocyanate. Toxicity studies have shown that these synthetic cross-linking reagents are cytotoxic to a certain extent and may impair the biocompatibility of the chitosan delivery system.

Recently, the naturally occurring genipin (isolated from *Genipa Americana* and *Gardenia jasminoides Ellis*) has been used to promote cross-linking reactions between proteins and polysaccharides containing amino moieties. The biocompatibility of genipin in humans has not yet been assessed, while in vitro tests and injection in rats did not show cytotoxicity. Based on biochemical data on genipin safety it was concluded that the cross-linked complexes formed with genipin were not cytotoxic for the animal and human cells tested so far [124]. Moreover, the gelling of chitosan solutions treated with low amounts of genipin (0.05 – 0.20 %) at close to neutral pH in presence of glycerol phosphate can be controlled by changing the genipin concentration in the solution [125]. Importantly, the chitosan bacteriostatic activity remains unaffected after the cross-linking reaction [126]. Furthermore, genipin was successfully employed for controlled cross-linking of collagen extracts in a relatively short time-frame [127]. In addition, genipin-fixed collagen-based biological tissues of various origins have demonstrated improved mechanical properties and resistance to enzymatic degradation compared to non-cross-linked tissues [128, 129].

By varying the concentration of genipin, the cross-linking degree of chitosan and/or chitosan with another biopolymer can be modulated. In an example, genipin was used for blending with chitosan aiming tissue engineering applications [130]. Higher genipin concentration (2.5 % w/w of gelatin) negatively affected properties desirable for dressing applications such as wettability and swelling degree of the blends. On the other hand mouse fibroblast adhesion and proliferation on substrates

increased due to the fact that gelatin contains Arg-Gly-Asp (RGD) attachment site, a major recognition sequence for cell adhesion and proliferation [131]. The relative comparison of biological response involving cell proliferation and viability on chitosan-gelatin scaffolds suggested that blending of the two biopolymers could improve the cellular efficiency. Furthermore, chitosan–gelatin scaffolds were cytocompatible with buffalo embryonic stem cells [132]. This study disclosed for the first time that the chitosan–gelatin scaffolds were promising candidates for stem-cell-based tissue engineering, considered as the next generation of skin substitutes. Stem cells, as cells being able to renew themselves through mitotic cell division and differentiating into a diverse range of specialized cell types, have been increasingly reported to confer benefits *in vivo* as agents of angiogenesis and multilineage restoration in the face of soft tissue defects [133, 134]. In yet another example chitosan has been cross-linked with genipin to obtain an asymmetric structure chitosan membrane further loaded with type I collagen particles (CGC membrane). Cell adhesion tests after 7 days of dynamic culture revealed a flat cell morphology and good spreading on the membrane scaffold. In animal studies, this potential skin substitute seeded with fibroblast and grown for 7 days, was more effective for healing wounds that the commercial ones. Histological *in vivo* assessment indicated that covering the wound with CGC membrane resulted in epithelialization and reconstruction [135].

Water soluble carbodiimides such as 1-ethyl-3-(3-dimethylaminopropyl) carbodiimide (EDC) or N-(3-Dimethylaminopropyl)-N′-ethylcarbodiimide hydrochloride (EDAC) have been frequently applied as cross-linking agents for biological materials. Carboxyl residues in biopolymers are activated with carbodiimides usually in the presence of N-hydroxysuccinimide (NHS). The activated carboxyl groups then react with nucleophiles such as primary amine groups to form stable zero-length amide bonds [136]. Byproducts of the reaction are easily rinsed away leaving a stable non-cytotoxic matrix. Accordingly, carbodiimides have become popular in a wide range of tissue engineering-based applications [137]. In one of the studies chitosan was covalently coupled to type I collagen by using EDC [138]. The platelet deposition and endothelial cell culture experiments showed that the chitosan/collagen matrices had good cell and excellent blood compatibility, therefore suggesting creation of an appropriate environment for the regeneration of endothelial cells in tissue regeneration. In another study, sponge scaffolds comprising different ratios of chitosan, collagen and hyaluronic acid cross-linked with EDC displayed a steady improvement of the biostability observed with increasing chitosan concentration, suggesting greater extent of cross-linking. The biocompatibility test showed high proliferation of fibroblasts cultured on these sponges [62].

All these findings suggested that genipin and carbodiimides are promising cross-linkers of biopolymers and blends thereof for fabrication of wound dressing materials. In this thesis, both reagents were used for biopolymers cross-linking in order to rule the exploitation characteristics of the obtained materials.

1.5.3 Modification/blending of biopolymers using enzymatic tools

The enzymatic methods for polymer modification rely on the high specificity of the biocatalysts at mild reaction conditions to achieve targeted functionalisation, whereas eliminating a series of complicated protection/deprotection steps, typical for the chemical synthetic routes. Enzymatic modifications of natural polymers are less frequently reported than the conventional chemical modifications; however, this trend is progressively changing. Recent studies clearly indicate that the modification of natural polymers with enzymes is an environmentally friendly alternative to the chemical methods using harsh conditions [139]. However, despite the increasing number of reports on using of biotools for tuning of biopolymer properties, their functionalisation using active compounds aiming at wound healing and dermal engineering application are still sparsely reported.

Enzymatic functionalisation/cross-linking

The enzymatic tools for functionalisation are selected on the basis of the chemical structure of biopolymers, functional groups and targeted enzyme activities related. These usually include oxidases (e.g. tyrosinase, peroxidase, laccase), transferases (transglutaminase) and isomerise (protein disulphide isomerise) type of enzymes. The same enzymatically-assisted reactions are employed to cross-link and blend biopolymers in order to improve the exploitation characteristics of the materials, i.e. stability at use.

Grafting of phenolic compounds onto chitosan using tyrosinase (EC 1.14.18.1) to confer water solubility under basic conditions has been reported [140]. The tyrosinase converts the phenol moieties into electrophilic o-quinones in a wide variety of phenolic substrates, which subsequently undergo non-enzymatic reactions with chitosan amino groups to yield either Schiff bases or Michael type adducts. However, coupling reactions of the phenolic active species result in a complex mixture of mono- and oligomeric products grafted on chitosan. On the plus side, the modified chitosan is soluble in both acidic and basic media. In addition, the tyrosinase-catalysed modification of chitosan with phenols dramatically alters the rheological and surface properties of the biopolymer. Generally, this reaction would allow for grafting of any phenol group-containing molecule and therefore introducing various functionalities into polysaccharides that contain amino residues. For example, grafting of 3,4-dihydroxyphenethylamine onto chitosan could find application as a water-resistant adhesive [141]. In another study various phenolic substrates with different molecular weights to induce enzymatic gelation of chitosan were used [142]. Interaction between chitosan and polymers, such as poly(4-hydroxystyrene) in the mixture of methanol and water has been also reported [143]. The increased interest in blending of two or more natural derived compounds to improve their physicochemical properties resulted in many publications in the field. Chitosan was blended with sericin containing peptides using tyrosinase [144]. Following the same route chitosan was combined with proteins, such

as silk fibroin [145], and collagen hydrolysate gelatin to induce gelation [146]. The so obtained gels showed improved mechanical properties when compared to gels formed by gelatin cooling.

Transglutaminases (EC 2.3.2.13) catalyse the formation of a highly resistant to chemical and enzymatic degradation covalent bond between a primary amino group of lysin and the γ-carboxamide group of protein-bound glutamine. Preparation of chitosan-protein gels using transglutaminases has been reported. Although chitosan was not required to obtain strong gels from gelatine (as in the case of tyrosinase), it was observed that its presence leads to faster gelation, and the resulting protein-polysaccharide gels were mechanically stronger [146].

Horseradish peroxidase (HRP)-catalysed gelation system has been studied as a novel and effective route for obtaining hydrogels from various biopolymers. HRP catalyses the oxidation of donors using H_2O_2 resulting in polyphenols linked at the aromatic ring by C-C and C-O coupling of phenolic moieties. The versatility of the HRP-catalysed gelation has been demonstrated on the biopolymer derivatives bearing phenolic groups such as modified polysaccharides, e.g. hyaluronic acid [147], alginate [148], dextran [149], carboxymethylcellulose [150] and chitosan [151], and proteins such as gelatine [152]. Simultaneous conjugation and hydrogelation of phenol-bearing polysaccharides and proteins using horseradish peroxidase is also reported [153]. The gelation time of the resulting systems decreased with increasing the enzyme concentration and was controllable from a few seconds to several min. The tuneable gelation, biodegradability, mechanical properties, and cell adhesiveness of the obtained polysaccharide-protein conjugated hydrogels indicate high potential for a wide range of applications, among which scaffolds for tissue engineering and carriers for drug delivery systems. Recently, HRP was used to cross-link chitosan derivatives prepared by conjugation of chitosan and phenol containing α-hydroxy acids to produce biodegradable injectable hydrogels for medical purposes [93]. In the same study was shown that these hydrogels showed good biocompatibility by in vitro culturing of chondrocytes and can be readily degraded by lysozyme.

Enzymatic depolymerisation of chitosan

Chitosan can be controllably depolymerised by various enzymes, including lysozyme and especially chitosanases [92, 154]. In general, the efficacy of chitosan oligomers for wound healing is superior to chitosan macromolecules. A mixture of chitosan oligomers up to the hexamer including D-glucosamine have been compared with macromolecules in a linear incisional wound model in rats. The wound breaking strength in the cases where chitosan oligomers were applied was higher than in the macromolecule-treated group of wounds. Collagenase activity also followed the same trend [155]. In another study, chitosan oligomers were found to inhibit the growth of deleterious bacteria and to boost immune function [156].

1.6 Dressing design

The design of a dressing depends on the type of the wound, its thickness, position on the body, exudate volume, the stage of the healing process (early, late) and age of the affected individual. The modern dressings are mainly classified according to the materials from which they are produced and generally occur in the design of (hydro)gels, thin films/coatings and foam sheets (i.e. sponges).

Hydrogels are highly absorbent water-insoluble networks of polymer chains with high degree of flexibility similar to that of the natural tissue. The hydrogels are normally classified according to the nature of network formation as physical and chemical hydrogels. The physical hydrogels are obtained by reversible electrostatic interactions (e.g. PEC) or through secondary interactions (e.g. hydrogen bonds), while the chemical hydrogels are covalently cross-linked. Hydrogels are useful for exudative wounds because of their high absorptive capacity. In addition, they provide excellent pain relief by cooling the wound. Nevertheless, due to their low adherence hydrogels should be covered by an outer layer of tape, netting or roll bandage. They were found particularly useful for the treatment of deep partial thickness wounds.

Hydrophilic **foam dressings** are permeable to oxygen and water vapour. They usually have a hydrophobic backing and some have an adhesive surface to make the application easier. Sponges are more easily saturated with wound exudates than hydrogels, hence their changing frequency is considerably higher, especially during early wound healing when exudation is greater. Foam dressings are ideally suited for superficial, and dry and semi-dry wounds, in addition to chronic ulcers since they provide padding that can relieve pressure over bony prominences. From a technological point of view, the production of a foam dressing is an easy process consisting only of freeze-drying of a moulded suspension of the dressing components.

Thin **transparent film dressings** have low absorption capacity, thus not useful for wounds with significant exudates. Sometimes films are used as top layers to keep other dressings in place, e.g. over ointment or hydrogel dressing. Moreover, film dressings are used for the later stage healing, when the wound exudates are minimised. If applied alone, transparent films allow for on-site inspection of the healing progress without removal of the dressing. Films/coatings bearing active functions could be an ideal solution for the combined wound treatment and monitoring of the wound status.

1.7 Research objectives

The main objective of this thesis is the development of functional biopolymer-based materials upgraded with bioactive molecules based on understanding and targeted intervention in chronic wound management. Since the dressing design should be optimised according to the particular clinical application (type, cause and size of the wound; location on the body), as examples the dressings in the form of sponges and films/coatings, and nanoparticle formulations will be generated during the work realisation. To this end, the following specific objectives have been set up:

- **Generation of cross-linked biopolymer(s) sponges using chemical techniques (Chapter 2).** The optimisation of the cross-linking process is the crucial step in the development of stable in the physiological environment materials. The obtained sponges will serve as a base for further upgrading with active functions.
- **Impregnation of the cross-linked biopolymer(s) platforms with bioactive molecules and evaluation of their functional properties (Chapter 3).** The functionalised sponges will be investigated for the capacity to inhibit the enzymes related with prolonged inflammation in chronic wounds.
- **Permanent modification of biopolymer platforms with bioactive agents, e.g. thiol-bearing compounds (Chapter 4).** The thiolated protocols will set up the basis for further processing of thiolated biopolymers in various designs.
- **Layer-by-layer build-up of active multilayered films/coatings (Chapter 5).** Nano-scale materials will comprise thiol-modified chitosan and oppositely charged glycosaminoglycans. The multilayered assemblies will be studied for controlled adsorption of the major chronic wound enzymes and the fibroblasts attachment/proliferation.
- **Formation of nano/micro-particles from thiolated chitosan conjugates under ultrasonic irradiation (Chapter 6).** Especially the feasibility of the new strategy for nanoparticles generation, stability improvement and functionalisation in a single-step sonochemical process will be studied.

The experimental set-up of the thesis and the summary of the investigation and overall objectives are given on Scheme 1.1.

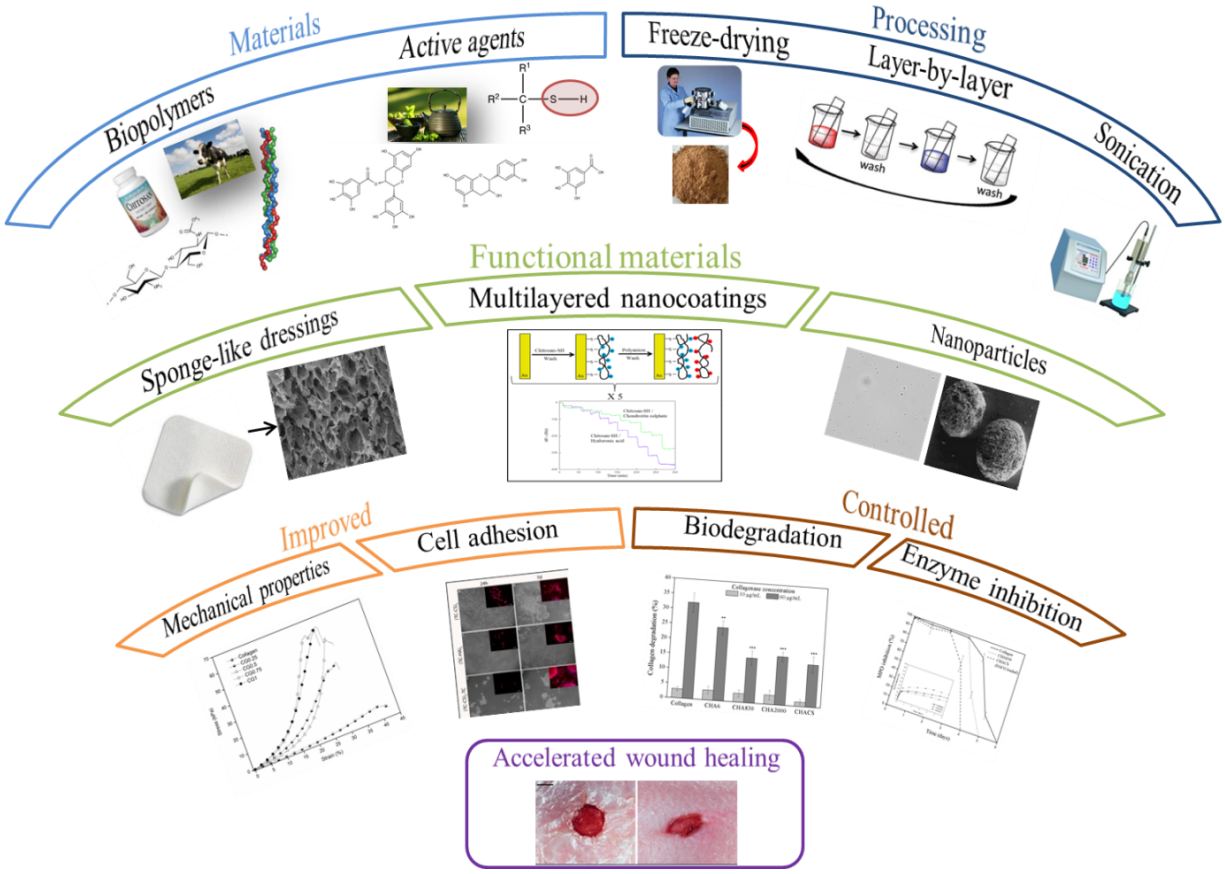

Scheme 1. 1 Summary of the work carried out during the thesis development

Section B

Dressing platforms loaded with plant polyphenols

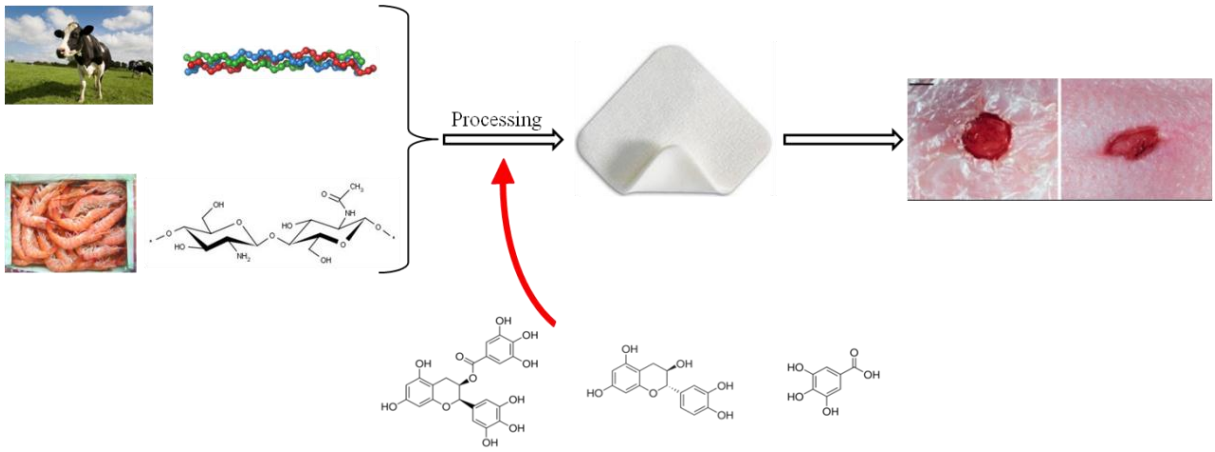

This section is based on the following publications:

1. Díaz-González M, Rocasalbas G, **Francesko A**, Touriño S, Torres JL, Tzanov T (2012) Inhibition of deleterious chronic wound enzymes with plant polyphenols. *Biocatalysis and Biotransformation* 30(1), 102-110
2. **Francesko A**, Rocasalbas G, Touriño S, Mattu C, Gentile P, Chiono V, Ciardelli G, Tzanov T (2011) Cross-linked collagen sponges loaded with plant polyphenols with inhibitory activity towards chronic wound enzymes. *Biotechnology Journal* 6(10), 1208-1218
3. **Francesko A**, Soares da Costa D, Reis RL, Pashkuleva I, Tzanov T (2012) Functional biopolymer-based matrices for modulation of chronic wound enzyme activities. *Acta Biomaterialia*, accepted for publication

---

Chapter 2

Cross-linked biopolymer sponges

2.1 Introduction

Biopolymers nowadays play increasingly important role in applications where the materials are in direct contact with body tissue due to their biodegradability, biocompatibility, low immunoreactivity and ability to integrate with a particular cell type/tissue. Their unique physicochemical and biological properties have been exploited in variety of commercially available wound dressings [25]. Among them, collagen - the most abundant structural component of the ECM - is largely employed in dressings to create optimal moist conditions for wound healing and absorb proteases from wound exudates [157]. In addition, collagen ensures fibroblasts adhesion and growth, leading to the formation of new granulation tissue and epithelium at the wound site [158]. Hyaluronic acid is an important moisturising constituent of the ECM. Chitosan (CS), sharing structural similarities with naturally occurring GAGs, possesses intrinsic antimicrobial properties and accelerates early phase wound healing [39]. Assembling of collagen, HA and/or CS into composite materials has displayed advantages in tissue regeneration applications over the use of any of these biopolymers alone [159, 160].

Wound dressings, on the other hand, require high stability during the extended treatment duration combined with low frequency of dressing changes as recommendable for chronic wounds treatment. This stability-at-use might be compromised by the intrinsic susceptibility of the biopolymer components to enzymatic degradation in contact with biological fluids. Furthermore, their digested fragments, especially from collagen, are many times more immunoreactive than macromolecule *per se* [161]. The application of suitable chemical cross-linkers, depending on the functional group availability, overcomes the enzymatic degradability of biopolymeric materials. Naturally-derived genipin is widely used nowadays for covalent cross-linking of biopolymers due to its low cytotoxicity. It efficiently reacts with primary amines and has been reported for cross-linking of many biopolymers and blends thereof [162, 163]. Water soluble EDAC is another well-known cross-linker usually applied in combination with N-hydroxysuccinimide to form “zero length” bonds between polymers [137].

The current study focuses on generation of the biopolymer-based sponges with improved enzymatic stability, mechanical performance and hydrophilicity through cross-linking with genipin and EDAC. The exploitation characteristics of either single biopolymer (i.e. collagen) or composite sponge-like dressings were investigated as a function of the cross-linker concentration or the biopolymer composition, respectively. Moreover, the combined intrinsic properties of the individual biopolymers – collagen, hyaluronic acid and chitosan – in a composite dressing material and the optimisation of the biopolymer composition of such dressing for chronic wound treatment are discussed.

2.2 Materials and methods

2.2.1 Biopolymers

Collagen type I from bovine skin was kindly supplied by Lohmann & Rauscher International GmbH & Co. (Germany). Hyaluronic acid sodium salts of different Mw (6, 830 and 2000 kDa) from Lifecore Biomedical (USA) and ultrapure chitosan (Mw ~50 kDa) from KitoZyme (Belgium) were used for the experiments.

2.2.2 Reagents

Collagenase from *Clostridium histolyticum* (277.50 U/mg solid, one unit liberates peptides from collagen equivalent in ninhydrin colour (at 570 nm) to 1.0 μmol of leucine in 5 h at pH 7.4 and 37 ºC in presence of calcium ions), EDAC and NHS were purchased from Sigma-Aldrich. Genipin was purchased from Challenge Bioproducts (Taiwan). EnzChek® kit was purchased from Life Technologies (Spain). All other reagents were of analytical grade purchased from Sigma-Aldrich and used as received.

2.2.3 Preparation of biopolymer sponges

All individual biopolymer solutions were prepared in concentration of 1 % (w/v). Collagen and CS were dissolved in 1 % acetic acid, while HAs were dissolved in distilled water. The prepared collagen solution was used as such or mixed as follow: collagen-hyaluronic acid (CHA) in 9:1 weight ratio, and collagen-hyaluronic acid-chitosan (CHACS) in ratio 4.5:1:4.5. The mixtures were homogenised for 20 min, poured at Petri dishes with 3 mm thickness and freeze-dried to obtain porous biopolymer sponges. Thereafter, to study the cross-linker effect, the collagen sponges were immersed in genipin solution (0.25, 0.50, 0.75 and 1.00 mM) in phosphate buffered saline (PBS, pH 7.4) and let to react for 3 h at 37 ºC. Finally, the genipin cross-linked collagen samples were thoroughly washed with double distilled water and freeze-dried again.

On the other hand, to study the effect of the materials composition, the freeze-dried composite sponges were cross-linked in 96 % ethanol containing EDAC (50 mM) / NHS (10 mM) for 24 h, thoroughly washed with distilled water and freeze-dried again. CHA specimens were named after the Mw of the used HA (CHA6, CHA830, and CHA2000). CHACS specimen was prepared using HA with Mw of 830 kDa.

2.2.4 Determination of the degree of collagen cross-linking with genipin

The cross-linking degree of the genipin cross-linked collagens was determined by ninhydrin assay and was defined as the ratio between the amount of amino groups involved in the cross-linking, and the amount of free amino groups in the non-cross-linked samples [128].The samples were weighed and further heated with ninhydrin solution for 20 min at 100 °C. After cooling, the solutions were transferred into a 96-well microplate and their absorbance was recorded at 570 nm (microplate reader Infinite M200, Tecan, Austria). The amount of free amino groups in the samples was determined using glycine standards. After reaction with ninhydrin, the amount of free amino groups in the tested samples is proportional to the optical absorbance of the solution.

2.2.5 Scanning electron microscopy (SEM)

SEM images were taken on the cross-sections of the cross-linked collagen sponges in magnification of x100 using scanning electron microscope (JSM 5610, JEOL Ltd Japan). The samples were previously sputter coated with gold. Data of the mean pore size ± standard deviation of each experimental group (n=5) are reported.

2.2.6 Fourier transform infrared spectroscopy (FTIR)

Infrared spectra of the non-cross-linked and cross-linked composite sponges were recorded using Perkin Elmer Spectrum 100 FT-IR spectrometer utilising the attenuated total reflectance technique. Spectra were acquired with an average of 75 scans.

2.2.7 Tensile testing

Strip-shaped sponges (30 x 10 x 3 mm) cross-linked with different cross-linking reagents were subjected to uniaxial tensile test in a wet state at room temperature using universal mechanical testing machine INSTRON 5540. After removing the excess of PBS (pH 7.4) by gentle contact with filter paper, the specimens were stretched at a crosshead speed of 5 mm/min until failure (n=5).

2.2.8 Biostability of the cross-linked biopolymer sponges

In vitro biodegradation tests of the sponges were carried out by incubating the specimens in 50 mM Tris-HCl (pH 7.4, 40 mM $CaCl_2$) containing collagenase at 37 ºC for 24 h. The resulting mixtures

were centrifuged at 4000 rpm for 10 min and the supernatant hydrolysed in 6 M HCl for 24 h at 90 ºC. Hydroxyproline (Hyp) content of the hydrolysate was determined according to the method described by Reddy and Enwemeka [164]. The percentage of collagen in the hydrolysate was based on the assumption that collagen contains approximately 14 % Hyp [165]. All measurements were done in one assay to avoid inter-assay variability. Five samples were evaluated for each composition and the results are expressed as mean values ± standard deviation.

2.2.9 Swelling behaviour of the biopolymer sponges

Specimens were evaluated for their ability to absorb physiological fluid [166]. The sponges were weighed (Wi) before immersing in PBS (pH 7.4) for 24 h. The swollen samples were withdrawn and weighed again without dripping (Ws). The capacity to absorb physiological fluid was defined as the ratio between the bounded fluid (Ws - Wi) and the dry weight of the sample (Wi).

2.2.10 Extent of collagenase adsorption onto the biopolymer composite sponges

Collagenase binding onto the cross-linked composite sponges was studied in 500 μL of 50 mM PBS (pH 7.4, 40 mM CaCl2) containing 2 μg/mL collagenase by incubating 10 mg of cross-linked specimens for 24 h at 37 ºC. Thereafter, the supernatants were collected and analysed for remaining collagenase activity using EnzChek®. Briefly, the remaining in the supernatants collagenase was left to cleave a gelatin-fluorescein conjugate in dark at room temperature for 6 h after which the fluorescence was measured (495/515 nm) using a microplate reader Infinite M200, Tecan (Austria). The results are expressed as the percentage of collagenase binding onto the materials (inversely proportional to the enzymatic activity in the supernatant) ± standard deviation (n=5).

2.2.11 Statistical analysis

All data are presented as mean values ± standard deviation. For multiple comparisons of composite sponges, statistical analysis by a one way analysis of variance (ANOVA) followed by post-hoc Tukey test was performed using Graph Pad Prism Software 5.04 for Windows (USA). Statistical significance was considered at $p < 0.01$.

2.3 Results and discussion

2.3.1 Genipin cross-linked collagen sponges

According to the EN ISO 10993-1 Standard the chronic wound dressings are classified as materials having direct contact with injured skin and the time of activity longer than 24 h. Elevated enzymatic activity in chronic wounds requires therefore increased stability-at-use of the biopolymer carrier applied as a dressing material. The bifunctional cross-linking reagent genipin reacts promptly with amino groups in biopolymers. Two reaction pathways for cross-linking at the neutral pH (used in the study) are possible. The faster one goes through nucleophilic attack by the amino groups on the C-3 atom in genipin dihydropyran ring, followed by opening of the ring and attack by the secondary amino group on the newly formed aldehyde group [167]. As a result, stable condensation products containing tertiary amine are obtained. The subsequent slower reaction is a nucleophilic substitution of the ester group of genipin to form an amide linkage. Simultaneously, an oxygen radical-induced polymerisation occurs between genipin molecules already attached to amino groups leading to cross-linkers built by short genipin copolymers [168]. The resulting cross-linked biopolymer matrices typically possess good mechanical properties, reduced swelling, slower degradation rate and good biocompatibility.

Characterisation of genipin cross-linked collagen sponges

As expected, the cross-linking degree increased with higher concentrations of genipin used (Table 2.1). Cross-linking degree of 24 % and 67 % was achieved with 0.25 and 1 mM genipin, respectively. The degree of cross-linking depends on the reagent concentration, as well as on the number and availability of anchoring points (e.g. amine functional groups) [169]. In this study up to 1 mM genipin for cross-linking was used considering that further increase of genipin concentration could induce significant cell death [127]. On the other hand, the sponges obtained with less than 1 mM genipin displayed suitable for the envisaged application mechanical properties, swelling behaviour and proteolytic stability.

Table 2. 1 Denomination and the cross-linking degree of the genipin treated collagen sponges

Specimen denomination	Genipin concentration (mM)	Cross-linking degree (%)	Mean pore size (μm)
Collagen	0	-	129±21
CG0.25	0.25	24.0±1.2	106±31
CG0.5	0.50	35.9±0.3	100±34
CG0.75	0.75	50.4±5.2	99±45
CG1	1.00	67.0±2.7	92±27

The microstructure of the material, such as porosity, pore shape, size, and distribution has prominent influence on cell intrusion, proliferation and function in tissue repair. Lien et al. [170] studied the effect of porosity of the genipin cross-linked gelatin on ECM secretion and found a macroporous structure as preferable for proliferation of chondrocytes and ECM production.

Pore size between 50 and 150 μm are indicated as optimal for improved ECM production [171]. Cross-sectional morphology of the sponges obtained in this study showed typical for freeze-dried collagen macroporous structure with three-dimensional interconnected pores of various shapes and homogeneous distribution (Figure 2.1). The mean pore diameters ranged from 92 to 129 μm, and decreased as genipin concentration increased (Table 2.1).

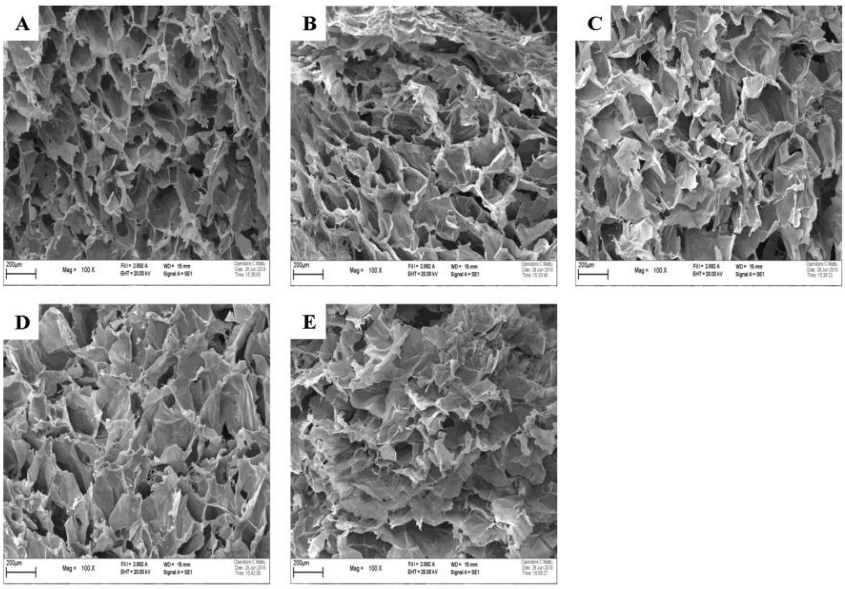

Figure 2. 1 SEM images of collagen sponges. (A) Uncross-linked, cross-linked with (B) 0.25 mM, (C) 0.50 mM, (D) 0.75 and (E) 1.00 mM genipin.

The obtained stress-strain curves of the sponges showed typical for freeze-dried collagen behaviour with three distinguished regions: toe, linear and failure region (Figure 2.2) [172]. An increase in elastic modulus and decrease of the elongation of genipin treated collagen sponges was observed increasing the cross-linking degree (Table 2.2).

Table 2. 2 Mechanical properties of the genipin cross-linked collagen sponges

Specimen	Young's modulus (kPa)	Elongation (mm)
Collagen	7.7±0.3	11.8±0.9
CG0.25	43.8±9.5	6.5±0.8
CG0.5	60.6±5.9	6.4±1.1
CG0.75	66.8±8.7	5.8±1.4
CG1	72.0±23.4	6.1±1.2

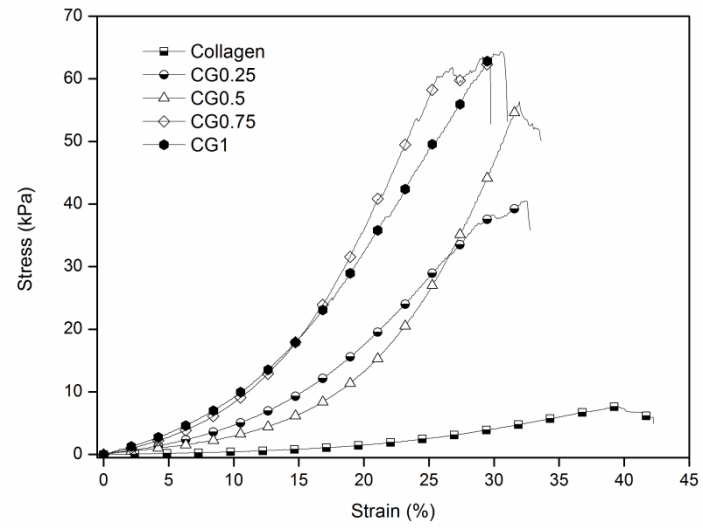

Figure 2. 2 Representative stress-strain curves of uncross-linked and collagen sponges cross-linked with different concentrations of genipin.

Collagen in biological tissues possesses low stretchability and high tensile strength unlike the materials prepared from collagen extracts. Both intra- and intermolecular cross-links may stabilise the collagen fibres. Studies on genipin fixation of biological tissues showed that intermolecular cross-links within collagen brought about increased ultimate tensile strength and stiffness [128, 129].On the contrary, intramolecular cross-links modify the collagen fibres along their preferential orientation, and have little effect on the mechanical strength. Thus, the orientation of the fibres plays a crucial role in the mechanical properties of cross-linked collagens [173]. However, in collagen extracts the fibrils are not aligned and do not have preferential orientation. Consequently, the cross-linking should improve the overall tensile strength of the material independent on the direction of the stress applied. The considerable increase in elastic modulus observed after genipin treatment is probably due to both intermolecular and intramolecular stabilisation of the sponges, and can be tuned varying the amount of genipin cross-linker.

Exploitation characteristics of genipin cross-linked collagen sponges

The ability of the dressing to bind biological fluids is an important factor in wound repair, and wounds are best treated in moist environment. Since the amount of exudates in chronic wounds varies depending on the wound type, location on the body and its status, there is no general recommendation for the water uptake properties of the dressings. The hydrophilic nature of the biopolymer material determines its fluid retention capacity. Cross-linking treatment results in the consumption of hydrophilic groups in the biopolymer and subsequently, swelling decreases. As expected, in this study the swelling of the sponges decreased with the increase of cross-linking degree (Figure 2.3). The type of cross-linker used does not alter significantly the water uptake, but rather the cross-linking degree

[174]. Since the generated dressings have a porous structure (Figure 2.1) the fluid uptake did not cause significant volume expansion and deformation of the specimens. The finding is important for the ease of the dressing removal.

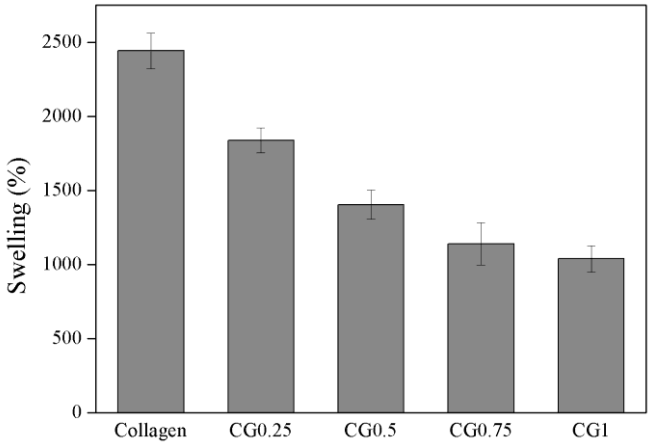

Figure 2. 3 Swelling capacity of uncross-linked and collagen sponges cross-linked with various genipin concentrations

In vitro test for biodegradability of genipin cross-linked collagen sponges showed considerable increase of their resistance (up to 94 % when 1 mM of genipin was used) to collagenase digestion after cross-linking (Figure 2.4). The uncross-linked collagen sponge was completely digested after 24 h incubation with collagenase. Although the biostability of the cross-linked sponges was in agreement with the cross-linking degree it should be noticed that at higher genipin concentrations, sponges with different cross-linking degree showed similar resistance to enzymatic digestion. The cross-linking degree of the sponges treated with 0.75 mM and 1 mM genipin was 50 % and 67 % respectively (Table 2.1), while the difference in their stability towards proteolysis was within 1 % (Figure 2.4). In contrast, both cross-linking degree and biostability of the samples treated with 0.5 mM and 0.75 mM genipin differed considerably (Table 2.1, Figure 2.4).

This suggests that the improved biostability was not only due to cross-linking, but also possibly due to reduced accessibility of collagenase to the cleavage sites in the cross-linked collagen network [169].This effect will be studied in the continuation through collagenase binding on the cross-linked biopolymer composite materials. In addition, the sponges cross-linked with 0.5 mM and higher genipin concentration conserved their structural integrity in the enzymatic digestion experiments. Preservation of the material integrity is one of the important properties of the dressing that would allow for its easy removal from the wound site.

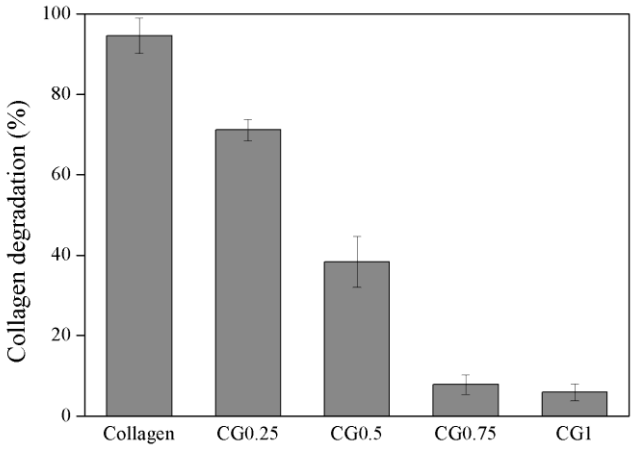

Figure 2. 4 Percentage of collagen degradation from the uncross-linked and sponges cross-linked with various genipin concentrations

2.3.2 EDAC cross-linked biopolymer composite sponges

Characterisation of cross-linked biopolymer composite sponges

EDAC-mediated cross-linking can undergo two distinct pathways depending on the available functional groups in polymers: either formation of amide linkages by activation of carboxylic moieties to react with free amines, or an acid anhydride formation from two carboxyl groups and further reaction with hydroxyl groups to yield ester bonds may occur [175]. Both pathways are likely to be followed for CHAs and CHACS to form inter- and intra-molecular cross-links between the biopolymers (e.g. some examples of intermolecular cross-linking are shown in Scheme 2.1).

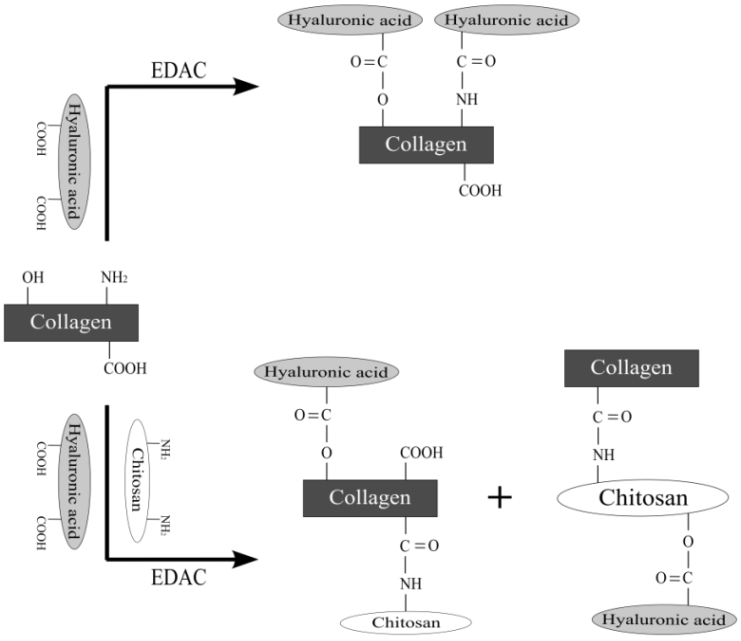

Scheme 2. 1 Cross-linking of the biopolymers with EDAC

After collagen treatment with EDAC, increase in the intensity of the amide I (C=O stretching at 1630 cm^{-1}) and amide II (N-H bending at 1543 cm^{-1}) bands was observed (Figure 2.5A,b). These signals together with the less intensive symmetric stretching band of carboxylate salts at 1399 cm^{-1} and the ester band with higher intensity at 1079 cm^{-1} confirmed the covalent cross-linking of the biopolymer. The intensity of the ester band became more pronounced in the spectra of the cross-linked CHA sponges, for simplicity represented only with CHA830 spectrum (Figure 2.5A,c). This indicated a higher esterification yield for these samples compared to collagen alone. In addition, the changes were more pronounced in CHA sponges containing higher Mw HA compared to CHA6 (Figure 2.5B). The latter observation could be explained with the higher number of carboxylic groups in a single molecule that increases the probability of acid anhydride formation mediated by EDAC and thus, subsequent ester bonding. On the other hand, the increased involvement of the carboxyl groups in these specimens to form acid anhydrides led to the lower extent of amide cross-linking, confirmed by the lower intensities of the amide I and amide II bands compared to CHA6. Finally, with the addition of chitosan to CHA830 sponge, a pronounced peak attributed to the mixed stretching and bending vibrations of the C–O–C bond (1150–970 cm-1) appeared and overlapped the ester peak (Figure 2.5A,d). The FTIR spectrum of CHACS hybrid sponge is rather complicated and shows overlapping effects of all three biopolymers after cross-linking.

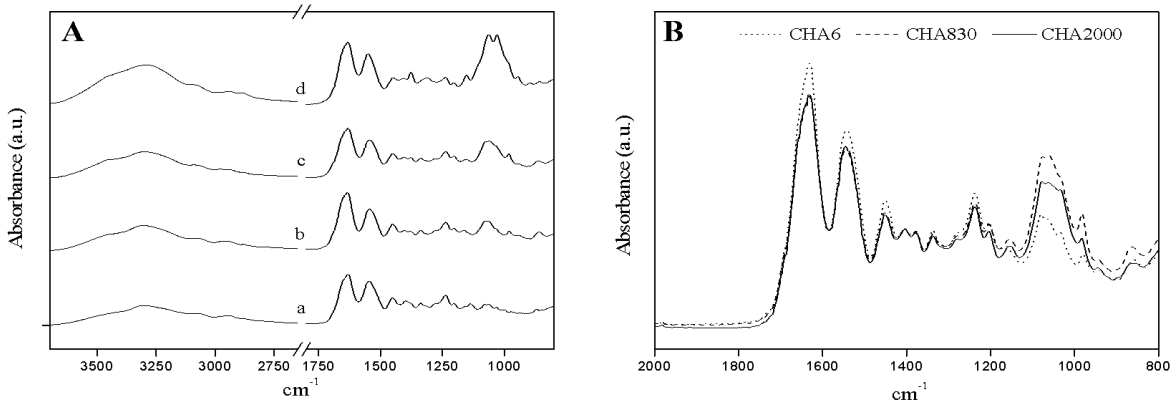

Figure 2. 5 Representative FTIR A) spectra of a) collagen, and EDAC cross-linked biopolymer matrices: b) collagen, c) CHA830, d) CHACS. B) normalised spectra of CHA6 (dot line), CHA830 (dashed line), CHA2000 (solid line)

The results from uniaxial tensile tests performed on the cross-linked biopolymer sponges showed increase in both the material elastic modulus and failure strain for CHA and CHACS specimens compared to the pure collagen sponge (Figure 2.6). Although amongst CHAs the modulus did not differ significantly, its values were higher for CHA830 and CHA2000 compared to CHA6 (Figure 2.6A). The elasticity of the composite matrices further increased with the addition of chitosan. Similarly, CHA specimens with higher Mw and CHACS displayed significant ($p<0.001$) increase in

the strain at break, while those of CHA6 were not considerably different from the cross-linked collagen (Figure 2.6B).

As the results for the genipin treated collagen indicated, cross-linking improves the elastic modulus of biopolymer materials, however negatively affecting their stretchability. To overcome this problem, hydrophilic in nature polymers could be used in a combination with cross-linking, resulting in increased water retention capacity and energy storage of the matrices, and consequently, higher stretchability and tensile strength [172]. This study confirms that the addition of polysaccharides, such as chitosan and high molecular weight hyaluronic acid into collagen-based matrices, in combination with chemical cross-linking is an efficient strategy to improve both elastic modulus and material stretchability.

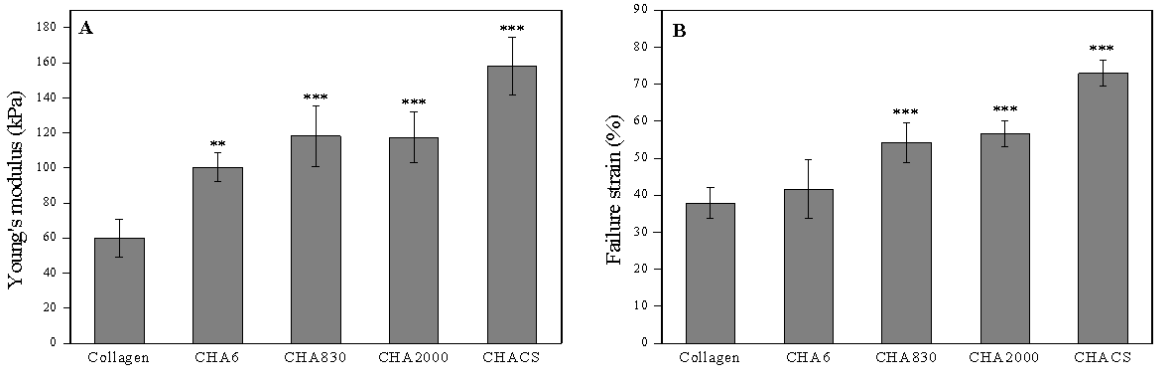

Figure 2. 6 A) Linear elastic (Young's) modulus and B) failure strain for the cross-linked, hydrated (PBS, pH 7.4) biopolymer composite sponges. Statistical differences are related to the collagen sponge and represented as **p<0.01 and ***p<0.001

Exploitation characteristics of cross-linked biopolymer composite sponges

In acute wounds the collagenases contribute to the controlled reconstruction of the damaged skin during wound closure and remodelling. In chronic wounds, however, their elevated levels cause uncontrolled breakdown of the newly formed ECM and impair the healing process. It is therefore crucial to maintain the collagenases active during the tissue reconstruction but interfere with their pathophysiologically persistent activation. One of the strategies for chronic wound treatment is based on the removal of these enzymes from the wound exudates by enzyme adsorption onto the dressing material [176]. Therefore, in this study the extent of collagenase binding onto the developed collagen-based sponges was evaluated *in vitro*.

Although in many cases collagenase adsorption onto collagenous substrates occurs within 1 h, the process is much slower on dense (e.g. cross-linked) matrices [71]. In order to assure equilibrium binding the biopolymer sponges were incubated for 24 h with the enzyme in concentration not causing degradation of the materials (2 μg/mL, results not shown), and the activity of the supernatants were further determined. All enzymatic solutions incubated with the sponges displayed lower activities

compared to the control, meaning that collagenase was adsorbed on all specimens (Figure 2.7A). As expected, the extent of binding decreased with the decrease of the substrate (collagen) content in the sponges. The protein adsorption on the cross-linked collagen was 52 %, while the addition of HA to the blends led to 38 % protein adsorption on CHA6, 22 % on both CHA830 and CHA2000, and only 9 % on CHACS sponges.

Despite that the extent of collagenase adsorption differed between the experimental groups, *in vitro* test for material biostability revealed similar (>95 %) resistance to collagenase (10 μg/mL) degradation for all cross-linked biopolymer sponges (Figure 2.7B). However, using higher enzyme concentration (60 μg/mL) made possible to distinguish between the enzymatic sensitivity of different experimental groups, the results being in agreement with the enzymatic adsorption tests. More than 30 % of the protein was digested from the pure collagen sponge, whereas the biostability of the sponges significantly increased after addition of HA and CS ($p<0.01$ for CHA6, $p<0.001$ for CHA830, CHA2000 and CHACS). Also, it is worthy to mention that even when higher enzyme concentration was used all sponges could preserve their structural integrity during incubation – an important property of a dressing material that allows for its easy removal from the wound site.

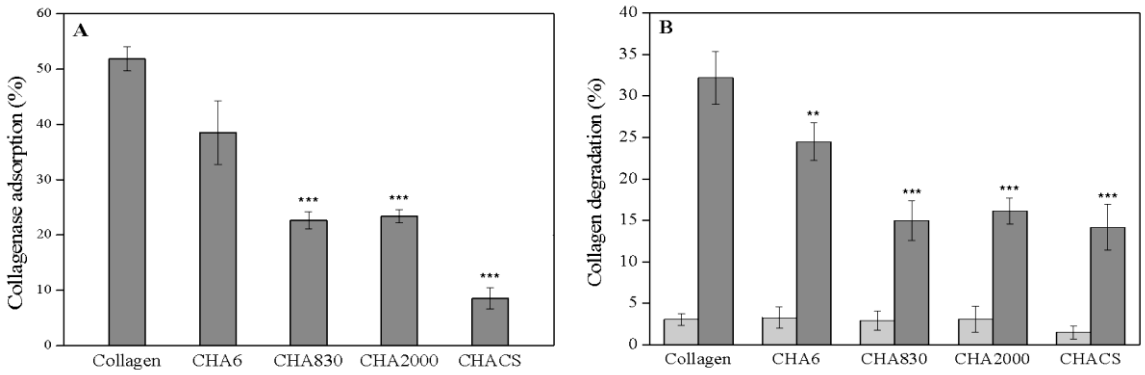

Figure 2. 7 A) Binding extent of collagenase onto the cross-linked collagen-based matrices and B) collagen proteolysis by 10 μg/mL (light grey bars) and 60 μg/mL (dark grey bars) collagenase from the cross-linked collagen-based matrices. Statistical differences are related to the collagen sponge and represented as **p<0.01 and ***p<0.001

It is known that the susceptibility of insoluble substrates, e.g. biopolymer matrices, to enzymatic transformations is inversely proportional to the cross-linking degree of the material. Higher cross-linking density of the substrate results in reduced surface area [169], lower accessibility of the enzyme to the binding sites and consecutively limited enzymatic adsorption and efficiency [177]. Thus, the inclusion of more cross-linking points (amino and carboxylic groups) by the addition of HA and CS to the collagen-based sponge resulted in improved biostability of the materials, but limited collagenase adsorption.

As already mentioned (see section 2.3.1), besides the extent of cross-linking in the matrix, the most important parameter influencing the swelling of the biopolymer constructs is the hydrophilicity of its constituents [174]. Again, owing to the diverse and dynamic nature of all chronic wounds, there is no general recommendation for the fluid uptake capacity of the corresponding dressings as long as the material maintains its form and stability after swelling to be easily removed from the wound site. In this study the addition of HA of different Mw to collagen altered differently the swelling of the CHA systems without causing a significant volume expansion of the specimens (Figure 2.8). While CHA6 did not differ from the cross-linked collagen in swelling, the addition of HA with higher molecular weights resulted in significant increase in fluid uptake ($p<0.01$ and $p<0.001$ for CHA830 and CHA2000, respectively).

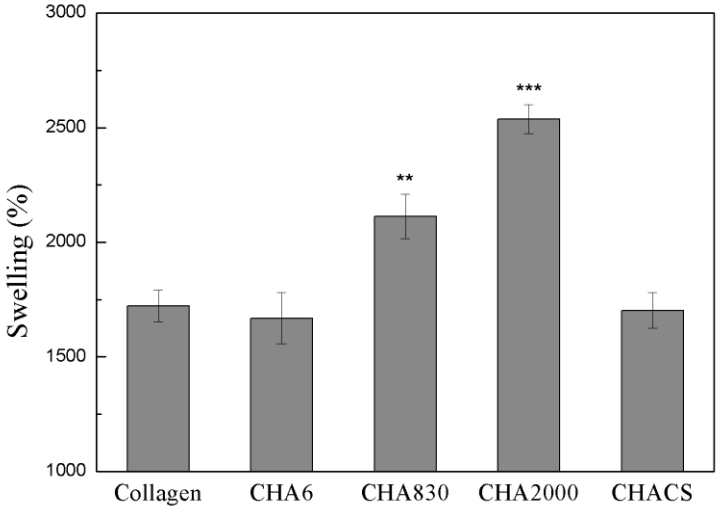

Figure 2. 8 Swelling of the cross-linked biopolymer matrices after 24 h incubation in PBS (pH 7.4). Statistical differences are related to the collagen sponge and represented as **p<0.01 and ***p<0.001

The presence of HA in collagen-based sponges is expected from one side to increase the swelling due to the high hydrophilicity of this polymer, but from another, to increase the cross-linking density of the system and affect negatively the swelling [166]. Although the results from the biostability test and collagenase binding studies indicated higher cross-linking densities in the specimens prepared with HA with longer polymer chains, the latter retained more fluid compared to CHA6. The high affinity of HA for physiological fluids originates from the high density of negative charges that bind a cloud of cations, most notably Na^+ (here from PBS), which are osmotically active and promote swelling [53]. In order to estimate the anionic character of HA used in the study, the ζ -potential of HA solutions were determined (Nano-ZS from Malvern, UK). These values for HAs of 6, 830 and 2000 kDa were -5.3 ± 1.2, -17.1 ± 2.2 and -16.6 ± 1.1 mV, respectively. Thus, it can be hypothesised that HA with higher Mw would retain more fluid compared to HA of low Mw and, in spite of its densely

cross-linked structure, would enhance the hydrophilic properties of CHA system. The addition of CS to CHA830 decreased the swelling capacity of the specimen due to further cross-linking reactions with the amino groups from CS [171].

2.4 Conclusions

Low stability of biopolymers in contact with chronic wound exudates requires the use of cross-linking agents to diminish the susceptibility of biopolymer-based dressings to enzymatic degradations. In this study two chemical cross-linkers were tested to improve bulk properties and biostability of freeze-dried collagen and various biopolymer composite sponges. Collagen sponges cross-linked with genipin displayed beneficial for the extracellular matrix reconstruction macroporous structure able to retain more than 10-fold of their own weight of physiological fluid without deformation. By varying the amount of genipin, tuning of the mechanical properties and biostability of the materials was achieved. On the other hand, biopolymer composite sponges comprised collagen-hyaluronic acid and collagen-hyaluronic acid-chitosan were stabilised with EDAC through amide- and ester-bond formation. The physico-mechanical properties of the bio-composites were easily adjustable by altering their polymer composition, i.e. through the formation of additional cross-links after collagen blending with hyaluronic acid and chitosan. Additionally, the composite sponges also exhibited improved biostability compared to the collagen one. Improved swelling was achieved only by addition of hyaluronic acid with higher molecular weights (830 and 2000 kDa).

Chapter 3

Biopolymer sponges loaded with plant polyphenols

3.1 Introduction

During the persistent inflammation in chronic wounds numerous mutually causative cellular events lead to overexpression of proteolytic and neutrophil-derived oxidative enzymes. For example, total MMPs activity, being predominantly collagenases, is up to 30-fold greater in chronic than in acute wound fluids [17], resulting in a protease/antiprotease imbalance and excessive breakdown of the ECM. The proteolytic damage of the tissue is further promoted by oxidation of the natural protease inhibitors with hypochlorous acid generated by myeloperoxidase [178]. It is believed that bringing the counts of the deleterious chronic wound enzymes down to the levels found in acute wounds would allow healing to progress through the restoration of the balance between molecule degradation and production [179]. Therefore, the multifactorial nature of the chronic wounds requires the use of active agents to interfere more efficiently at molecular level with the biochemical events governing the ECM breakdown. The latter can be achieved by topical application of bioactive molecules, e.g. enzyme inhibitors.

Polyphenolic structures present in plant extracts are lately gaining considerable medical significance due to their therapeutic properties coupled with low toxicity to animal cells [180]. As such, different polyphenolic compounds have been already reported as wound healing promoters [181, 182], accounted for their antioxidant activity [183]. Moreover, the propensity of these compounds to bind proteins presumably accounts for the fact that polyphenols were able to inhibit virtually every enzyme tested with *in vitro* [180]. The previous studies in the group indicated that by the application of *Hamamelis virginiana* (witch-hazel) polyphenolic extracts controlled inhibition of major chronic wound enzyme activities (myeloperoxidase and collagenase) could be achieved [184]. On the other hand, biopolymeric platforms are increasingly used for delivery of active compounds into the wound site. The ability of polyphenols to complex with proteins and polysaccharides could be exploited for improving the biopolymers stability to enzymatic degradation [185], in addition to upgrade of these platforms with an active agent.

This work aims to functionalise different biopolymer-based sponges developed in Chapter 2 by integrating *Hamamelis virginiana* extract or single polyphenolic units from *Camellia sinensis* to generate active chronic wound dressings. The capacity of such devices to address the persistent inflammation in chronic wounds was evaluated *in vitro* by inhibition of MPO, taking into account the continuous influx of this enzyme to the wound site and the duration of such effect. In addition, inhibition of collagenase was also assessed with an intention to achieve a dual effect: i) attenuation of the deleterious chronic wound proteolytic activity, and ii) additional stabilisation of the biopolymeric platforms.

3.2 Materials and methods

3.2.1 Sponges and reagents

Collagen sponges cross-linked with genipin and biopolymer composite sponges cross-linked with EDAC developed in Chapter 2 were used in this study. Highly purified MPO from human leukocytes (1550 U/mg solid, one unit will produce an increase in absorbance at 470 nm of 1.0 per min at pH 7.0 and 25 °C, calculated from the initial rate of reaction using guaiacol substrate) was purchased from Planta Natural Products (Austria). Collagenase from *Clostridium histolyticum* (277.50 U/mg solid, one unit liberates peptides from collagen equivalent in ninhydrin colour (at 570 nm) to 1.0 μmol of leucine in 5 h at pH 7.4 and 37 ºC in presence of calcium ions) and N-(3-[2-Furyl]Acryloyl)-Leu-Gly-Pro-Ala (FALGPA) were obtained from Sigma-Aldrich. If not indicated otherwise, all other reagents were of analytical grade purchased from Sigma-Aldrich and used as received.

3.2.2 Active agents - polyphenols

Purified single polyphenolic units from *Camellia sinensis* – epigallocatechin gallate (EGCG), catechin (CAT) and gallic acid (GA) – were purchased from Sigma-Aldrich (Scheme 3.1). *Hamamelis virginiana* stems were provided by Martin Bauer GmbH (Alveslohe, Germany). Phenolic extracts were obtained following the previously reported method [186]. The extraction was carried out by the colleagues in the group. Briefly, chopped stems of the plant were incubated in an acetone/water mixture for 24 h at room temperature. The solid was filtered off, and the acetone was evaporated at reduced pressure. The remaining solution was defatted with n-hexane, and the oligomeric fraction was extracted with ethyl acetate. After drying this organic phase under vacuum, the obtained pellet was dissolved in deionised water, and the solution was filtered through a porous plate. The organic dry fraction (OWH) was finally obtained by freeze-drying.

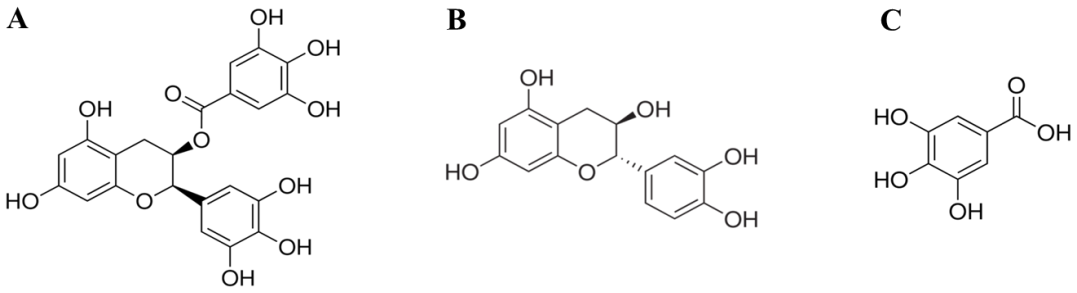

Scheme 3. 1 Structure of polyphenolic units from Camellia sinesis: A) EGCG, B) CAT and C) GA

3.2.3 Loading of the biopolymer sponges with polyphenols

The cross-linked sponges were loaded with polyphenols by immersing specimens of 10 mg into 1 mL of aqueous polyphenols solutions at 4 ºC for 24 h. The impregnation time was chosen according to the literature to assure equilibrium loading of the polyphenols [187]. Thereafter the samples were freeze-dried. Since the collagen sponge cross-linked with 1 mM genipin displayed the highest mechanical and enzyme stability among all samples studied, this specimen was chosen for loading with *Hamamelis virginiana* polyphenols. These polyphenols-loaded specimens were denominated as CG1P0.5, CG1P1 and CG1P2 (treated with 0.5, 1 and 2 mg/mL of polyphenols, respectively). On the other hand, due to the large number of experimental groups, for simplicity only collagen, CHA830 and CHACS specimens were loaded using 1 mM aqueous solutions of EGCG, CAT or GA.

3.2.4 Polyphenols binding onto the biopolymer sponges and release studies

The experiments for the release of *Hamamelis virginiana* polyphenols were conducted by immersing 10 mg of sample in 1 mL dH_2O at room temperature. At defined time periods 20 μL of solution were withdrawn and the polyphenols concentration was determined by the Folin-Ciocalteu's spectrophotometric method, measuring absorbance at 760 nm [188]. In the case of polyphenols single units the uptake by the sponges was estimated by comparison of the total phenol content in solution before and after incubation with cross-linked specimens. Moreover, their cumulative release was measured. The experiments for the cumulative release of polyphenols were started by immersing 5 mg of specimens in 500 μL dH_2O. At defined time periods the sponges were transferred into the same amount of fresh dH_2O. The total phenol content at each time point was determined as described above. The calibration curves were prepared using different concentrations of the corresponding polyphenolic extract/compounds.

3.2.5 Swelling behaviour of the biopolymer dressings

Cross-linked specimens impregnated with plant polyphenols were evaluated for their ability to absorb physiological fluid [166]. The sponges were first weighed (Wi) and then immersed in PBS pH 7.4 for 24 h. The swollen samples were withdrawn and weighed again without dripping (Ws). Their capacity to absorb physiological fluid was defined as the ratio between the retained fluid (Ws - Wi) and the dry weight of the sample (Wi). Five samples of each specimen were evaluated for swelling.

3.2.6 Biostability of the biopolymer dressings

Biodegradation tests were carried out *in vitro* by incubation of the dressings impregnated with polyphenols in 50 mM Tris-HCl (pH 7.4, with 40 mM $CaCl_2$) containing 60 μg/mL collagenase at 37 ºC for 24 h. After complete hydrolysis of the supernatants in 6 N HCl for 24 h at 90 ºC and neutralisation with 6 N NaOH, the Hyp content was determined by the method described by Reddy and Enwemeka [164]. The calculation was based on the assumption that collagen contains approximately 14 % Hyp [165].

3.2.7 Collagenase inhibition with polyphenols

Inhibition of collagenase activity was determined either by monitoring collagen degradation or cleavage of the specific collagenase substrate FALGPA using the enzyme pre-incubated with different polyphenols. For the polyphenolic extract from *Hamamelis virginiana* collagenase (10 μg/mL) was pre-incubated for 24 h at room temperature with different amount of polyphenols (0.2, 0.5, 1 and 2 mg/mL) in Tris-HCl buffer containing 100 mM $CaCl_2$ (pH 7.4). Subsequently, non-cross-linked collagen (10 mg) was treated with the pre-incubated enzyme for 24 h at 37 ºC. Hyp content of the resulting mixtures was analysed as previously described and the percentage of collagen degradation was determined. The enzyme inhibition was calculated as the difference in the percentage of collagen digestion by native collagenase and by polyphenols-incubated collagenase.

Inhibition of collagenase activity by single polyphenolic units from *Camellia sinensis* was determined using FALGPA as a substrate [189]. Collagenase (5 μg/mL) hydrolysis of FALGPA (1 mM) incubated with different concentrations of polyphenols for 1 h in 50 mM Tricine buffer (pH 7.5) containing 100 mM $CaCl_2$ and 400 mM NaCl, was monitored at 345 nm during 5 min. The results are expressed as the concentration required for the inhibition of 50 % FALGPA hydrolysis by collagenase (IC_{50}) ± standard deviation (n=3).

3.2.8 Myeloperoxidase inhibition assay

The inhibitory effect of the polyphenols and polyphenols loaded sponges on MPO activity was measured using guaiacol as a substrate. Different polyphenols concentrations were incubated for 1 h with MPO (0.60 U) and guaiacol (167 mM) buffered with 500 μL of 50 mM PBS pH 6.6 at 37 ºC. Thereafter, 270 μL aliquots were placed in a 96-well microplate and the enzymatic reaction was started by adding 30 μL of 10 mM H_2O_2. The change in absorbance at 470 nm was monitored and the activity determined by the rate of absorbance increase per min. The capacity of the polyphenols to inhibit MPO is expressed in IC_{50} values.

The inhibitory effect of the polyphenols released from the biopolymer sponges on MPO activity was determined after specimens (2 mg) incubation with the enzyme (0.60 U). After different incubation times the enzymatic activity was determined as described above and expressed as a percentage of enzyme inhibition compared to the control (sponges without polyphenols). All measurements were carried out in triplicate.

3.2.9 Cell viability, morphology and distribution

The sponges were sterilised by ethylene oxide and hydrated in PBS for 1 h before seeding with mouse NIH 3T3 fibroblasts or L929 human fibroblast-like cell lines (European Collection of Cell Cultures, UK) at 50000 and 100000 cells/sponge concentrations, respectively. The cultures were carried out in Dulbecco's modified eagle's medium (DMEM; Sigma-Aldrich, USA) supplemented with 10 % of fetal bovine serum (FBS, Biochrom AG, Germany) and 1 % antibiotic/antimycotic (Gibco, USA). Cells were cultured at 37 ºC under a humidified atmosphere of 5 % CO2.

For the genipin cross-linked collagen sponges, cell viability was evaluated using MTT (3-dimethylthiazol-2,5-diphenyltetrazolium bromide) colorimetric assay. After culturing the cells for 24 hours, the medium was removed, 10 % MTT solution (5 mg/mL in DMEM) was added to the cell monolayers, and the multi-well plates were incubated at 37 °C for another 4 h. After discarding the supernatants, the dark blue formazan crystals were dissolved by adding 100 µL of dimethylsulphoxide (DMSO) and quantified spectrophotometrically (Secomam, Anthelie light, version 3.8, Contardi, Italy) at 570 nm (n=3).

For the biopolymer composite sponges, cell viability was determined at 24, 48 and 72 h by CellTiter 96 Aqueous One Solution Cell Proliferation Assay (Promega, USA). The absorbance was measured at 490 nm using a microplate reader (Synergie HT, Bio-Tek, USA). Three samples of each specimen were characterised per time point.

3.2.10 Statistical analysis

All data are presented as mean values ± standard deviation. For multiple comparisons of composite sponges, statistical analysis by a one way analysis of variance (ANOVA) followed by post-hoc Tukey test was performed using Graph Pad Prism Software 5.04 for Windows (USA). Statistical significance was considered at $p < 0.01$.

3.3 Results and discussion

The multifactorial nature of all chronic wounds, characterised with prolonged inflammation and deleterious concentrations of oxidative and proteolytic enzymes, emphasizes the necessity for investigation of dressing materials with the ability to actively modulate the wound environment at molecular level and stimulate the healing. As a part of the immune response, MPO plays a major role in many diseases by catalysing the formation of the potent antimicrobial oxidant HClO from Cl^- in presence of H_2O_2. However, the persistent activity of MPO-H_2O_2 system during prolonged inflammation, such as in chronic wounds, and the consequent HClO accumulation at the wound site may adversely affect the tissue regeneration [190]. It is therefore essential that the chronic wound treatment include controlled MPO inhibition, which may also contribute to the control of the proteolytic activity [191]. Plant polyphenols exert their beneficial effect acting as both MPO inhibitors and MPO substrates, thereby deviating the enzyme from its catalytic cycle of HClO generation [184]. To this end, the cross-linked biopolymer-based sponges were impregnated with bioactive molecules, e.g. plant polyphenols, and evaluated *in vitro* as chronic wound dressings.

3.3.1 Collagen sponges loaded with *Hammamelis virginiana* polyphenols

Stability-at-use and swelling

Surprisingly, treatment with *Hamamelis virginiana* polyphenols (0.5 mg/mL) considerably increased the collagen degradation (65 %) by collagenase (60 μg/mL) compared to degradation of the cross-linked collagen without polyphenols (Figure 3.1), thus adversely affecting the stability-at-use of the dressing. On the other hand, when the samples were treated with higher polyphenols concentration the biostability was partially recovered. When 1 mg/mL polyphenols was used for loading collagen degradation decreased to 36 %, and further increasing concentration (2 mg/mL) resulted in 22 % collagen degradation.

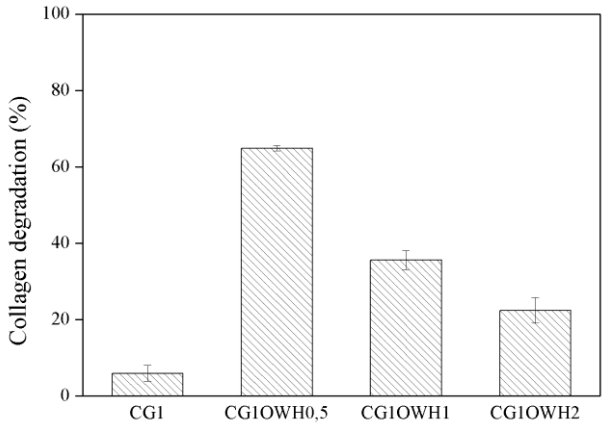

Figure 3. 1 Percentage of collagen degradation from the collagen sponges cross-linked with 1.00 mM genipin and further loaded with different polyphenols concentration (0.5, 1 and 2 mg/mL)

In order to clarify these findings, the protein degradation from uncross-linked collagen after treatment with collagenase pre-incubated with polyphenols was measured by released hydroxyproline. Collagenase incubation with polyphenols brought about dose dependent inhibition of the collagenolytic activity (Figure 3.2). The polyphenols (0.2 mg/mL) exhibited about 10 % collagenase inhibition measured by collagen degradation, whereas the inhibition of up to 73 % was achieved when the enzyme was pre-incubated with 2 mg/mL polyphenols.

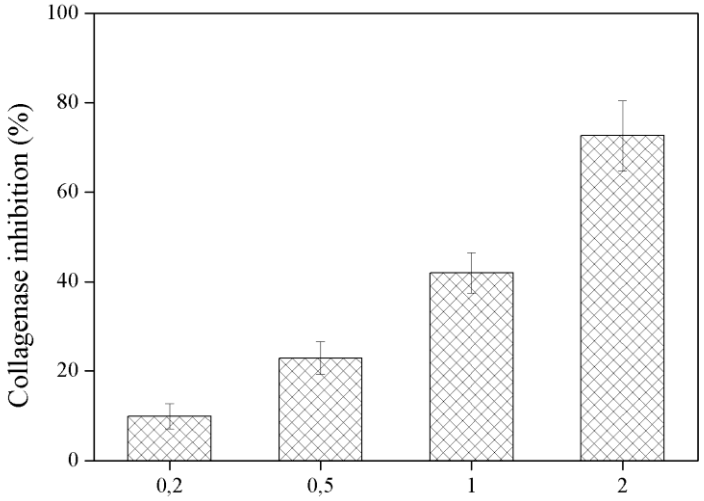

Figure 3. 2 The percentages of collagenase activity inhibition with polyphenols at different concentrations

The possibility that the polyphenols cleave the genipin bridges described in Chapter 2 is rather improbable. On the other hand, at pH 7.4 used in the study the structure of the *Hamamelis virginiana* polyphenols in the extract might be altered resulting in increase of the gallic acid content [186]. Unlike the other phenolic structures containing galloyl moiety, gallic acid does not promote collagen stabilisation [192]. Moreover, polyphenols organize along the collagen macromolecules interacting via hydrogen bonds and hydrophobic interactions [180]. It might be hypothesised that the interaction of the polyphenols with the cross-linked collagen matrix exerts a plasticising effect on the structure making it more accessible to enzymatic attack, thereby promoting increased collagen degradation. Nevertheless, higher concentrations of polyphenols were found to effectively inhibit the proteolytic degradation of collagen, and thus partially compensate the loss of biostability.

Moreover, due to the above mentioned nature of the polyphenols interactions with proteins it was not expected that their loading would significantly influence the swelling properties of the sponges, unlike the genipin covalent cross-linking. Some authors report even increase of the water binding capacity of collagen/phenolics aggregates [193]. In this study the genipin (1 mM) cross-linked sponges with or without polyphenols could all bind similar amounts of physiological fluid (results not shown).

Myeloperoxidase inhibition

All samples containing *Hamamelis virginiana* polyphenols showed efficient inhibition of MPO activity (Figure 3.3A) depending on polyphenol concentration, while inhibition was not observed with the cross-linked collagen control (result not shown). Large part of the activity was reduced within 1 h for all specimens used. It was also found that the MPO inhibition is related to the polyphenols release profiles from the cross-linked biopolymer platform (Figure 3.3B). Most of the polyphenols from the sponge treated with 0.5 mg/mL extract were released within the first hour. On the other hand, for the samples treated with 1 mg/mL and 2 mg/mL polyphenols, the release continued up to 3 days showing initial burst release followed by sustained release of small amounts of polyphenols (Figure 3.3C). Such duration of the active agent release corresponds to the need for less frequent changing of the chronic wound dressing.

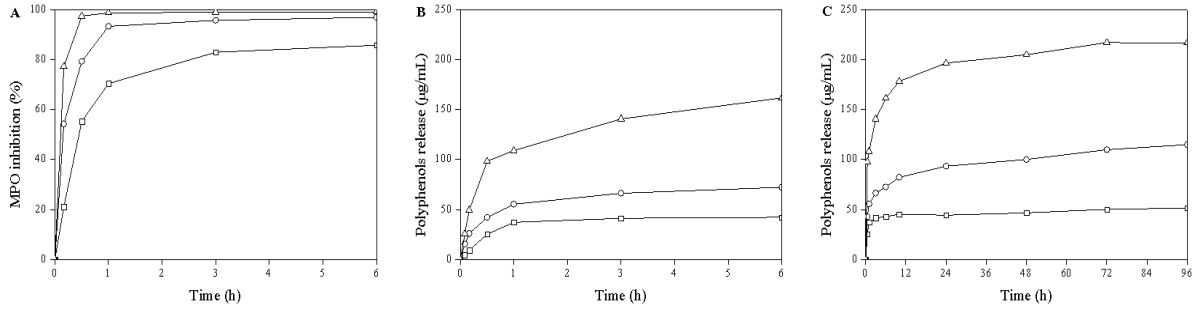

Figure 3. 3 Time-course inhibition of MPO by *Hamamelis virginiana* polyphenols released from the collagen-based sponges (A), and polyphenols release from the sponges within 6 h (B) and 96 h (C). Collagen sponges were cross-linked with 1 mM of genipin and further loaded with various polyphenols concentrations: 0.5 mg/mL (□), 1 mg/mL (○) and 2 mg/mL (Δ).

In addition to be an integral component of the innate immune response, the MPO plays major role in many diseases by catalysing the formation of HClO from Cl^- in the presence of H_2O_2, contributing to tissue damage during inflammation. As already mentioned, by controlling the activity of MPO in chronic wound site it is possible to control the levels of HClO and consequently the proteolytic activity. It is therefore essential that besides protease inhibition, the chronic wound healing approach include controlled MPO inhibition.

Cytotoxicity evaluation

MTT test showed good viability of NIH-3T3 mouse fibroblasts cultured in a medium which was previously in contact with the collagen, genipin cross-linked collagen and sponges loaded with various concentrations of polyphenols for 24 h (Figure 3.4). Nevertheless, a slight decrease in biocompatibility was observed after collagen cross-linking with 1 mM genipin and further after addition of polyphenols. Maximum reduction of 14 % of the fibroblast activity was observed for collagen cross-linked with genipin and loaded with 2 mg/mL polyphenols.

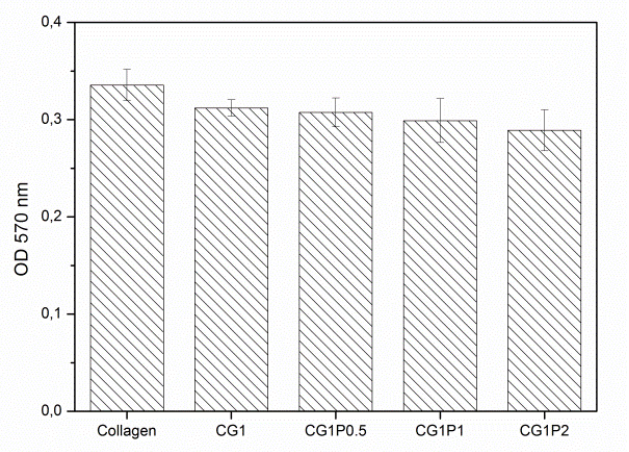

Figure 3. 4 Toxicity effects of uncross-linked, collagen cross-linked with 1 mM of genipin and cross-linked collagen sponges loaded with different polyphenols concentration (0.5, 1 and 2 mg/mL) on fibroblasts measured by MTT colorimetric assay at 24 h.

Although fibroblast cytotoxicity does not directly correlate with impairment of wound healing process in humans, the sensitivity of these cells gives insight to the biocompatibility of the systems. The MTT assay, a method to assess metabolic activity in cells, does not reflect cell death directly although it is accepted as an indicator for cytotoxicity measurements [194]. Usually up to 20 % reduction in cell viability is acceptable *in vivo* [192]. Since the decrease in fibroblast viability for all samples did not reach 20 %, it can be considered that the prepared sponges presented good biocompatibility profile for dermal applications. The cytotoxicity-provoking concentration usually exceeds by several folds the beneficial effects-providing concentration of phenolics [195, 196].

3.3.2 Biopolymer composite sponges loaded with green tea polyphenols

Stability-at-use and swelling

Unlike for the dressing materials treated with *Hamamelis virginiana* polyphenols, the treatment of the EDAC cross-linked biopolymer composite sponges with the single polyphenolic units from *Camellia sinensis* did not affect negatively the biostability of the materials against collagenase (60 μg/mL) degradation (Figure 3.5A). Specimens loaded with EGCG displayed the lowest degradation (less than 5 %) regardless to their biopolymer composition. Although not as efficient as EGCG, CAT also brought about significant increase in the dressing resistances to enzymatic degradation. In this case, the values for collagen degradation obtained for experimental groups with different biopolymer composition followed the same trend as in the case of dressings without polyphenols. Treatment with GA did not affect the materials biostability which is in good agreement with literature [192].

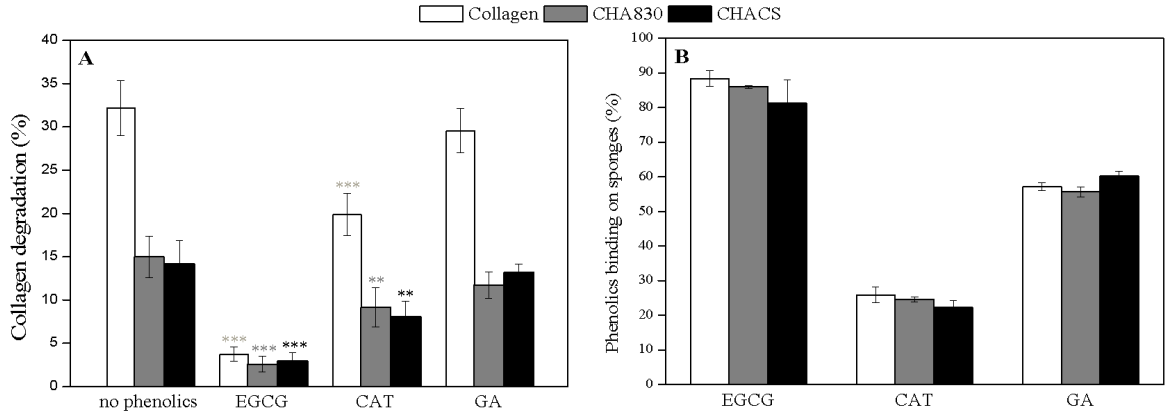

Figure 3. 5 A) Collagen proteolysis in cross-linked biopolymers matrices without and loaded with polyphenols by 60 μg/mL collagenase, and B) extent of polyphenols binding onto cross-linked specimens: Collagen (white bars), CHA830 (grey bars) and CHACS (black bars). Statistical differences in the biostability of the non-treated and polyphenols loaded specimens are represented as **p<0.01 and ***p<0.001, in light grey, dark grey and black if related to Collagen, CHA830 and CHACS, respectively

Some phenolic compounds exert a well-known improvement in the stability of protein/polysaccharide matrices towards enzymatic degradation through phenols-biopolymers interactions [185, 197] and enzyme inhibition [180]. In most cases, The extent of biostability improvement is proportional to the number of phenol moieties in the polyphenolic compound [187]. Thus, the highest potential of EGCG to stabilise biopolymer sponges could be related to its high number of phenolic groups able to react with the biopolymers (Figure 3.5B), and its highest potential for collagenase inhibition (Table 3.1). Although GA binds stronger to the sponges compared to CAT, the higher potential of CAT to inhibit collagenase still provided improved biostability of the materials. In conclusion, EGCG and CAT were found to effectively inhibit the proteolytic degradation of collagen, and thus have potential to partially compensate the loss of materials biostability.

Table 3. 1 IC_{50} values for collagenase inhibition by single unit polyphenols

Polyphenol compound	IC_{50} collagenase (μM)
EGCG	92±8
CAT	152±11
GA	298±23

On the other hand, loading of the biopolymer matrices with polyphenols did not cause changes in the swelling behaviour of any experimental group (results not shown). Their concentration used in this study (1 mM) was probably too low to influence the swelling capacity of the cross-linked sponges.

Myeloperoxidase inhibition and durability of the inhibition effect

Since the inhibition of MPO activity by biopolymer platforms loaded with *Hamamelis virginiana* polyphenols was related to their release profile, the MPO inhibition caused by the released single unit polyphenols was also investigated *in vitro*. In this case, in order to simulate the chronic inflammation, i.e. continuous influx of neutrophil derived MPO to the wound site, at each reading point the incubation solutions were replaced with new solutions containing the fresh enzyme. Thus, the MPO inhibition in each reading point corresponds only to the effect of the polyphenols released between the two reading points. The durability of such effect was evaluated up to six days.

Table 3. 2 IC_{50} values for MPO inhibition by single unit polyphenols

Polyphenol compound	IC_{50} MPO (μM)
EGCG	15±1
CAT	21±2
GA	29±1

Although CAT reduces stronger than GA the MPO activity (Table 3.2), the lowest extent of CAT binding on the materials (Figure 3.5B) might have led to the least efficient initial MPO inhibition with CAT-loaded dressings (Figure 3.6). Moreover, except for CAT-loaded collagen, all GA- and CAT-loaded dressings inhibited MPO during only up to 6 h despite that their release continued after this point (Figure 3.6B,C). The possible reasons for such short period of efficiency could be: i) a large part of the active agent was released within the first few hours as in the case of CAT-loaded sponges (Figure 3.6B inset), and ii) the initial burst release was followed by a slow release of phenolics, apparently insufficient to achieve an inhibitory effect as in the case of GA-loaded sponges (Figure 3.6C inset). On the other hand, the pattern for EGCG was of initial burst release followed by a sufficient for MPO inhibition sustained release (Figure 3.6A inset). The inhibitory potential of EGCG-loaded systems was also due to the high binding affinity of EGCG onto the biopolymer sponges.

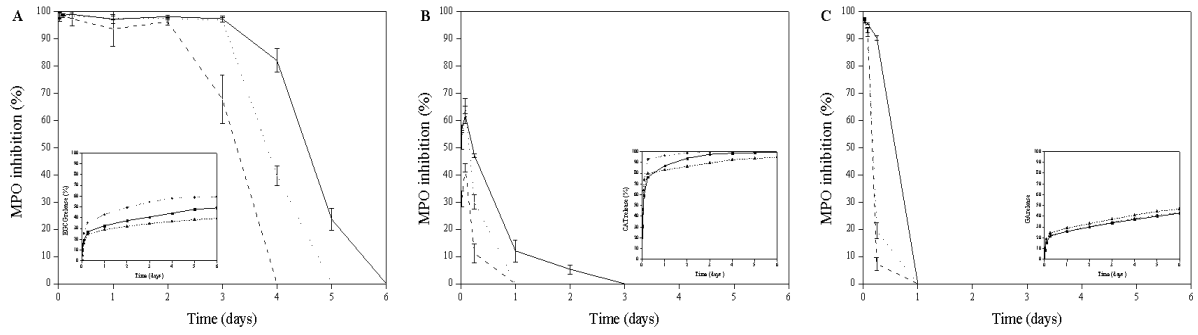

Figure 3. 6 Time-course inhibition of MPO by polyphenols: A) EGCG, B) CAT and C) GA released from the cross-linked Collagen (solid line), CHA830 (dot line) and CHACS (dash line). The inset graphs show the polyphenols release patterns from the corresponding biopolymer composite matrices.

Finally, the EGCG released from CHACS sponge maintained the MPO inhibitory capacity up to 3 days, whereas when released from CHA830 and collagen alone the effect was prolonged up to 4 and 5 days, respectively (Figure 3.6A). Strong complexation of polyphenols with chitosan at neutral pH was possibly the reason for the slowest release pattern from CHACS sponge [197].

In vitro evaluation of cell viability and morphology

Although fibroblasts were metabolically active on all biopolymer matrices over the studied period, some differences were observed among the experimental groups at the end of 72 h (Figure 3.7). The results clearly demonstrated the effect of the HA molecular weight on the cells viability: while there was no significant difference in viability after adding low molecular weight HA (6 kDa), the values were significantly ($p<0.001$) lower for the sponges containing longer HA chains (CHA830, CHA2000 and CHACS). Moreover, the cells cultured in contact with the collagen, CHA6 and CHACS sponges showed progressive increase in their metabolic activity during the whole period of culture. However, the addition of HA with higher molecular weight (CHA830 and CHA2000) resulted in an increase of the metabolic activity only during the first 48 h, which then was maintained or decreased. The reduced cell viability in the specimens containing longer HA chains can be assigned to their increased hydrophilicity related with reduced fibroblast cell growth [198]. On the other hand, this study confirms that different molecular weights of HA can be used to tune cell differentiation [199] and rule different cell responses [200].

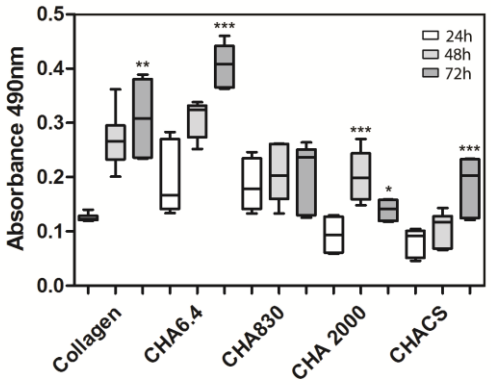

Figure 3. 7 Time-course evaluation of fibroblasts metabolic activity using MTS assay. Statistical differences are represented as * $p<0.05$, ** $p<0.01$ and *** $p<0.001$

SEM analysis showed that adherent cells could be observed on all cross-linked sponges at the end of the culture period – 72 h (Figure 3.8). It is worthy to notice the different morphology of the cells on different specimens: when cultured on collagen sponge, fibroblasts show typical spindle morphology, establishing several contacts with neighbouring cells. More elongated cells are visible on CHA6 and

CHA830, while round cells indicating a poor attachment to the surface of the sponge are observed for CHA2000 and CHACS. The amount of cells detected in CHACS sponges is remarkably lower when compared to the other specimens, due to the presence of chitosan in the formulation, related with the poor cell adhesion [44].

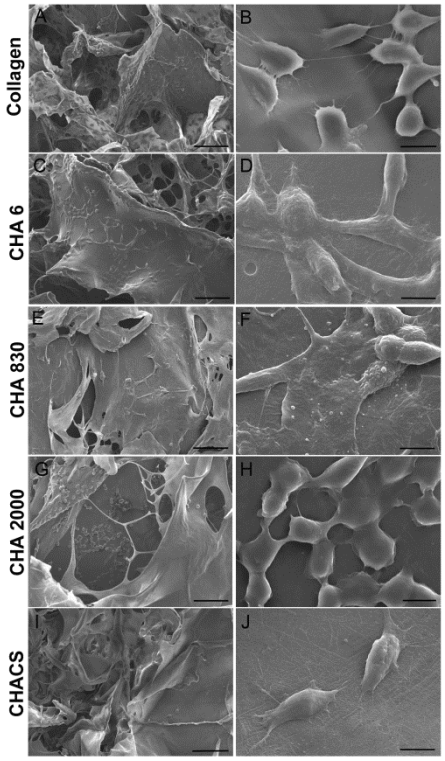

Figure 3. 8 Morphology of the fibroblasts cultured for 3 days onto cross-linked Collagen (A-B), CHA6 (C-D), CHA830 (E-F), CHA2000 (G-H), CHACS (I-J). Scale bars correspond to 100 µm (left-side images) and 10 µm (right-side images).

Finally, the cytotoxicity of the biopolymer composite sponges before and after loading them with the polyphenols was compared. Generally, the loading of the sponges with polyphenols in the concentration used (1 mM) did not induce significant difference in the cytotoxicity of the matrices; the only significantly lower metabolic activities ($p<0.01$) were found for the cells cultured on the GA-loaded composite sponges (Figure 3.9). Thus, the overall results for the biocompatibility demonstrated that the composition of the biopolymer-based material can have stronger influence on cell viability than functional polyphenolic compounds *per se*.

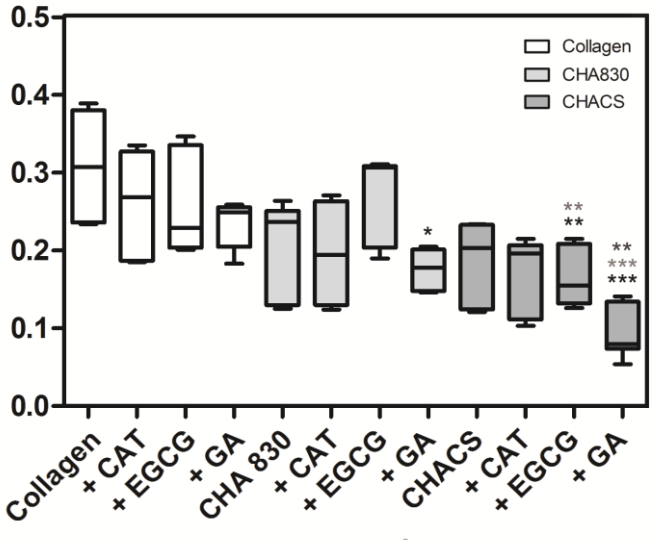

Figure 3. 9 Effect of the polyphenols loaded sponges on fibroblasts viability after 3 days in culture. Statistical differences are represented as * p<0.05, ** p<0.01 and *** p<0.001, in black, light grey or dark grey, if related to Collagen, CHA830 or CHACS, respectively.

3.4 Conclusions

An efficient chronic wound treatment approach requires the application of stable-at-use biocompatible dressing platforms upgraded with active functions for the control of the inflammation-related enzymatic activities at the wound site. To this end, chemically cross-linked collagen and biopolymer composite sponges comprising collagen-hyaluronic acid and collagen-hyaluronic acid-chitosan (obtained in Chapter 2) were functionalised by impregnating them with natural bioactive compounds, e.g. *Hamamelis virginiana* extract and single polyphenolic units from *Camellia sinensis*. Whereas the polyphenols incorporation did not affect swelling behaviour of any of the cross-linked specimens, their biostability was differently altered. Impregnation of *Hamamelis virginiana* extract to collagen sponge induced its higher susceptibility to collagenase digestion. This negative effect could be diminished by using higher polyphenols concentrations to inhibit proteolytic degradation of collagen. An efficient myeloperoxidase inhibition (within 1 h) occurred due to the initial burst release of the polyphenolic extract from the collagen-based platform. Nevertheless, sustained release of the extract was observed over three days, indicating the prolonged active function of such dressing. On the contrary, all biopolymer composite sponges loaded with EGCG and CAT (but not GA) exhibited improved biostability to collagenase degradation compared to non-treated materials. As expected, these dressings efficiently inhibited the inflammation-related MPO activity *in vitro*. The duration of the MPO inhibition effect could be tuned by the biopolymer composition of the materials and proper selection of the polyphenolic compound.

Section C

Thiolated biopolymers and derived functional nanomaterials

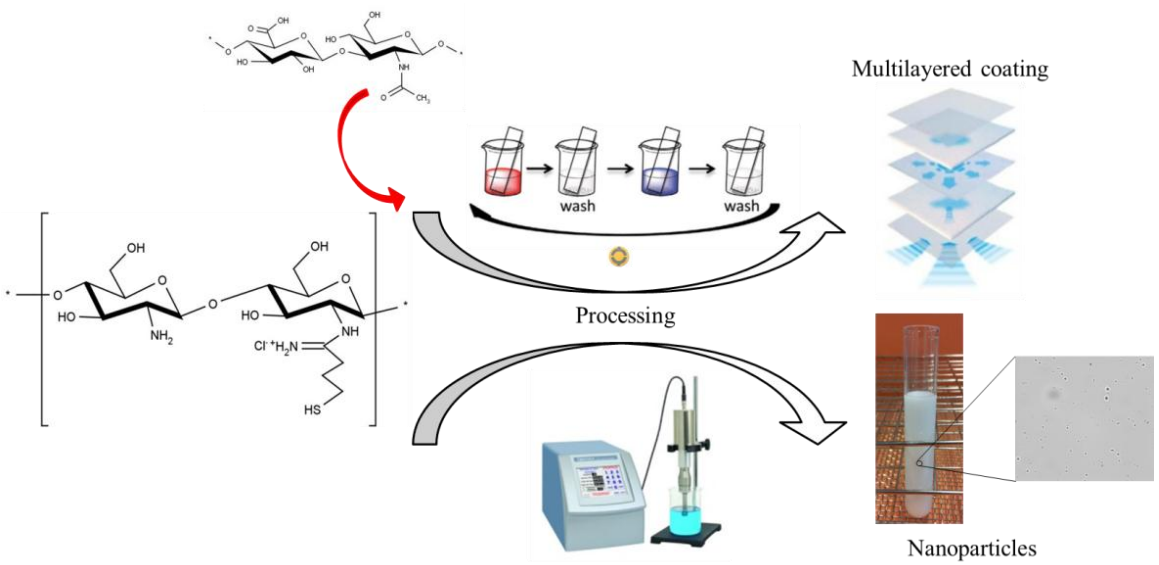

Chapter 4

Thiolated biopolymers

4.1 Introduction

While acute wound healing can be enhanced by dressings based on a single biopolymer or their blends, the persistent inflammation related with aberrant expression of myeloperoxidase and MMPs in chronic wounds must be treated differently. Some dressings on the market combine biopolymers with therapeutics, most of them antimicrobials on an empirical basis. However, the need to heal chronic wounds faster will require the development of biopolymer-therapeutic combinations acting on specific molecular targets in wound environment. Functionalisation of biopolymer platforms with wound healing promoting agents means development of active dressings able to counteract the chronic wound pathogens (e.g. deleterious enzymes).

The activation/inhibition of MMPs (e.g. collagenase) could be regulated by oxidation/reduction of the cysteine ligand coordinating Zn^{2+} in the enzymes active centre using thiol compounds [74], or non-specifically with the same functionality through metal chelation [75]. In addition, these versatile compounds were reported to inhibit the human myeloperoxidase [79], directly involved in the regulation of MMPs activity [191]. Thus, thiol-functionalised biopolymers should be able to control both collagenase and myeloperoxidase activities through different mechanisms. In line with this, due to their reactivity biopolymers can be easily modified via chemical techniques through covalent grafting of a bioactive agent. In such cases the active function would act from the polymer matrix, without release to the wound.

This work focuses on permanent modification of two biopolymers, chitosan and aminocellulose, by immobilisation of different thiol bearing compounds and optimisation of the protocols in order to achieve the maximum thiolation yields, i.e. the amounts of free thiols immobilised onto the polymer backbone. The effect of the thiolated conjugates, e.g. chitosan, on the chronic wound enzyme activities was evaluated *in vitro*. To this end, the rate inhibition of myeloperoxidase and collagenase activities as a function of the chitosan modification degree was investigated.

4.2 Materials and methods

4.2.1 Biopolymers and reagents

Ultra-pure chitosan (~50 kDa) was obtained from KytoZyme. Aminocellulose conjugate (Scheme 4.1) was prepared by nucleophilic displacement reaction of p-toluenesulfonic acid ester of cellulose (cellulose tosylate) with ethylendiamine (EDA) and characterised by means of NMR at the Centre of Excellence for Polysaccharide Research, Friedrich Schiller University of Jena, Germany, and kindly provided as 1 % aqueous solution with pH~9.2.

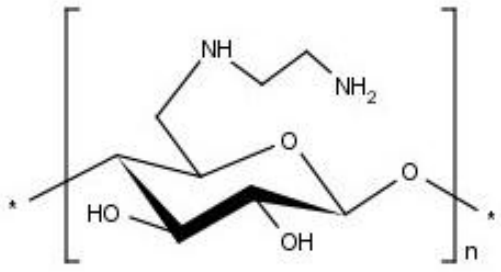

Scheme 4. 1 Schematic representation of aminocellulose structure

Reagents for thiolation used were: 2-Iminothiolane hydrochloride (Traut's reagent) and imidoester cross-linker - dimethyl 3,3'-dithiobispropionimidate dihydrochloride (DTBP). Dithiothreitol (DTT) was used to cleave disulphide bond in DTBP-cross-linked biopolymer to obtain free thiols. 5,5'-dithiobis (2-nitrobenzoic acid) - Ellman's reagent was used for quantification of free thiol groups immobilised onto biopolymer backbones. Highly purified MPO from human leukocytes (1550 U/mg solid, one unit will produce an increase in absorbance at 470 nm of 1.0 per min at pH 7.0 and 25 °C, calculated from the initial rate of reaction using guaiacol substrate) was purchased from Planta Natural Products (Austria). FALGPA was obtained from Sigma-Aldrich. All other reagents were of analytical grade purchased from Sigma-Aldrich and used as received.

4.2.2 Chitosan thiolation

The synthesis of thiolated chitosan (TC) was carried out in a one-step coupling reaction between 2-iminothiolane HCl and primary amino groups of chitosan, according to Bernkop-Schnürch et al. [109]. Briefly, chitosan was dissolved in CH_3COOH (1%, v/v). The pH of the solution was adjusted to 6 with NaOH (5 M) Traut's reagent added and the solution was stirred overnight at closed vessel in dark. The resulting mixture was dialysed two times for 24 h against 1 mM HCl containing NaCl (1 %) and finally for three days in 1 mM HCl. Dialysed products were freeze-dried and stored at +4 °C until

further use. Batches differing in the thiolation degree were prepared altering the amount of the coupling reagent in the reaction mixture and the thiolated conjugates were designated accordingly (Table 4.1).

Table 4. 1 Denomination of the thiolated chitosan conjugates

Thiolated specimen	Chitosan:2-iminothiolane HCl (w/w)
Chitosan	-
TC10-1	10:1
TC5-1	5:1
TC5-2	5:2
TC2-1	2:1

4.2.3 Synthesis of thiolated aminocellulose

The thiolation of aminocellulose was achieved by cross-linking with disulphide containing homobifunctional imidoester - DTBP and subsequent cleavage of disulphides with DTT. The thiolation protocol was optimised for obtaining the highest amount of free thiol groups onto the biopolymer, in terms of DTBP concentration and pH of the reaction.

Optimisation of the imidoester concentration

Aminocellulose solution (5 mL) of was brought to pH 8 with 1 M HCl. DTBP was added at different concentrations, pH readjusted to 8 and reaction allowed to proceed in closed tubes at room temperature for 30 min. To stop the reaction pH was dropped to 3 and thereafter 150 mM of DTT was added, pH adjusted to 7 and the solutions were left 45 min at 37 ºC for disulphide reduction. The resulting mixture was dialysed 2 times against 3 L of 1 mM HCl solution for 24 h, and finally extensively against 1 mM HCl for three days. The products were then freeze-dried. Control sample was prepared the same way just omitting imidoester.

Optimisation of the reaction pH

Aminocellulose conjugate was brought to the desired pH (7, 8 and 9) with 1 M HCl and DTBP was added in the final concentration 5 mM. Thereafter, the reaction protocol described above was repeated. Control sample was prepared at pH 3 to assure that the imidoester does not react with primary amines from aminocellulose.

4.2.4 Quantification of the thiol groups immobilised onto biopolymers

The amount of free thiol groups immobilised on biopolymers was determined spectrophotometrically using Ellman's reagent. First, 1 mg of specimen was hydrated in 500 μL of 0.5 M phosphate buffer (PB), pH 8.0 and then 500 μL of Ellman's reagent solution (3 mg of the reagent dissolved in 10 mL PB) was added. The samples were incubated for 3 h at room temperature in dark. After centrifugation (5000 rpm, 5 min), the absorbance was measured at 450 nm. L-cysteine standards were used to build the calibration curve.

Sulphur elemental analysis (EuroVector 3011 CHNS Elemental Analyzer, Italy) was performed to determine total sulphur content in the conjugates.

4.2.5 ζ-potential measurements

The ζ-potential of the chitosan some and thiolated chitosan solutions was determined at 25 °C (Nano-ZS from Malvern, UK) after the appropriate dilution of conjugates in ultrapure-grade water. The instrument was previously calibrated with a ± 66 mV latex standard.

4.2.6 Enzymes assays

The inhibitory effects of thiolated chitosan (2 mg) on collagenase and MPO activities were measured by the same methods applied in Sections B 3.2.7. and B 3.2.8.

4.3 Results and discussion

4.3.1 Thiolated chitosan

2-Iminothiolane HCl is a compound that reacts with primary amines to add a small spacer arm (8.1 Å) terminated by a free sulfhydryl group. The reaction is well established for the modification of proteins [201]. On the other hand, it can be applied for modification of other biopolymers, being especially efficient with those bearing comparatively much more amino groups than proteins. The advantage of Traut's reagent over other thiolation compounds is that its sulphhydryl group is not in the free form, in which it is sensitive to air oxidation [202], but rather forms part of the cyclic thioimidate. Other advantages include one-step coupling with amines from polymers to immobilise free thiol groups, mild reaction conditions and improved cationic character of the conjugate polymers due to the established amidine linkages (Scheme 4.2) [1]. The latter was confirmed by ζ-potential measurements (Table 4.2).

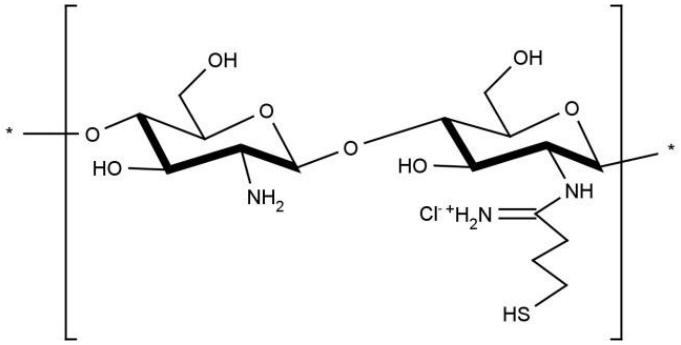

Scheme 4. 2 Proposed structure of the obtained thiolated chitosan [1]

Table 4. 2 ζ-potential of some thiolated chitosan solutions (0.5 mg/mL) prepared in 0.15 M NaCl, pH 5.5

Specimen	ζ-potential (mV)
Chitosan	6.97±0.50
TC10-1	13.20±0.46
TC5-2	13.30±0.94

The sulphur content in the samples (Table 4.3) increased with the increase of 2-iminothiolane HCl concentration, demonstrating a successful coupling with chitosan. Between 31 and 43 % of the total sulphur content was in the form of disulphide bridges, oxidised during the time consuming dialysis step of the conjugates preparation.

It is also worthy to notice that the ζ-potential values (Table 4.2) increased with the chitosan thiolation independently of the degree of the modification (Table 4.3). Thus, the cationic character of the thiolated chitosan did not depend on the percentage of the polymer thiolation, but rather on the modification itself.

Table 4. 3 Total sulphur content, percentage of free thiol groups, and disulphide content in the obtained thiolated chitosan conjugates

Specimen	Total sulphur content (%, w/w)	Free thiol groups (μmol/g of conjugate)	Free thiol groups (% of total S)	S-S (% of total S)
Chitosan	-	-	-	-
TC10-1	2.08	158±8	61	39
TC5-1	3.61	288±4	69	31
TC5-2	5.43	515±53	60	40
TC2-1	5.82	582±35	57	43

4.3.2 Thiolated aminocellulose

The thiolation of aminocellulose was achieved in the reaction with homobifunctional -S-S- bearing imidoester cross-linker – DTBP and subsequent cleavage of disulphides with DTT (Scheme 4.3). The imidoester functional group is one of the most specific acylating groups available for the modification of primary amines and has minimal cross reactivity towards other nucleophilic groups [203]. This reaction has been used previously to cross-link proteins, e.g. for stabilisation of collagen matrices [204]. Unlike the modification with Traut's reagent, the reaction products obtained in the reaction with the imidoester do not alter the overall charge of the polymer [205]. Imidoesters react with primary amines at pH 7-10.

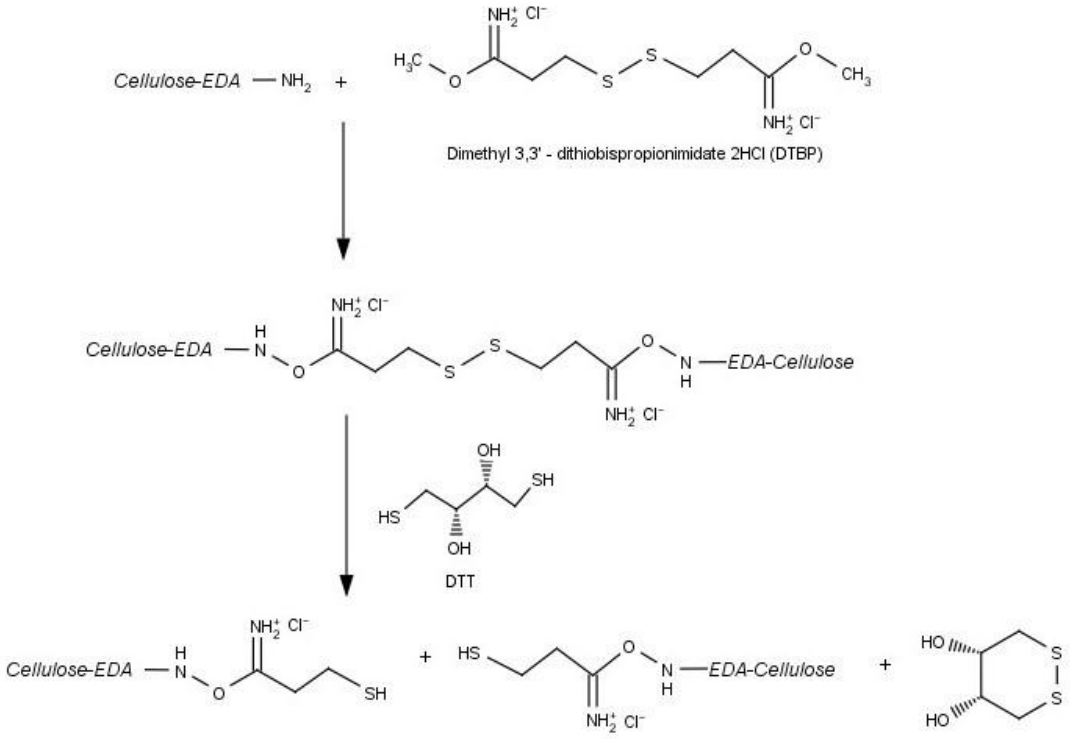

Scheme 4. 3 Synthetic pathway for thiolation of the aminocellulose conjugate

The protocol was firstly optimised in terms of the reagent concentration. To this end, different concentrations of DTBP were used for the modification while pH of the reaction was kept constant. Results indicated a good correlation between increasing DTBP concentration in the range of 0.5 – 5 mM and free thiol groups immobilised onto EDA-cellulose (Figure 4.1). Further increase of DTBP concentration (10 mM) did not result in the higher thiolation grade of the conjugate. Therefore, 5 mM concentration was chosen to carry out the further experiments.

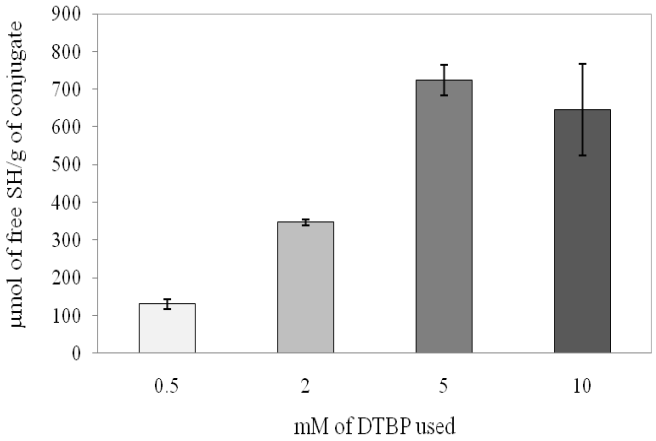

Figure 4. 1 Amount of free thiol groups immobilised onto EDA-cellulose prepared using different concentrations of DTBP

The thiolation protocol was also optimised in terms of the pH of the cross-linking reaction, where the concentration of 5 mM of DTBP was kept constant. Control sample was prepared at pH 3, in which no thiol groups were detected confirming that the reaction is not possible at lower pH (Figure 4.2). In this experiment, the highest thiol content of 694±31 μmol/g of conjugate was found for the specimen prepared at pH 8 followed by the sample prepared at pH 7 (358±9 μmol/g) and at pH 9 (289±6 μmol/g). Therefore, pH 8 and 5 mM of DTBP were chosen as the optimal to yield the highest amount of free thiol groups immobilised onto the biopolymer backbone.

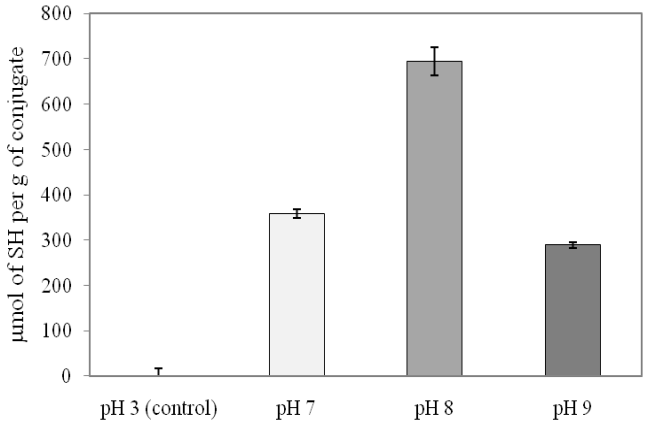

Figure 4. 2 Amount of free thiol groups immobilised onto EDA-cellulose prepared at different pH

Finally, the reproducibility of the thiolation protocol used has been evaluated. For this purpose the thiolation has been repeated three times and the aminocellulose modification degrees have been compared. No substantial differences have been found comparing the amount of free thiol groups immobilised onto the aminocellulose in three independent experiments. Thus, the thiolation protocol used had good reproducibility (Table 4.4).

Table 4. 4 Amount of free thiol groups immobilised onto aminocellulose prepared using the same reaction conditions for three independent experiments

Experiment	DTBP concentration (mM)	Reaction pH	–SH (mmol/g conjugate)
1	5	8	699±15
2	5	8	724±40
3	5	8	694±31

4.3.3 Effect of thiolated chitosan on myeloperoxidase and collagenase activities

The identification of elevated levels of oxidative MPO and matrix degrading proteolytic MMPs in chronic wound fluids [17, 206] led to a considerable interest for these enzymes as potential therapeutic targets [207, 208]. The product of the MPO-induced oxidation of physiological chloride in the presence of H_2O_2 is the potent antimicrobial oxidant HClO. However, the persistent activity of the MPO-H_2O_2 system may adversely affect the tissues under pathological conditions. The accumulated HClO is able to oxidatively modify lipids, DNA and (lipo)proteins by halogenation, nitration and oxidative cross-linking. On the other hand, collagenases are able to hydrolyse the triple helical regions of collagen under physiological conditions during many repairing processes. Therefore, it is crucial to maintain MPO and MMPs active during the host defence (MPO induces HClO generation needed for the bacterial killing) and reconstruction of the ECM (involving collagenases), but interfere with their pathophysiologically persistent activation.

Some authors reported thiolated polymers as efficient inhibitors of zinc-dependent enzymes through metal chelation [209]. However, others found that the binding tendency of thiols immobilised onto polymers in solution is not high enough to develop effective ion depletion from the active sites of enzymes, unlike when such systems are applied as coating components due to different polymer chains rearrangement [210].

The thiolated chitosan conjugates obtained in this work were able to inhibit the activity of MPO in solution (Figure 4.3). Moreover, the degree of MPO inhibition could be tuned by the percentage of the chitosan thiolation. However, no reduction of collagenase activity by thiolated conjugates was found measured using FALGPA as a substrate (results not shown). Furthermore, the IC_{50} values for MPO and collagenase inhibition by 2-iminothiolane HCl were of 85 ± 2 μM and 24 ± 3 mM, respectively.

This large difference indicates that chitosan with much higher thiolation grade is needed to inhibit collagenase in solution and to be detected by the enzymatic assay used.

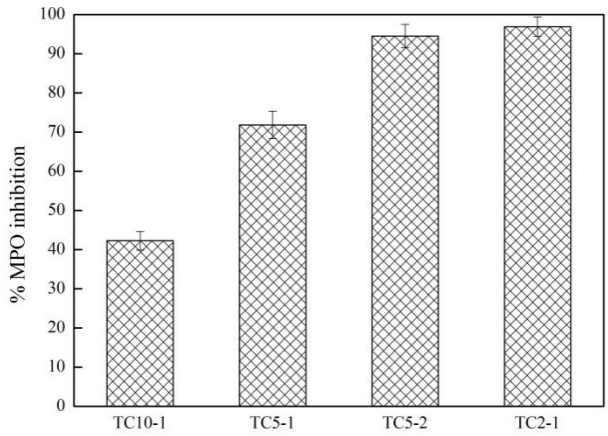

Figure 4. 3 Effect of thiolated chitosan conjugates on MPO activity measured with guaiacol as substrate

4.4 Conclusions

Permanent modification of chitosan and aminocellulose to introduce free thiol groups has been achieved using different chemical approaches. In the first, chitosan was thiolated in a one-step coupling with 2-iminothiolane HCl. Total sulphur content as well as the amount of free thiol groups immobilised on the conjugates depended on the amount of the reagent used for the reaction. On the other hand, thiolation of aminocellulose was carried out in two steps, by cross-linking of the polymer with disulphide containing imidoester and subsequent reduction of -S-S- bridges with dithiothreitol. The thiolation protocol was optimised in terms of the imidoester concentration (5 mM) and pH of the cross-linking reaction (pH 8). Preliminary results show that the thiolated conjugates are efficient myeloperoxidase inhibitors, where the extent of inhibition could be controlled by the degree of the polymer modification. However, no reduction of collagenase activity by thiolated conjugates was found.

Chapter 5

Functional nanocoatings based on thiolated chitosan

This chapter is based on the following publication:

1. **Francesko A**, Soares da Costa D, Lisboa P, Reis RL, Pashkuleva I, Tzanov T (2012) GAGs-thiolated chitosan assemblies for chronic wounds treatment: control of enzyme activity and cell attachment. *Journal of Materials Chemistry* 22, 19438-19446

5.1 Introduction

Most of the approaches for chronic wounds management are based on the topical application or the release of active compounds from the dressing platforms into the wound [211]. Despite some of the approaches include controlled release of active agents [25] the biggest concern, however, remain the side effects due to the accumulation of immunoreactive compounds at the wound site [26], i.e. overdoses. The permanent immobilisation of the active agents on the surface of the dressing would prevent from overdoses in clinical application. On the other hand, the modification of surfaces is nowadays a key aspect in biotechnology including development of substrates for regenerative medicine [212]. By alteration of the surface functionality controlled chemical and biological interactions can be achieved [213].

This study aims in development of a functional coating able to control the activities of deleterious proteolytic enzymes found in chronic wounds through specific surface interactions for promoting the healing process. To this end, the thiolated chitosan prepared in Chapter 4 was used to build PEM structures by assembling with the GAGs, chondroitin sulphate (CSU) and hyaluronic acid, as counterions. The preparation of such assemblies through layer-by-layer approach is a convenient technique for surface functionalisation and to impart specific surface bio-activity towards e.g. proteins and cells [214, 215]. From a technological point of view, the alternate deposition of oppositely charged polymers represent a simple way for surface modification, while rendering it suitable for the interaction with biological tissues in a relatively predictable way [216]. Moreover, control of the physicochemical and biological properties of multilayer coatings/films can be achieved by adjusting the process parameters such as pH, layer number, cross-linking and nature of the outermost layer [217].

To this end, the capacity of the fabricated multilayered structures for removal of collagenase from biological fluids by enzymatic adsorption was evaluated *in vitro*. Build-up of the coatings onto gold surfaces was assessed in situ by quartz crystal microbalance with dissipation (QCM-D). Since no inhibition of collagenase could be detected using spectrophotometric assay (Chapter 4), QCM-D was also used to study the affinity of collagenase towards surfaces coated with thiolated chitosan. Finally, the nature of the outermost layer was investigated in terms of fibroblasts adhesion and proliferation.

5.2 Materials and methods

5.2.1 Polyelectrolytes and reagents

Hyaluronic acid with different Mw (6 kDa, 830 kDa and 2000 kDa) from Lifecore Biomedical (USA) and the sodium salt of chondroitin sulphate (~20 kDa, DS 0.9) kindly supplied by Innovent (Germany) were used. Medical grade chitosan (~50 kDa, DDA 87 %) from Kitozyme (Belgium) was used for further thiolation as described in Chapter 4. Two batches with different thiolation degrees (TC10-1 and TC5-2) together with chitosan control were selected for PEM assembling. Collagenase from Clostridium histolyticum (0.27 U/mg solid, one unit hydrolyses 1.0 μmol of FALGPA per minute at pH 7.5 and 25 ºC in the presence of calcium ions) were purchased from Sigma-Aldrich. Unless specified otherwise, all other reagents and buffers were of analytical grade purchased from Sigma-Aldrich and used as received.

5.2.2 Layer-by-layer assembly of PEM coatings and collagenase adsorption

Solutions of chitosan, thiolated conjugates and glycosaminoglycans (0.5 mg/mL) containing NaCl (0.15 M) were prepared, and the pH adjusted to 5.5 with HCl or NaOH solutions. The ζ -potential of each solution was determined at 25 °C (Nano-ZS from Malvern, UK). The deposition of the polyelectrolytes was carried out at the same temperature and at a constant flow rate (75 μL/min) onto the surface of Au coated sensor crystals (Q-Sense, Sweden). The crystals were first cleaned with H_2O_2(30%) / NH_4OH(25%) / H_2O (1:1:5) for 10 min at 75 ºC. The process was followed in situ by QCM-D E4 system (Q-Sense, Sweden). The baseline was built using a 0.15 M NaCl solution. Different multilayered systems were built by consecutive depositions of polycation (CS, TC10-1 or TC5-2) and polyanion (HA with different molecular weight or CSU) solutions. The solutions were injected into the measurement chamber for 10 min followed by a rinsing step (10 min) with 0.15 M NaCl, pH 5.5. This procedure was repeated 5 times to obtain five bi-layer substrates. Collagenase (0.1 mg/mL in 0.15 M NaCl, pH 5.5) deposition was monitored in situ by QCM-D for 3 h at a constant flow of 10 μL/min. At the end of this time a rinsing step with a protein-free solution was applied (1 h) to remove weakly and unadsorbed protein. Each study was performed in triplicate. For graphical simplification the evolutions of the normalised frequency ($\Delta f/\upsilon$) and dissipation (ΔD) shifts as functions of time of one representative per experimental group and only for the 9th harmonic are shown. Coating growth (thickness variation) as a function of the layer number and the amount of collagenase adsorbed on coatings was estimated using the Voigt model (Q-Tools software, Q-Sense). By using this model the values for the coating thickness obtained for the first layer adsorption are usually non-reproducible, therefore these values were excluded from the data [218].

5.2.3 Characterisation of PEM coatings

The PEM coatings were characterised by X-ray photoelectron spectroscopy and contact angle measurements. Multilayered systems were deposited on Au coated (100 Å) glass microscopy slides (Sigma-Aldrich), cut into pieces of 1 cm^2 and cleaned using the same protocol as the one described for QCM crystals. Custom made dipping robot was used for the biopolymers deposition. The assembling process was performed using the same conditions (solution concentration, pH, ionic strength and deposition/rinsing times) described in section 5.2.2. Multilayered systems differing in layer number (1, 3, 7 and 11) and composition of the outermost layer were prepared.

X-ray photoelectron spectroscopy

X-ray photoelectron spectroscopy (XPS) analyses were performed on a PHI 5500 Multitechnique System (Physical Electronics, USA) using monochromatic Al-Kα X-ray source (hυ 1486.6 eV), placed perpendicularly to the analyser axis and calibrated using 3d5/2 line of Ag with a full width at half maximum (FWHM) of 0.8 eV. The analysed area was a circle of 0.8 mm diameter, and the resolution chosen for the spectra was 187.5 eV of pass energy and 0.8 eV/step for survey spectra, and 0.1 eV/step for each analysed element. Binding energies were referenced by setting the Au4f7/2 at 84.0 eV. Surface elemental composition was determined using the standard Scofield photoemission cross sections.

Contact angle measurements

The hydrophilicity of the PEM coatings prepared on the Au coated glass microscopy slides was assessed by means of static contact angle measurements (sessile drop method) with ultra-pure water, using drop shape analysis system DSA 100, Kruss, GmbH (Germany), equipped with ½ CCD camera. The volume of the liquid droplet was 5 μL. Ten measurements at room temperature were taken for each sample.

5.2.4 Cell adhesion, proliferation and morphology

PEM coatings of 5 and 5½ bi-layers were sterilised by UV radiation for 15 min and washed with PBS. The substrates were seeded with L929 human fibroblast-like cell line (European Collection of Cell Cultures, UK) at concentration of 16500 cells/cm^2 in DMEM supplemented with 10 % of FBS (Biochrom AG, Germany) and 1 % antibiotic/antimycotic (Gibco, USA). Cells were cultured for 1 and 7 days at 37 ºC under a humidified atmosphere of 5 % CO_2.

The morphology of the cells was observed by SEM (Leica Cambridge S-360, 15kV) and fluorescence microscopy (Zeiss Imager Z1, Germany). The samples were washed twice with PBS and fixed either

in 2.5 % glutaraldehyde in PBS (for SEM) or in 10 % neutral buffered formalin for 1 h at 4 ºC for immunostaining assays. For the SEM analysis, samples were washed twice in PBS, dehydrated in a graded series of ethanol, and finally, dried using hexamethyldisilazane. Cytoskeleton organisation was analysed after treatment of the cells with 0.2 % Triton X-100 in PBS for 5 min and 3 % bovine serum albumin (BSA) in PBS for 30 min at room temperature. Phalloidin–TRITC conjugate was used (1:200 in PBS for 30 min) to assess cytoskeleton organisation. Nuclei were counterstained with 1 μg/mL 4,6-diamidina-2-phenylin (DAPI) for 30 min. Samples were washed with PBS, mounted with Vectashield® (Vector) in glass slides and images were acquired with an Axio Cam MRm (Zeiss).

5.2.5 Statistical analysis

All data are presented as mean ± standard deviation. For multiple comparisons, statistical analysis by a one way analysis of variance (ANOVA) followed by post-hoc Tukey test was performed using Graph Pad Prism Software 5.04 for windows (USA). Statistical significance was considered at $p < 0.01$.

5.3 Results and discussion

5.3.1 Build-up of polyelectrolyte multilayered coatings

Being natural components of the ECM, GAGs were selected as building elements for PEM coatings. They are also capable to adsorb wound exudates while providing favourable for wound healing moist environment. In this work HA (pKa~3 [219]) with different Mw and CSU (pKa~3.5 for higher ionic strengths [220]) were used. CS (pKa~6.5 [221]) has similar structure to the natural GAGs but it bears positive charge. Moreover, as commented in Chapter 4, by thiolation of chitosan using 2-iminothiolane HCl, the cationic character of the polymer improves. This allows for assembling via electrostatic interactions with the negatively charged GAGs (Figure 5.1).

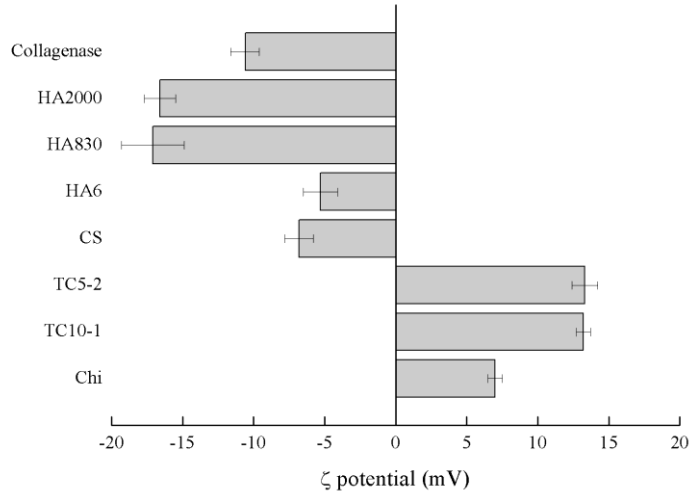

Figure 5. 1 ζ-potential of collagenase and the polyelectrolytes used for the QCM-D studies. Polyelectrolytes (0.5 mg/mL) and collagenase (0.1 mg/mL) solutions were prepared in 0.150 M NaCl, pH 5.5

Effect of the chitosan thiolation degree on build-up of PEMs

The stepwise adsorption of polyelectrolytes was monitored *in situ* by QCM-D, and the effect of the chitosan thiolation degree and molecular weight of GAGs on the growth of the coatings was assessed. The successful build-up of the PEM constructs using layer-by-layer process was confirmed by the decrease in $\Delta f/\upsilon$ and increase of ΔD after each polyelectrolyte deposition (Figure 5.2a-b). Bigger changes in $\Delta f/\upsilon$ and ΔD shifts were observed for the first layer when thiolated chitosan was used as a polycation instead of unmodified chitosan. This difference was expected because of the well-known high affinity of the thiol groups to Au [222]. Changes in the frequency and dissipation shifts become more pronounced after the deposition of the 6th layer for all experimental groups and especially for the systems built with thiolated chitosan conjugates. These data indicated an exponential growth confirmed by calculation of thickness variation using the Voigt model (Figure 5.2c). The results imply polyelectrolytes diffuse "in and out" of the coating during the build-up process [223]. Interestingly,

the thickness variation in respect of layer number was higher when thiol-modified compared to non-modified chitosan was used, where the thiolation degree promoted the growth, as the final thicknesses for the 5½ bi-layer systems were of 27±2 nm, 37±2 nm and 52±5 nm for CS/CSU, TC10-1/CSU and TC5-2/CSU, respectively. Thus, the improved cationic character after chitosan thiolation with 2-iminothiolane HCl (Table 4.2) induces stronger electrostatic interactions with chondroitin sulphate and together with better deposition of the first layer favours the PEM coating growth.

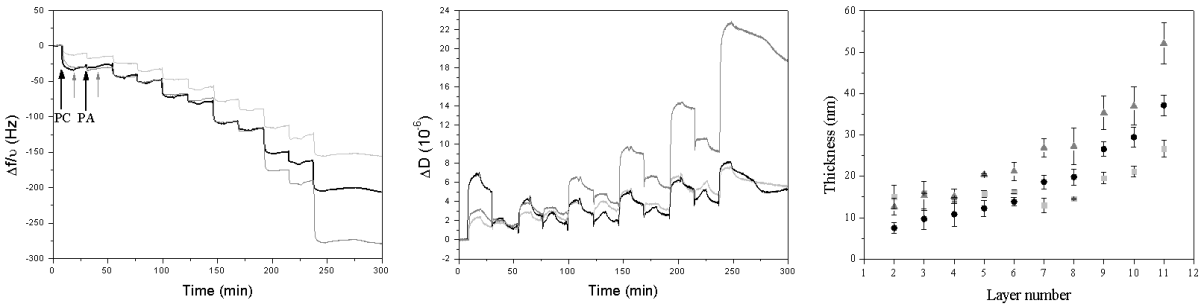

Figure 5. 2 Build-up assessments of 5½ bi-layers of CS/CSU (light grey), TC10-1/CSU (black) and TC5-2/CSU (dark grey). Signals for normalized a) frequency (Δf/υ) and b) dissipation (ΔD) were obtained during QCM-D monitoring. Labelled arrows indicate polyelectrolyte injection (PC for polycation, PA for polyanion), whereas small arrows without labels indicate rinsing with 0.15M NaCl, pH 5.5. c) Thickness evolution of the obtained PEMs estimated using the Voigt model for three independent experiments

Finally, although the stability of the PEM coatings was not investigated here, the partial oxidation of the free thiol groups is expected to occur after deposition in situ [224]. This would lead to the formation of disulphide cross-links in chitosan that would certainly improve the mechanical properties of the systems containing thiolated conjugates and enhance their stability in biological fluids. Chemical cross-linking has been already investigated as an approach to increase the stability of PEMs [225] and improve their mechanical properties [226].

Effect of molecular weight of glycosaminoglycans on build-up of PEMs

QCM-D experiments were also conducted to investigate the effect of Mw of polyanion on the build-up of multilayered coatings containing thiolated chitosan. HA with three molecular weights (6 kDa, 830 kDa and 2000 kDa) was used for building multilayered systems with TC5-2 (Figure 5.3a-b).

Initially, the PEMs grew regularly for all experimental groups. However, the system containing HA with lowest Mw becomes unstable after the addition of the 8th layer; re-dissolution of the formed complex upon the contact with the following polyelectrolyte solution was observed. Similar effect has been previously observed for other weak PEMs [225]. Although the negative charge of HA with Mw of 6 kDa was similar to the one of CSU (Figure 5.1), in the latter case a stable complex with polycation was formed.

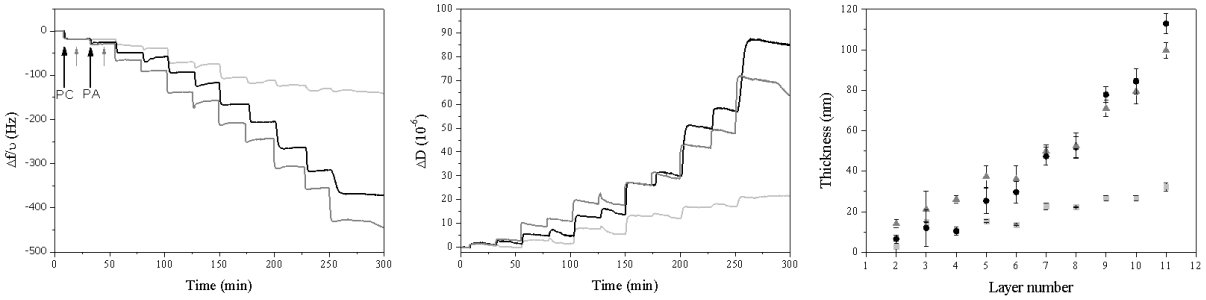

Figure 5. 3 Build-up assessments of 5½ bi-layers of TC5-2/HA using hyaluronic acid with different Mw: 6 kDa (light grey), 830 kDa (black) and 2000 kDa (dark grey). Signals for normalized a) frequency (Δf/υ) and b) dissipation (ΔD) were obtained during QCM-D monitoring. Labelled arrows indicate polyelectrolyte injection (PC for polycation, PA for polyanion), whereas small arrows without labels indicate rinsing with 0.15M NaCl, pH 5.5. c) Thickness evolution of the obtained PEMs estimated using the Voigt model for three independent experiments.

Efficient GAGs-biomolecules binding relies on multivalent interactions or so-called cluster effect [227]. Out of this, two are the possible reasons for the results observed with the low Mw HA: the unavailability of enough reaction centres (because of the lower Mw) or their inadequate distribution, i.e. their conformation does not allow effective binding through cluster effect. Thus, we can speculate that CSU takes a conformation favouring the interactions with TC which is not the case with low molecular weight HA. In addition, previous reports showed that Mw plays an important role for efficient immobilisation of sugars onto many surfaces, where oligosaccharides and monosaccharides cannot be densely and stably immobilised if they are not coupled to larger moieties, support this result [228, 229]. Thus, the Mw of 6 kDa is too low to allow for sufficient deposition onto the oppositely charged surface and when the amounts of the deposited polyelectrolytes increase (after 8th layer) re-dissolution occurs.

The PEM coatings containing HA of higher average molecular weight displayed higher stability and grew exponentially (Figure 5.3c); Δf/υ and ΔD shifts became more pronounced after the deposition of 6th layer. Slightly larger increase was detected for HA of 830 kDa compared to 2000 kDa, due to the better diffusion of the HA with lower Mw into the coating, which is in a good agreement with the literature data for the exponentially growing PEM systems [230]. The calculated thicknesses were of 32±2 nm, 113±5 nm and 100±4 nm for PEMs with HA of 6 kDa, 830 kDa and 2000 kDa, respectively. These results confirm the instability of the PEM system build up with low molecular weight HA.

5.3.2 XPS analysis

XPS measurements were performed to confirm the successful deposition of the polyelectrolytes. Out of the measurements it was possible to estimate the surface coverage by analysing Au atomic concentrations at the different steps of deposition (Table 5.1). As could be expected, the XPS analysis showed a steady decrease in the intensity of the Au signal with increasing number of deposited layers.

Table 5. 1 Au and S content (%) for various multilayered systems deposited onto gold covered microscopy slides

System	Au (4f)	S (2p)
Gold surface	99.99*	-
TC5-2	16.19	1.37
$(TC5\text{-}2/HA830)_1TC5\text{-}2$	1.97	1.66
$(TC5\text{-}2/HA830)_3TC5\text{-}2$	0.18	1.42
$(TC5\text{-}2/HA830)_5TC5\text{-}2$	0.08	1.60
$(CS/HA830)_5CS$	0.12	-

*According to the manufacturer

The obtained value for Au signal (16.19 %) after the deposition of the first layer is in agreement with previously reported values for monolayers of thiolated polymers deposited onto gold surfaces [231]. After 5½ bi-layers deposition of TC/HA830 system only a negligible Au signal was detected (0.08 %), the value lower than the one measured for CS/HA830 system for the same number of deposited bi-layers (0.12 %). This is in agreement with QCM-D results confirming better build-up and surface coverage for the PEMs containing thiolated compared to non-modified chitosan.

The presence of S was also observed for all PEMs terminating with TC5-2, where the signal did not vary considerably between the experimental groups (Table 5.1). The binding energies and the possible oxidation states of S in the TC5-2 deposited on the gold were obtained from the high resolution XPS spectra of S2p core level. The S2p high resolution spectrum (not presented) showed two dominant peaks at 162.4 eV and 163.6 eV that are assigned to bound S atoms (S2p3/2 and S2p1/2) on the Au surface (thiols and disulphides). Two additional peaks appear in the spectrum of multilayered (5½ bi-layers) TC5-2/HA830 system (Figure 5.4): an intensive peak at 164.3 eV corresponding to unbound thiols and a lower intensity peak at above 168 eV due to partial sulphur oxidation or presence of impurities in the sample [231]. These values were in agreement with literature data [222, 232].

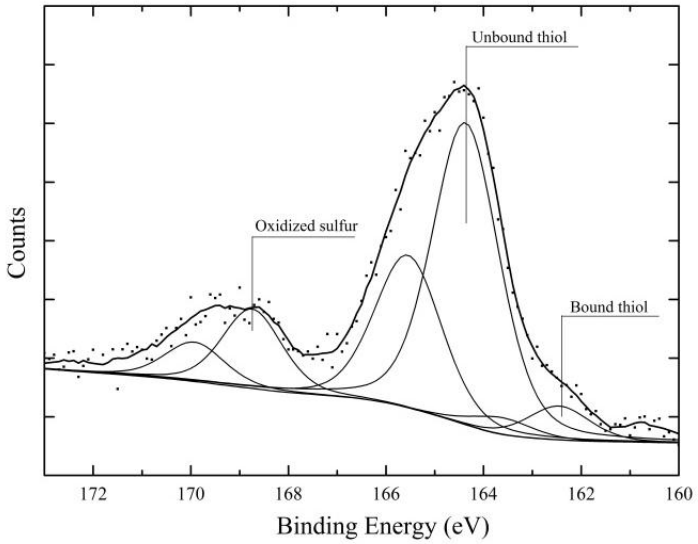

Figure 5. 4 S2p spectrum of TC5-2/HA830 multilayer system consisting of 5½ bi-layers adsorbed onto gold surface acquired by XPS. Polyelectrolytes were deposited onto gold from 0.15M NaCl, pH 5.5 solution, using concentrations of 0.5 mg/mL. The S peaks were fit using three S2p doublets with a 2:1 area ratio and a splitting of 1.2 eV. The positions of the S2p3/2 peaks assigned to bound thiolate, unbound thiol and oxidized S species are shown.

5.3.3 Collagenase adsorption on PEM coatings

Coating of surfaces through PEM deposition has been extensively investigated as a way to rule the protein attachment on such surfaces required for different applications and controlled attachment could be achieved by changing an ambient pH, system cross-linking and selection of the outermost layer [218, 233]. Moreover, the incorporation of the proteins can be further controlled by an appropriate functionalisation of the PEM components before or even after their construction [234]. As one of the efficient ways to inactivate the proteases in the wound environment is through the selective or non-selective protein adsorption [235, 236], the PEM coatings prepared in this study have been evaluated for their capacity to adsorb collagenase from solution. The effect of chitosan thiolation and the charge of the outermost layer have been considered as variables.

The amount of collagenase adsorption onto PEMs with different terminate layer is showed in Figure 5.5. The adsorption was performed at pH 5.5, the same as the one applied in the process of PEMs build-up. This pH was chosen to ensure the optimum protein adsorption since it is near to the isoelectric point of collagenase (pI in the range 5.35 - 6.20 [237]) and thus, minimal lateral interactions and compact conformation of protein onto surface occur [238]. The collagenase is negatively charged at these conditions (Figure 5.1) and has higher affinity to positively charged chitosan surfaces regardless of chitosan modification. These results confirmed the dominant role of the electrostatic interactions during protein adsorption [214, 239].

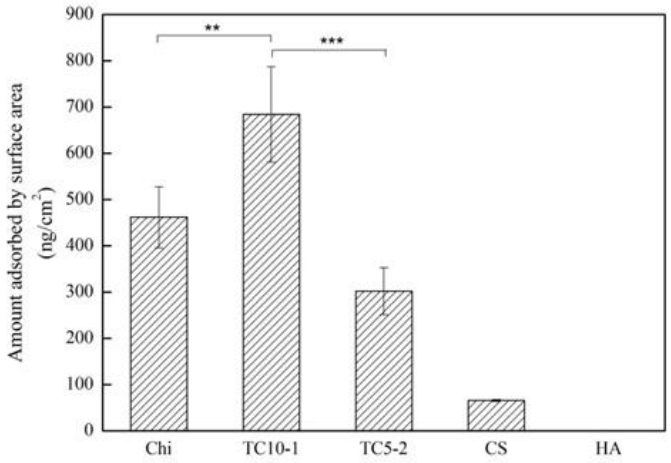

Figure 5. 5 Variation of collagenase adsorption (0.1 mg/mL) onto PEMs with different outermost layer in terms of amount adsorbed by surface area. The results were obtained by extracting the data acquired with QCM-D and calculated using the Voigt model. PEM coatings comprised 10 layers in case of polyanion and 11 in case of polycation outermost layer. For the PEMs terminating with polycation CS was used, whereas for those terminating with polyanion TC5-2 served as a counter polyelectrolyte. Polyelectrolytes were deposited onto gold from 0.15 M NaCl, pH 5.5 solution, using concentrations of 0.5 mg/mL. **p<0.01 and ***p<0.001

Besides electrostatic interactions, the affinity of chitosan towards collagenase could be explained by the high content of amino groups that allows for the sorption of the Zn^{2+} coordinated in the active site of the enzyme. Further, collagenase adsorption onto TC10-1 outermost surface was significantly higher than in the case of chitosan ($p<0.01$). This was expected since inclusion of free thiols in the chitosan structure improves its Zn^{2+} binding capacity [210] and thus the adsorption of collagenase. Surprisingly, collagenase adsorption was not higher on the TC5-2 surface in comparison with chitosan. Although with inclusion of higher amount of thiol groups improved collagenase adsorption was expected, this was not the case. One possible explanation may be that a highly cross-linked structure is formed *in situ* after TC5-2 deposition via intra- and inter-molecular disulphide cross-linking which is promoted in the formulations with high percentages of free thiol groups due to their proximity [240]. The formation of such structure would impede the availability of the remaining free thiols and consequently the sorption capacity towards Zn^{2+}. This result is consistent with the decrease in protein adsorption after cross-linking of the PEM systems [218].

On the other hand, adsorption of collagenase onto like-charged surfaces was different. Whereas the enzyme was not adsorbed onto HA outermost layer, adsorption onto CSU containing surface occurred. This result confirms that not only electrostatic interactions, but also other non-ionic factors can influence protein adsorption [241]. Again, GAGs-protein binding relies on multivalent interactions, some of them very difficult to measure experimentally [242], where, besides other factors, spatial distribution of negative charges in GAGs plays an important role [243]. Also, HA displays higher negative charge (Figure 5.1) which may be the explanation for stronger repulsion of the like-charged enzyme. Another factor that may influence the protein adsorption is the surface hydrophilicity. Normally, the protein attachment decreases with wettability [244]. The CSU-

terminated assemblies had contact angles of 54±4º, whereas HA-terminated exhibited 40±4º, being thus more hydrophilic.

5.3.4 Cell culture studies

Fibroblasts behaviour on the obtained PEM coatings was evaluated in terms of cell adhesion, morphology and cytoskeleton organisation. Bright-field images (Figure 5.6) showed that after 24 h the cells adhered better on GAG-terminated coatings (Figure 5.6A,C) than on thiolated chitosan (Figure 5.6E,G). Moreover, the number of fibroblasts on CSU-terminated coatings (Figure 5.6A-B) was similar to the control, tissue culture polystyrene surface (TCPS) surfaces (Figure 5.6I-J).

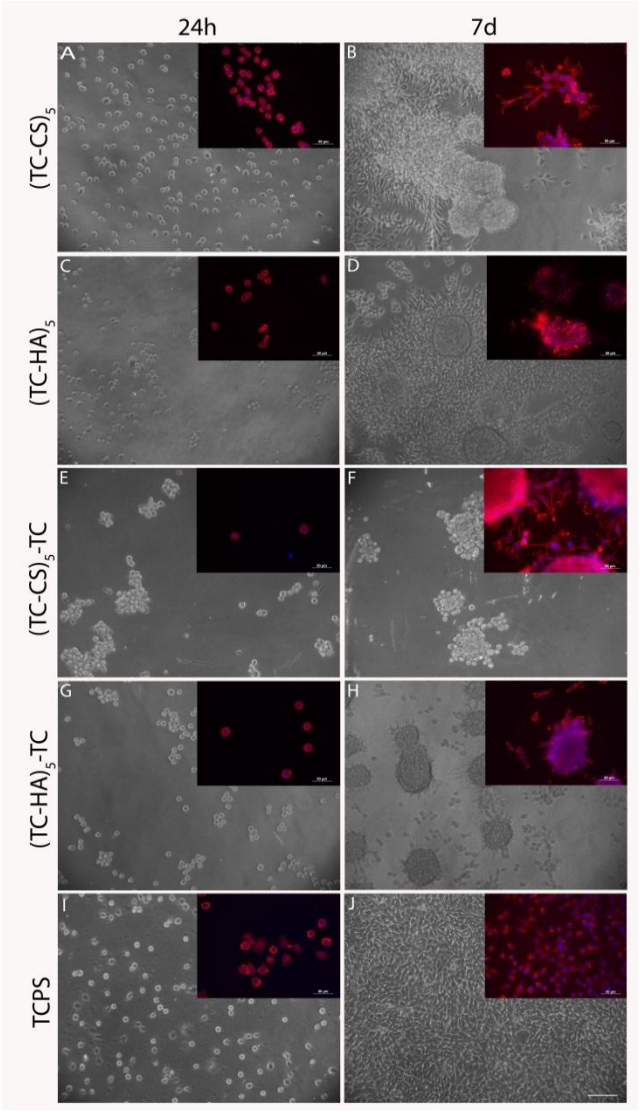

Figure 5. 6 Morphology of L929 cells cultured for 24 h and 7 d on (A-B) CSU-terminated; (C-D) HA830-terminated, (E-F) TC terminated (TC5-2/CSU system, (G-H) TC terminated (TC/HA830 system) and (I-J) TCPS (scale bar=100 μm) . Insets show fluorescence microscopy images of DAPI and phalloidin staining

Different cell morphology was also observed as a response to the terminal layer; after 24 h, cells cultured in contact with thiolated chitosan remain round and compact (Figure 5.6E,G). These results

are in agreement with previously reported data about the poor cellular adhesion on the chitosan [43, 44]. On the other hand, when the outermost layer is GAG (HA or CSU), cells are elongated with a morphology more similar to the cells cultured on TCPS (Figure 5.6A,C,I).

After one week of culture the cells tend to organise in clustered structures on the thiolated chitosan (Figure 5.6F,H; Figure 5.7C-D). This behaviour has been previously associated with defensive mechanisms by which cells are able to survive under unfavourable conditions [245].

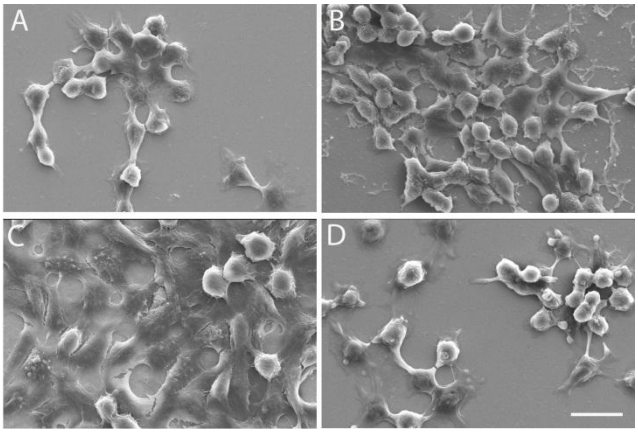

Figure 5. 7 Morphology of L929 cells cultured for 7 d on (A) $(TC\text{-}CS)_5$; (B) $(TC\text{-}HA)_5$, (C) $(TC\text{-}CS)_5$-TC and (D) $(TC\text{-}HA)_5$-TC (scale bar=20 μm).

Also, the formation of the spheroid structures has already been reported for cells cultured on chitosan membranes [43, 245]. Although not that pronounced, similar behaviour was observed for the fibroblasts cultured in contact with the GAGs-terminated coatings (Figure 5.6B,D, Figure 5.7A-B). This result is consistent with the diffusion of the polyelectrolytes layer estimated by the QCM-D. The diffusion of the layers and its influence on the cell behaviour is also obvious for the TC-terminated coatings where the GAG layer below induces fibroblasts morphology that is similar to the one observed for the respective GAG-terminated coatings (Figure 5.6 insets).

5.4 Conclusions

Due to their cationic properties, the thiolated chitosan conjugates prepared in Chapter 4 were successfully combined with anionic glycosaminoglycans, chondroitin sulphate and hyaluronic acid, in a sequential multilayer fashion based on electrostatic interactions to build-up continuous multilayered assemblies onto gold surface. It was demonstrated that the fastness of the build-up process (with respect to the number of deposited layers) is promoted by the higher chitosan thiolation degree and molecular weight of glycosaminoglycans. Moreover, the proper selection of the outermost layer could be used to control the extent of collagenase adsorption onto the multilayered coatings. Chitosan-based surfaces were found to be more protein-adhesive than glycosaminoglycans ones. The extent of collagenase adsorption on thiolated chitosan surfaces also depends on the availability of free thiol groups able to bind the zinc in the active site of the enzyme. Finally, the multilayered structures terminating with thiolated chitosan were found to be fibroblast resistant, whereas glycosaminoglycans as outermost layer promoted the cell proliferation. Such tuneable inhibition/adsorption of the deleterious proteolytic enzymes and controlled cell proliferation applied in the wound site could bring restoration of the balance between tissue synthesis and degradation in chronic wounds necessary for healing.

Chapter 6

Thiolated chitosan nanoparticles

6.1 Introduction

Nano/micro-particles (NPs) are employed for protection of unstable active agents and ensure their sustained delivery to targeted tissue compartments [246], e.g. skin layers. When engineered in NPs, biopolymers display improved biological activities. If such systems are used as drug carriers, combined beneficial effects of biopolymer and loaded active agent for targeted application is expected. In order to combine this promising strategy with thiolated biopolymers, the aim of this study was to generate and characterise NPs based on thiolated chitosan.

Particles generation from thiolated conjugates has been already reported by using various techniques for their generation such as emulsification-solvent evaporation [247], coacervation/precipitation [248], air jet milling [249], cross-linking with sodium tripolyphosphate [250] and ionotropic gelation [251]. Engineered in nano-structures, the thiolated conjugates display improved mucoadhesive, permeation enhancing and anti-inflammatory properties, and enhance transfection and delivery of various bioactive molecules into various cells/tissues. However, by using these techniques for NPs preparation the broad size distributions of the particles are usually obtained, thus limiting the predictability of their physical and chemical interactions with the targeted tissues. In addition, many of these techniques lead to the formation of the particle systems that display large sizes (up to several tens of microns).

The generation of biopolymer-based NPs under sonication is recently gaining much of attention due to its simplicity and short processing time [252]. In this case the generation of biopolymer NPs is induced in a one-step environmentally friendly process. Moreover, some reports revealed the additional stabilisation of the NPs systems comprising thiol groups bearing biopolymers due to the ultrasound-induced oxidation of free thiols to disulphide bonds [31, 253].

Therefore, high power ultrasound was used to generate NPs from different thiolated chitosan conjugates and the resulting particles were evaluated regarding their size and cross-linking via -S-S- bonds formation, taking into account the pH of the ultrasonic bath and the chitosan thiolation degree. The effect of the particles cross-linking degree on the stability against lysozyme degradation and *in vitro* MPO inhibition efficacy was also assessed.

6.2 Materials and methods

6.2.1 Thiolated chitosan and reagents

Medical grade chitosan (~50 kDa, DDA 87 %) from Kitozyme (Belgium) was used for the thiolation as described in Chapter 4. Batches differing in thiolation degrees (TC10-1, TC5-1 and TC5-2) together with chitosan control were selected for NPs formation. These conjugates displayed 158±8, 288±4 and 515±53 μmol of free thiol groups per g of polymer, respectively, quantified spectrophotometrically in Chapter 4 (Table 4.3). Highly purified MPO from human leukocytes (1550 U/mg solid, one unit will produce an increase in absorbance at 470 nm of 1.0 per min at pH 7.0 and 25 °C, calculated from the initial rate of reaction using guaiacol substrate) was purchased from Planta Natural Products (Austria). Lysozyme from chicken egg white (111000 U/mg, 1 U corresponds to the amount of enzyme which decreases the absorbance at 450 nm by 0.001 per minute at pH 7.0 and 25°C using *Micrococcus luteus* as substrate) was supplied by Sigma-Aldrich. Edible grade sunflower oil was used as organic phase for the NPs preparation. Unless specified otherwise, all other reagents and buffers were of analytical grade purchased from Sigma-Aldrich and used as received.

6.2.2 Nano/micro-parcticles preparation

NPs were prepared by application of high-intensity ultrasound (17 W) using the method previously of Grinstaff and Suslick [254]. Briefly, two-phase mixtures containing 70 % of 1 mg/mL of chitosan or thiolated chitosan aqueous solution and 30 % of edible-grade sunflower oil were prepared. The high-intensity ultrasonic horn was positioned at the aqueous-organic interface and the solution was sonicated for 3 min with the amplitude of 30 % at 5 (±1) ºC. The resulted emulsion was kept at +4 ºC for 24 h in order to complete the obtained phase separation after which the non-encapsulated oil was withdrawn before further analysis. The volume of the oil withdrawn was quantified in order to determine the NPs encapsulation efficiency.

6.2.3 Determination of free thiol groups

Determination of free thiol groups in NPs suspensions was determined spectrophotometrically using Ellman's reagent. Aliquots of 500 μL of nanoparticle suspensions were diluted with 500 μL of 0.5 M PB (pH 8) containing Ellman's reagent (3 mg of the reagent in 10 mL PB). Following 3 h incubation at room temperature in the dark, the suspensions were centrifuged (5000 rpm, 5 min) and filtered through Whatman® 0.2 μm regenerated cellulose filters (Sigma-Aldrich). The absorbance of the

filtered solution was measured at 450 nm. L-cysteine standards were used to build the calibration curve.

6.2.4 Dynamic light scattering

Particle size and size distribution was measured by dynamic light scattering (DLS) using DL135 Particle Size Analyzer (Cordouan Technologies, France). Three samples of each nanoparticle suspension were measured at room temperature, acquiring 5 measurement cycles with 1 % signal-to-noise ratio. The data were analysed using NanoQ 1.2.1.1 software to calculate the mean particle diameter and polydispersity index (PDI).

6.2.5 Biostability of nanoparticles

The biostability of thiolated chitosan NPs was studied in a biodegradation test using lysosyme, a glycoside hydrolase enzyme. Nanoparticles formulations (1 mL) were incubated in 1 mL of 50 mM phosphate buffer, pH 6.6, in the presence of 10 μg/L lysozyme at 37 °C for 24 h. Samples of 250 μL were thereafter withdrawn and filtered through Whatman® 0.2 μm regenerated cellulose filters in order to remove intact particles from the hydrolysed solutions. The degraded chitosan was determined in the filtrate using the ninhydrin test. The degradation of nanoparticles was determined as the amount of hydrolysed chitosan leached from the nanoparticles and expressed in mM of glycine equivalents, used as a standard to develop the calibration curve.

6.2.6 Myeloperoxidase inhibition

The inhibitory effects of thiolated chitosan nanoparticles on MPO activity was assayed using the same method applied in Sections B, 3.2.8.

6.3 Results and discussion

6.3.1 Sonochemical generation of thiolated chitosan nanoparticles

High intensity ultrasonic irradiation of liquids is well known to produce both emulsification and acoustic cavitation – the formation, growth and implosive collapse of micron-sized bubbles in two-phased mixtures [255, 256]. Owing to the possibility of chemical reactions around the formed bubbles, this technique is successfully employed for generation of NPs from proteins and, lately, polysaccharides. If high intensity ultrasonic horn is positioned in the interface of biopolymer aqueous solution and organic phase (solvent), e.g. vegetable oil, biopolymer NPs will be formed (Scheme 6.1).

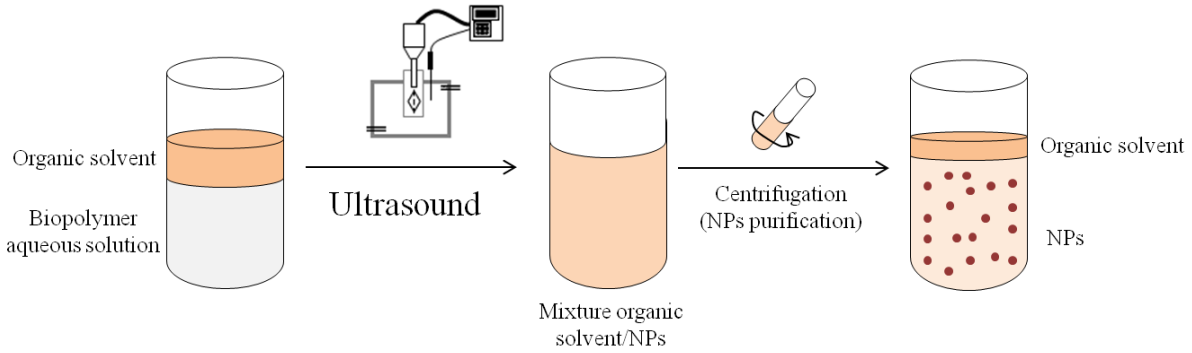

Scheme 6. 1 Sonochemical preparation of biopolymer NPs

In such cases the core of the particles is filled with oil, whereas the shell comprises the biopolymer [252]. In this study NPs from chitosan and thiolated chitosan with different modification degrees were produced in the fast (3 min) sonochemical process using sunflower oil as a cosolvent. Although the NPs generation occurred in the pH range from 3 to 6, differences in the oil encapsulation efficiency between the experimental groups have been found. In particular, higher chitosan thiolation degree and pH promoted the efficiency of oil encapsulation (Figure 6.1). This data can be of particular importance in the case of drug encapsulation, since the quantity of the oil encapsulated is the indirect measurement of the efficiency of the hydrophobic drug encapsulation. Moreover, optical microscopy images indicated the higher NPs density and smaller particles in the formulations obtained from thiolated conjugates compared to those obtained from chitosan (Figure 6.2).

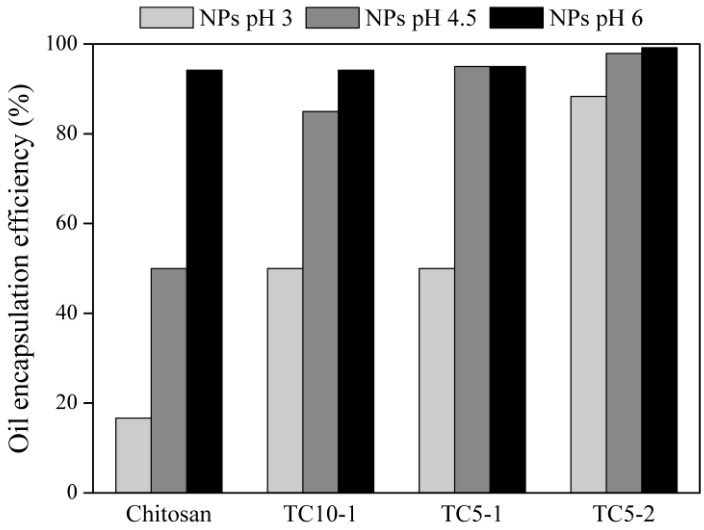

Figure 6. 1 Efficiency of oil encapsulation by chitosan and thiolated chitosans NPs

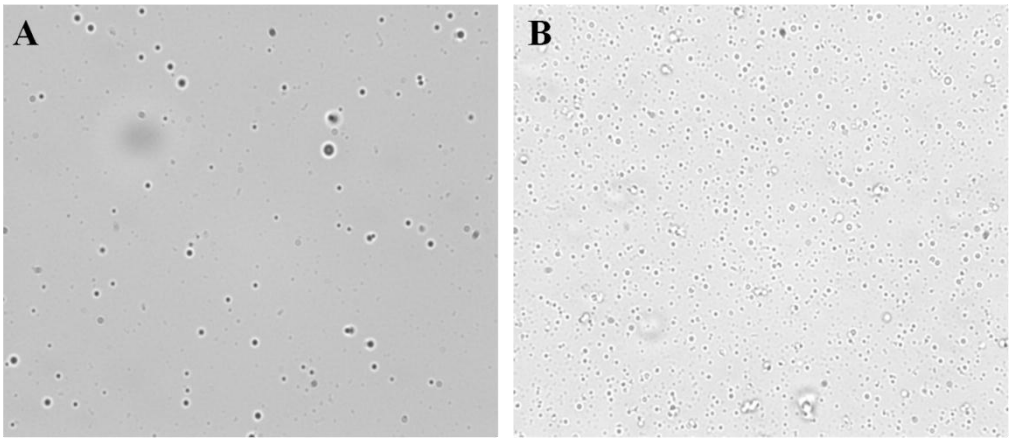

Figure 6. 2 Optical microscopy images of NPs obtained under sonication A) chitosan NPs, and B) thiolated chitosan (TC5-1) NPs

6.3.2 Degree of chitosan thiolation in nanoparticles

Compared to the -SH content in thiolated chitosan conjugates (TC10-1, TC5-1 and TC5-2) before sonication, all corresponding NPs formulations displayed less free thiol groups per gram of the freeze-dried polymer conjugate regardless of the process pH (Figure 6.3). Moreover, it has been found that the NPs processed at lower pH contained more -SH. Accordingly, all formulations sonicated at pH 6 contained the lowest amounts of free thiol groups, especially when obtained from TC5-1 and TC5-2 (the conjugates with higher degree of thiolation), where the -SH content was negligible (below 10 μmol/g of particles). These results indicated that an oxidation of free thiol groups into disulphide bridges, i.e. NPs cross-linking [247], takes place to different extents upon sonication.

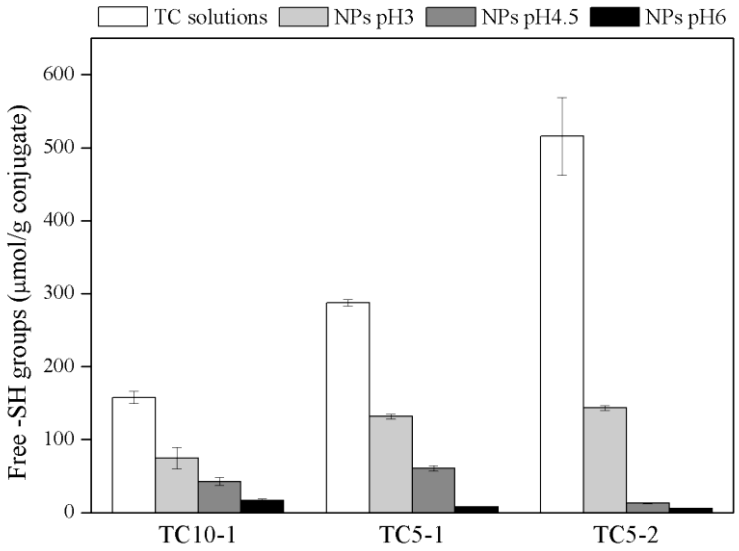

Figure 6. 3 Amount of free thiol groups in thiolated chitosan conjugates and the corresponding NPs formulations obtained at indicated pH values of the aqueous phase during the sonication process.

The oxidation of cysteine moieties in proteins by superoxide radical ($\cdot HO_2$) produced during the ultrasonic irradiation to cross-link the polymer was suggested as crucial for the formation of protein microparticles [31]. Although later studies revealed that -S-S- are not required for the sonochemical formation of protein NPs [257], these bonds undoubtedly play an important role in the particles stabilisation. Furthermore, it is well known that the oxidation of free thiol groups to disulphide bonds is promoted on higher pH in the presence of oxygen. In addition, the -S-S- formation is faster in the systems with high percentages of -SH due to their proximity [240]. Based on the above, it is expected that the extent of cross-linking via -S-S- formation is higher in the NPs formulations obtained from the thiolated chitosan with higher modification degrees and processed on higher pH. Indeed, these formulations contained less free thiol groups per gram of NPs and accordingly higher content of -S-S- bonds (Table 6.1).

Table 6. 1 Estimated percentage of disulphide bonds in the NPs formulations obtained from different thiolated chitosan conjugates at indicated pH values of the aqueous phase

NPs formulation	**% of –SH oxidised**		
	pH 3	**pH 4.5**	**pH 6**
TC10-1	52.7±9.4	73.0±3.5	89.4±1.1
TC5-1	54.3±1.2	79.0±1.2	97.3±0.1
TC5-2	72.2±0.6	97.5±0.1	98.9±0.1

Cross-linking of biopolymer-based materials, e.g. through the formation of disulphide bonds, brings about the increased stability of these systems in physiological conditions. If such systems are used as carriers for the protection and delivery of unstable active compounds, sustained drug liberation

resulting in prolonged effect is guaranteed [258]. On the other hand, the presence of free thiol groups amplifies the functional properties of biomaterials, including improved mucoadhesion [110], permeation enhancement [259], or inhibition of targeted enzymes, the latter described in Chapters 4 and 5. Therefore, the optimal thiol/disulphide content is driven by the specific application. In order to achieve the desired ratio, the oxidation of thiol groups during the preparation process has to be well controlled. In the present study it was demonstrated that the amount of -SH and -S-S- in the NPs formulation obtained from thiolated chitosan under sonication is easily adjustable by tuning the pH of the sonication bath and the conjugate thiolation degree.

6.3.3 Particle size and size distribution

DLS measurements revealed different influence of the sonication pH on the size of the chitosan and thiolated chitosan NPs. Whereas the mean particle size for the chitosan NPs increased with the pH from 3 to 6, the smaller particles were obtained after sonication of all thiolated conjugates on higher pH, especially when performed at pH 6 (Table 6.2). Accordingly, the NPs formulations obtained from the conjugate containing the highest amount of free thiol groups (TC5-2) exhibited the smallest particles of all experimental groups when processed at pH 4.5 and pH 6 (315±9 and 303±2 nm, respectively). Since the mean particle size decreases after the cross-linking through the formation of disulphide bonds [260], this finding is yet another indication of higher percentage of -S-S- in these samples and in agreement with the rapid oxidation of thiol groups on higher pH values [261]. It is also worthy to notice that regardless of the pH and conjugate used the mean particle sizes of all formulations were in the submicron range, probably owing to the low molecular weight (~50 kDa) of the chitosan used in the study [262].

Table 6. 2 Mean particle size of chitosan and thiolated chitosan NPs obtained at various pH values

NPs formulation	Mean particle size (nm)		
	pH 3	**pH 4.5**	**pH 6**
Chitosan	489±33	560±18	781±41
TC10-1	520±13	571±16	357±21
TC5-1	542±19	499±34	340±22
TC5-2	546±36	315±9	303±2

The mean particle sizes of the formulations obtained from thiolated chitosan conjugates did not change significantly after three months (Figure 6.4), revealing high physical stability of these systems. This finding is particularly important for the formulations displaying higher number of free thiol groups. In such cases the aggregation could be expected over prolonged periods due to inter-particle cross-linking via -S-S- formation. On the other hand, the average particle size of the chitosan NPs

systems increased for 152 nm, 355 nm and 288 nm in three months for the formulations obtained at pH 3, pH 4.5 and pH 6, respectively, thus display low stability against aggregation.

Finally, the particle size distribution was similar to that observed for the mean particle size. When obtained at higher pH (4.5 and 6) the chitosan NPs displayed broader size distributions compared to the particles obtained at pH 3 (Figure 6.5). Conversely, the narrowest size distributions between the thiolated chitosan NPs exhibited the formulations obtained at pH 6.

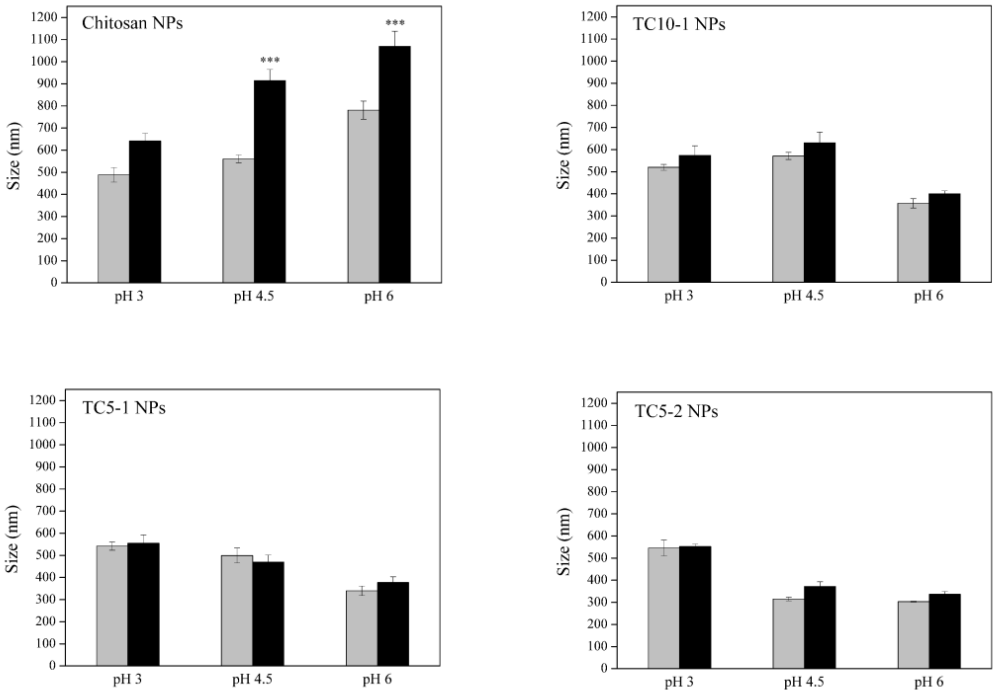

Figure 6. 4 Comparison of the mean particle sizes of chitosan NPs and NPs obtained from thiolated chitosan conjugates after one week (grey bars) and three months (black bars) storage

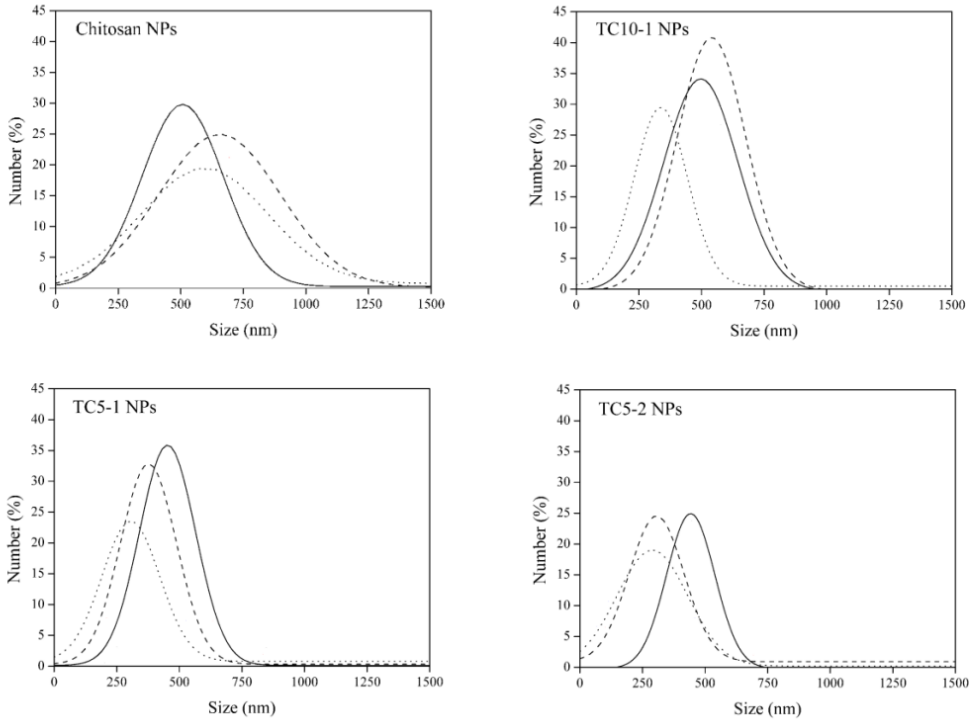

Figure 6. 5 Comparison of the Gaussian particles size distributions between the NPs formulations obtained at various pH values: pH 3 (solid line), pH 4.5 (dashed line) and pH 6 (dot line)

6.3.4 Biostability of nanoparticles

The degradation of thiolated chitosan NPs was tested in the presence of 10 μg/mL of lysozyme, an enzyme able to degrade chitosan and chitosan NPs [263], and commonly present in body fluids and skin [264, 265]. The biostability of the NPs against lysozyme was found to be dependent on the pH of sonication process: at low pHs the resulting particles showed higher degradation yields than at pH 6, which were found to be remarkably stable (Figure 6.6). In addition, the degradation behaviour was also influenced by the biopolymer thiolation degree: chitosan with the highest thiolation grade (TC5-2) developed particles extremely stable to lysozyme degradation regardless of pH of the sonication process. On the other hand, the NPs systems obtained from TC 10-1 and TC 5-1 at pH 3 and pH 4.5 were more easily degraded by the enzyme. Therefore, the biostability of the NPs was found to be inversely proportional to the amount of free thiols groups in the formulation. These results are in a good agreement with the hypothesis of the larger extent of cross-linking in the NPs processed from highly thiolated chitosan at pH 6 to impart the highest stability to lysozyme degradation.

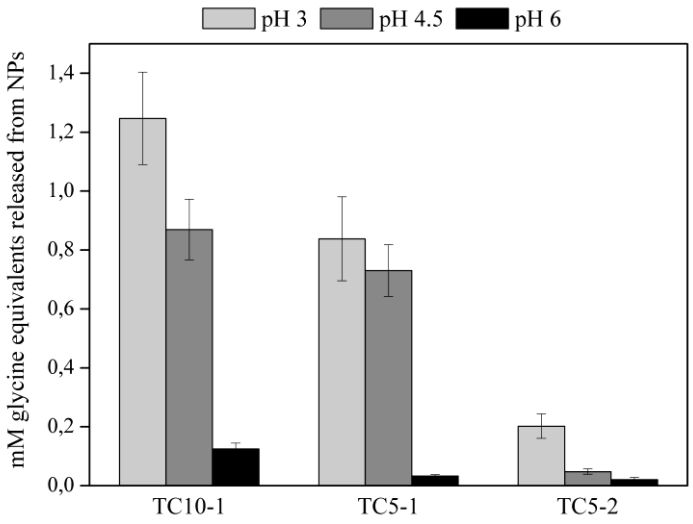

Figure 6. 6 Degradation of TC NPs by lysozyme

6.3.5 Myeloperoxidase inhibition

As expected, the amount of free thiol groups in the thiolated chitosan NPs (Figure 6.3) was directly proportional to their myeloperoxidase inhibition capacity (Figure 6.7). The NPs formulations obtained at pH 3 possessed the highest ability to inhibit enzymes regardless of the conjugate used for their preparation. The only two formulations able to inhibit more than 50 % of the enzymatic activity were those displaying more than 100 μmol of -SH per gram of nanoparticles – TC5-1 and TC5-2 fabricated at pH 3. Thus, the targeted functional properties could be tuned by both biopolymer thiolation degree and the pH of the ultrasonic bath.

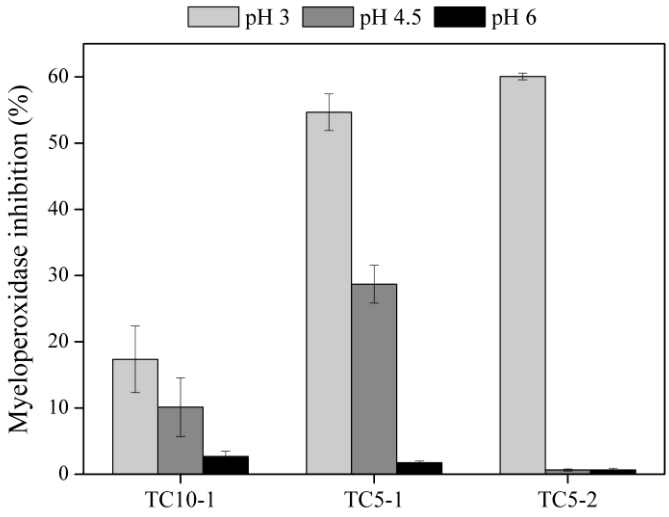

Figure 6. 7 Inhibition of MPO activity by with thiolated chitosan nanoparticles

6.4 Conclusions

Within this study the formation of the chitosan and various thiolated chitosan nanoparticle formulations was achieved in an ultrasonic process, and analysed regarding their size, bio- and physical stability and the capacity to inhibit myeloperoxidase activity. The applied strategy for the simultaneous nanoparticles generation, stability improvement and functionalisation was found to be feasible in a short (3 min) sonochemical process. In particular, chitosan thiolation degree and the pH of the sonication bath were crucial factors to achieve dimension and stability control as well as tuning of the enzyme inhibition ability of the nanoparticle formulations. However, a strong competition between the size and biodegradability of the nanoparticles on one, and their functional properties on another side was found due to the different ratios free/oxidised thiols obtained as a function of the processing conditions. The best compromise to achieve the combination of the exploitation and functional properties was found for the processing of the conjugate with the highest amount of free thiol groups (TC5-2) at low pH.

Section D

Final remarks

Chapter 7

Conclusions and future plans

7.1 Conclusions

A range of multifunctional materials aiming at chronic wounds healing applications were developed during the realisation of this thesis. These materials differentiate in design, biopolymer composition, nature of the loaded bioactive molecule and functionalisation approach used. Nonetheless, they all share a common feature: combined and controllable *in vitro* attenuation of the two main deleterious enzyme activities (collagenase and myeloperoxidase).

In the first approach, various biopolymer-based dressing sponges were produced using freeze-drying technique and chemically cross-linked in order to improve their bulk properties and resistance to enzymatic degradation. Controllable improvement of their physico-mechanical properties and biodegradability could be achieved through the formation of additional cross-links by altering: i) the cross-linking agent concentration, and ii) the polymer composition of the sponges, e.g. after collagen blending with hyaluronic acid and chitosan. This means easily adjustable exploitation characteristics of the dressing materials prior to loading of active functions. Once impregnated with plant-derived polyphenols, the results for myeloperoxidase inhibition were proportional to the release behaviour of the active agents. Large part of the enzyme activity was reduced within a few hours, corresponding to the need for the initial stimulation of the chronic wound healing process. In addition, the following sustained release allowed for the prolonged up to several days inhibition effects, in line with the requirement for less frequent dressing changes during the treatment.

In another approach two biopolymers bearing amino moieties were permanently modified using different thiolation protocols. The inhibitory effect of these conjugates against myeloperoxidase was dependent on the amount of thiol moieties immobilised onto biopolymers. Therefore, this parameter was used to achieve control of the enzyme activity in further studies. Thiolated conjugates were then used to obtain functional nanosized architectures in different designs. Multilayered surface nanocoatings were built using layer-by-layer technique based on electrostatic interactions between cationic thiolated chitosan and anionic glycosaminoglycans. This simple and convenient approach for surface modification was successfully applied to obtain functional coatings with specific bio-activity towards various bioentities. Indeed, the obtained materials were able to adsorb different amounts of collagenase or provide controllable interactions with skin fibroblasts depending on the nature of the outermost layer. On the other hand, thiolated chitosan nanoparticles were prepared by ultrasonic irradiation of the conjugates solutions. In this case, a simultaneous formation of functional nanoparticles and tuning of their exploitation and functional properties, i.e. size, biodegradability and myeloperoxidase inhibition capacity, was achieved.

7.2 Future perspectives

The results obtained during the realisation of this thesis demonstrated the possibility to control the activities of major chronic wound enzymes *in vitro* by the fabricated materials/formulations. These functional properties coupled to the good exploitation characteristics suggest these materials potentially useful in chronic wound management. Progressing ambitiously towards their clinical use, the first step is to extend the investigation to enzymatic activities in "real samples". Besides judging the potential to inhibit wound enzymes *ex vivo*, these studies are also employed to assess and compare the enzymatic activities in fluids collected from different wound types. The latter could serve as a base for the development of more accurate *in vitro* wound models by upgrading already existing ones with appropriate enzyme levels. Indeed, prior to *in vivo* assessment, single cell and models set-up around complex skin multicellular systems would allow more accurate investigation of fundamental processes such as cell-material interactions and protein synthesis in the presence of the dressing materials. To this end, wounds of varying depths and sizes could be performed on commercially available skin equivalents and parameters of wound healing (migration, proliferation and protein synthesis) monitored upon wound dressing applications in the environment with over-expressed enzymes. Such studies will be carried out during the realisation of EU project "Added value from high protein & high oil industrial co-streams" – APROPOS FP7-289170, where the GBMI group is a leader of WP3 "Up-grading intermediate products for end use applications". This WP foresees the fabrication of active medical skin care formulations and dressings similar to those developed in this thesis and their assessment in wound models.

Acknowledgments

Firstly, I would like to sincerely thank to my supervisor **Dr. Tzanko Tzanov** for the opportunity to embark on this journey and his guidance during my first years of investigation. His continued encouragement, assistance and direction have been invaluable through the realisation and completion of my PhD studies. **Благодаря!**

Secondly, I would like to express the gratitude to **Professors Georg M. Gübitz** (Institute of Environmental Biotechnology, Graz University of Technology), **Artur Cavaco-Paulo** (Department of Textile Engineering, Universidade do Minho), **Gianluca Ciardelli** (Department of Mechanics, Politecnico di Torino) and **Rui L. Reis** (3B's research group, Universidade do Minho) for the opportunities to spend short, but unforgettable moments in their research groups, work in the international environment and learn many new techniques. The acknowledgment wouldn't be complete without mentioning all their group members for fantastic receptions which made me feel like at home. Special thanks to **Dr. Iva Pashkuleva** for all the lost time and nerves after receiving my written works for improvements. **Danke! Obrigado! Grazie! Thank you!**

Much of the work, especially administrative, wouldn't be possible without the administration of the EQ department and the members of the CTT, who were always there when the bureaucracy becomes non-understandable. **Irene, Francina, Rosa, Mercè, Silvia, Susana, Clara** and others, sorry for the difficulties caused by language barriers in the beginning and **Gràcies!**

In no particular order I would like to thank to all the former and current members of the GBMI. For all the "lab" work, endless coffee breaks, laughs, and unforgettable moments and trip adventures we shared: **María, Carlos, Guillem, Gaffar, Kamelia, Mònica, Sonia, Mª Teresa, Kristina, Petya and others** who spent their time in the group for their scientific missions: **Gracias**!

When it was difficult, they were always here for me! Thanks to all of my friends, those far in Serbia as well as those who are here in Spain, for all their energy and support during these tough years. Thank you **Kizo** for the stomach and patience to hear my problems for three consecutive years. **Hvala!**

Above all I want to thank to my fiancée **Magui**, whose entrance in my life gave me the strength and will to accelerate the process of the work and completing the thesis. You have been an incredible support, motivator and encourager. Thank you for understanding all the complicated moments. Your example of success, your smile and positive energy made it possible for me. **Muito obrigado!**

This thesis I dedicated to my family for all their unquestionable support, not only during the last years, but also before this stage in my life. The biggest acknowledgment goes to my parents, **Mirjana**

and Slobodan, for the values they have taught me and the education they have provided me. No less recognition goes to my sister **Irena**, for the good (and quite difficult to follow) example you were making in every step of our childhood. **Najveće hvala!**

References

1. Bernkop-Schnürch, A., M. Hornof, and T. Zoidl, *Thiolated polymers—thiomers: synthesis and in vitro evaluation of chitosan–2-iminothiolane conjugates.* International Journal of Pharmaceutics, 2003. **260**(2): p. 229-237.
2. Lazarus, G.S., et al., *Definitions and guidelines for assessment of wounds and evaluation of healing.* Wound Repair and Regeneration, 1994. **2**(3): p. 165-170.
3. Papini, R., *Management of burn injuries of various depths.* BMJ, 2004. **329**(7458): p. 158-160.
4. Groeber, F., et al., *Skin tissue engineering — In vivo and in vitro applications.* Advanced Drug Delivery Reviews, 2011. **63**(4–5): p. 352-366.
5. Stadelmann, W.K., A.G. Digenis, and G.R. Tobin, *Physiology and healing dynamics of chronic cutaneous wounds.* The American Journal of Surgery, 1998. **176**(2, Supplement 1): p. 26S-38S.
6. Weiss, S.J., *Tissue Destruction by Neutrophils.* New England Journal of Medicine, 1989. **320**(6): p. 365-376.
7. Martin, P. and S.J. Leibovich, *Inflammatory cells during wound repair: the good, the bad and the ugly.* Trends in Cell Biology, 2005. **15**(11): p. 599-607.
8. Leibovich, S.J. and R. Ross, *The role of the macrophage in wound repair. A study with hydrocortisone and antimacrophage serum.* The American Journal of Pathology, 1975. **78**(1): p. 71-100.
9. Eming, S.A., et al., *Regulation of angiogenesis: Wound healing as a model.* Progress in Histochemistry and Cytochemistry, 2007. **42**(3): p. 115-170.
10. Diegelmann, R.F. and M.C. Evans, *Wound healing: an overview of acute, fibrotic and delayed healing.* Frontiers in bioscience, 2004. **9**: p. 283-289.
11. Bowler, P.G. and B.J. Davies, *The microbiology of infected and noninfected leg ulcers.* International Journal of Dermatology, 1999. **38**(8): p. 573-578.
12. Bowler, P.G., B.I. Duerden, and D.G. Armstrong, *Wound microbiology and associated approaches to wound management.* Clinical microbiology reviews, 2001. **14**(2): p. 244-269.
13. Diegelmann, R.F., *Excessive neutrophils characterize chronic pressure ulcers.* Wound Repair and Regeneration, 2003. **11**(6): p. 490-495.
14. Taylor, K.B., et al., *The Mechanism of Inhibition of Collagenase by TIMP-1.* Journal of Biological Chemistry, 1996. **271**(39): p. 23938-23945.
15. Wang, Y., et al., *Myeloperoxidase Inactivates TIMP-1 by Oxidizing Its N-terminal Cysteine Residue.* Journal of Biological Chemistry, 2007. **282**(44): p. 31826-31834.
16. Saarialho-Kere, U.K., *Patterns of matrix metalloproteinase and TIMP expression in chronic ulcers.* Archives of Dermatological Research, 1998. **290**(14): p. S47-S54.
17. Trengove, N.J., et al., *Analysis of the acute and chronic wound environments: the role of proteases and their inhibitors.* Wound Repair and Regeneration, 1999. **7**(6): p. 442-452.
18. Davies, M.J., *Myeloperoxidase-derived oxidation: mechanisms of biological damage and its prevention.* Journal of Clinical Biochemistry and Nutrition, 2011. **48**(1): p. 8-19.
19. Visse, R. and H. Nagase, *Matrix Metalloproteinases and Tissue Inhibitors of Metalloproteinases.* Circulation Research, 2003. **92**(8): p. 827-839.
20. Jacobsen, J.A., et al., *To bind zinc or not to bind zinc: An examination of innovative approaches to improved metalloproteinase inhibition.* Biochimica et Biophysica Acta (BBA) - Molecular Cell Research, 2010. **1803**(1): p. 72-94.
21. Parks, W.C., *Matrix metalloproteinases in repair.* Wound Repair and Regeneration, 1999. **7**(6): p. 423-432.
22. Yager, D.R. and B.C. Nwomeh, *The proteolytic environment of chronic wounds.* Wound Repair and Regeneration, 1999. **7**(6): p. 433-441.
23. Falabella, A.F., *Debridement and wound bed preparation.* Dermatologic Therapy, 2006. **19**(6): p. 317-325.

24. Wollina, U., M. Kinscher, and H. Fengler, *Maggot therapy in the treatment of wounds of exposed knee prostheses.* International Journal of Dermatology, 2005. **44**(10): p. 884-886.
25. Boateng, J.S., et al., *Wound healing dressings and drug delivery systems: a review.* Journal of pharmaceutical sciences, 2008. **97**(8): p. 2892-2923.
26. Atiyeh, B.S., et al., *Effect of silver on burn wound infection control and healing: Review of the literature.* Burns, 2007. **33**(2): p. 139-148.
27. Gupta, S., et al., *Guidelines for Managing Pressure Ulcers with Negative Pressure Wound Therapy.* Advances in Skin & Wound Care, 2004. **17**: p. 1-16.
28. Xie, X., M. McGregor, and N. Dendukuri, *The clinical effectiveness of negative pressure wound therapy: a systematic review.* Journal of wound care, 2010. **19**(11): p. 490-495.
29. Noble-Bell, G. and A. Forbes, *A systematic review of the effectiveness of negative pressure wound therapy in the management of diabetes foot ulcers.* International Wound Journal, 2008. **5**(2): p. 233-242.
30. Ubbink Dirk, T., et al. (2008) *Topical negative pressure for treating chronic wounds*. Cochrane Database of Systematic Reviews **16**, DOI: CD001898.
31. Suslick, K.S. and M.W. Grinstaff, *Protein microencapsulation of nonaqueous liquids.* Journal of the American Chemical Society, 1990. **112**(21): p. 7807-7809.
32. Ennis, W.J., et al., *Ultrasound therapy for recalcitrant diabetic foot ulcers: results of a randomized, double-blind, controlled, multicenter study.* Ostomy/wound management, 2005. **51**(8): p. 24-39.
33. Ennis, W.J., et al., *Evaluation of Clinical Effectiveness of MIST Ultrasound Therapy for the Healing of Chronic Wounds.* Advances in Skin & Wound Care, 2006. **19**(8): p. 437-446.
34. Queen, D., et al., *A dressing history.* International Wound Journal, 2004. **1**(1): p. 59-77.
35. Kim, I.-Y., et al., *Chitosan and its derivatives for tissue engineering applications.* Biotechnology Advances, 2008. **26**(1): p. 1-21.
36. Synowiecki, J. and N.A. Al-Khateeb, *Production, Properties, and Some New Applications of Chitin and Its Derivatives.* Critical Reviews in Food Science and Nutrition, 2003. **43**(2): p. 145-171.
37. Pa, J.-H. and T.L. Yu, *Light Scattering Study of Chitosan in Acetic Acid Aqueous Solutions.* Macromolecular Chemistry and Physics, 2001. **202**(7): p. 985-991.
38. Ohkawa, K., et al., *Electrospinning of Chitosan.* Macromolecular Rapid Communications, 2004. **25**(18): p. 1600-1605.
39. Ueno, H., et al., *Accelerating effects of chitosan for healing at early phase of experimental open wound in dogs.* Biomaterials, 1999. **20**(15): p. 1407-1414.
40. Wedmore, I., et al., *A Special Report on the Chitosan-based Hemostatic Dressing: Experience in Current Combat Operations.* The Journal of Trauma and Acute Care Surgery, 2006. **60**(3): p. 655-658 10.1097/01.ta.0000199392.91772.44.
41. Pietramaggiori, G., et al., *Effects of Poly-N-acetyl Glucosamine (pGlcNAc) Patch on Wound Healing in db/db Mouse.* The Journal of Trauma and Acute Care Surgery, 2008. **64**(3): p. 803-808 10.1097/01.ta.0000244382.13937.a8.
42. Shi, C., et al., *Therapeutic Potential of Chitosan and Its Derivatives in Regenerative Medicine.* Journal of Surgical Research, 2006. **133**(2): p. 185-192.
43. Zhu, A.-P. and N. Fang, *Adhesion Dynamics, Morphology, and Organization of 3T3 Fibroblast on Chitosan and Its Derivative: The Effect of O-Carboxymethylation.* Biomacromolecules, 2005. **6**(5): p. 2607-2614.
44. Lopez-Perez, P.M., et al., *Effect of chitosan membrane surface modification via plasma induced polymerization on the adhesion of osteoblast-like cells.* Journal of Materials Chemistry, 2007. **17**(38): p. 4064-4071.
45. Alves, N.M. and J.F. Mano, *Chitosan derivatives obtained by chemical modifications for biomedical and environmental applications.* International Journal of Biological Macromolecules, 2008. **43**(5): p. 401-414.
46. Khor, E., *Methods for the treatment of collagenous tissues for bioprostheses.* Biomaterials, 1997. **18**(2): p. 95-105.
47. Ruszczak, Z., *Effect of collagen matrices on dermal wound healing.* Advanced Drug Delivery Reviews, 2003. **55**(12): p. 1595-1611.

48. Schoof, H., et al., *Control of pore structure and size in freeze-dried collagen sponges.* Journal of Biomedical Materials Research, 2001. **58**(4): p. 352-357.
49. O'Brien, F.J., et al., *The effect of pore size on cell adhesion in collagen-GAG scaffolds.* Biomaterials, 2005. **26**(4): p. 433-441.
50. Ruszczak, Z. and W. Friess, *Collagen as a carrier for on-site delivery of antibacterial drugs.* Advanced Drug Delivery Reviews, 2003. **55**(12): p. 1679-1698.
51. Sai K, P. and M. Babu, *Collagen based dressings a review.* Burns, 2000. **26**(1): p. 54-62.
52. Mian, M., F. Beghè, and E. Mian, *Collagen as a pharmacological approach in wound healing.* International journal of tissue reactions, 1992. **14 Suppl**: p. 1-9.
53. Dhanasingh, A., et al., *Tailored hyaluronic acid hydrogels through hydrophilic prepolymer cross-linkers.* Soft Matter, 2010. **6**(3): p. 618-629.
54. Baeurle, S.A., et al., *Effect of the counterion behavior on the frictional–compressive properties of chondroitin sulfate solutions.* Polymer, 2009. **50**(7): p. 1805-1813.
55. Gilbert, M.E., et al., *Chondroitin Sulfate Hydrogel and Wound Healing in Rabbit Maxillary Sinus Mucosa.* The Laryngoscope, 2004. **114**(8): p. 1406-1409.
56. West, D., et al., *Angiogenesis induced by degradation products of hyaluronic acid.* Science, 1985. **228**(4705): p. 1324-1326.
57. Perng, C.-K., et al., *In Vivo Angiogenesis Effect of Porous Collagen Scaffold with Hyaluronic Acid Oligosaccharides.* Journal of Surgical Research, 2011. **168**(1): p. 9-15.
58. Hsieh, Y.-S., et al., *Effects of different molecular weight hyaluronan products on the expression of urokinase plasminogen activator and inhibitor and gelatinases during the early stage of osteoarthritis.* Journal of Orthopaedic Research, 2008. **26**(4): p. 475-484.
59. Kawasaki, K., et al., *Hyaluronic acid enhances proliferation and chondroitin sulfate synthesis in cultured chondrocytes embedded in collagen gels.* Journal of Cellular Physiology, 1999. **179**(2): p. 142-148.
60. Segura, T., et al., *Crosslinked hyaluronic acid hydrogels: a strategy to functionalize and pattern.* Biomaterials, 2005. **26**(4): p. 359-371.
61. Luo, Y., K.R. Kirker, and G.D. Prestwich, *Cross-linked hyaluronic acid hydrogel films: new biomaterials for drug delivery.* Journal of Controlled Release, 2000. **69**(1): p. 169-184.
62. Lin, Y.-C., et al., *Synthesis and characterization of collagen/hyaluronan/chitosan composite sponges for potential biomedical applications.* Acta Biomaterialia, 2009. **5**(7): p. 2591-2600.
63. Chang, C.-H., et al., *Gelatin–chondroitin–hyaluronan tri-copolymer scaffold for cartilage tissue engineering.* Biomaterials, 2003. **24**(26): p. 4853-4858.
64. Yerushalmi, N., A. Arad, and R. Margalit, *Molecular and Cellular Studies of Hyaluronic Acid-Modified Liposomes as Bioadhesive Carriers for Topical Drug Delivery in Wound Healing.* Archives of Biochemistry and Biophysics, 1994. **313**(2): p. 267-273.
65. Voinchet, V., P. Vasseur, and J. Kern, *Efficacy and Safety of Hyaluronic Acid in the Management of Acute Wounds.* American Journal of Clinical Dermatology, 2006. **7**(6): p. 353-357.
66. Muzzarelli, R., *Chitins and chitosans for the repair of wounded skin, nerve, cartilage and bone.* Carbohydrate polymers., 2009. **76**(2): p. 167-182.
67. Kim, M.-M. and S.-K. Kim, *Chitooligosaccharides inhibit activation and expression of matrix metalloproteinase-2 in human dermal fibroblasts.* FEBS Letters, 2006. **580**(11): p. 2661-2666.
68. Van Ta, Q., M.-M. Kim, and S.-K. Kim, *Inhibitory Effect of Chitooligosaccharides on Matrix Metalloproteinase-9 in Human Fibrosarcoma Cells (HT1080).* Marine Biotechnology, 2006. **8**(6): p. 593-599.
69. Gorzelanny, C., et al., *Specific Interaction between Chitosan and Matrix Metalloprotease 2 Decreases the Invasive Activity of Human Melanoma Cells.* Biomacromolecules, 2007. **8**(10): p. 3035-3040.
70. Cullen, B., et al., *The role of oxidised regenerated cellulose/collagen in chronic wound repair and its potential mechanism of action.* The International Journal of Biochemistry & Cell Biology, 2002. **34**(12): p. 1544-1556.
71. Metzmacher, I., et al., *A model describing the effect of enzymatic degradation on drug release from collagen minirods.* Eur J Pharm Biopharm, 2007. **67**(2): p. 349-360.

72. Seaman, S., *Dressing selection in chronic wound management.* Journal of the American Podiatric Medical Association, 2002. **92**(1): p. 24-33.
73. Giles, N.M., et al., *Metal and Redox Modulation of Cysteine Protein Function.* Chemistry & biology, 2003. **10**(8): p. 677-693.
74. Gu, Z., et al., *S-Nitrosylation of Matrix Metalloproteinases: Signaling Pathway to Neuronal Cell Death.* Science, 2002. **297**(5584): p. 1186-1190.
75. Andreassen, O.A., et al., *N-acetyl-L-cysteine improves survival and preserves motor performance in an animal model of familial amyotrophic lateral sclerosis.* Neuroreport, 2000. **11**(11): p. 2491-2493.
76. Marchant, N.S., Dickens Jr., Elmer Douglas, Kemp, Shannon M., *Inhibition of matrix metalloproteinases with polymers and pharmaceutical applications thereof*, T.B.F.G. Company, Editor. 2000 USA.
77. Bloor, S., *Use of acetylcysteine for the manufacture of a medicament for the treatment of chronic ulcers*, E. Patent, Editor. 2003, Johnson & Johnson Medical Ltd.
78. Fu, X., et al., *Hypochlorous Acid Oxygenates the Cysteine Switch Domain of Pro-matrilysin (MMP-7).* Journal of Biological Chemistry, 2001. **276**(44): p. 41279-41287.
79. Van Antwerpen, P., et al., *Thiol-containing molecules interact with the myeloperoxidase/H2O2/chloride system to inhibit LDL oxidation.* Biochemical and Biophysical Research Communications, 2005. **337**(1): p. 82-88.
80. Rice-Evans, C.A., N.J. Miller, and G. Paganga, *Structure-antioxidant activity relationships of flavonoids and phenolic acids.* Free Radical Biology and Medicine, 1996. **20**(7): p. 933-956.
81. Mira, L., et al., *Interactions of flavonoids with iron and copper ions: a mechanism for their antioxidant activity.* Free radical research, 2002. **36**(11): p. 1199-1208.
82. Pauff, J.M. and R. Hille, *Inhibition Studies of Bovine Xanthine Oxidase by Luteolin, Silibinin, Quercetin, and Curcumin.* Journal of Natural Products, 2009. **72**(4): p. 725-731.
83. Ding, Z., et al., *Anti-Inflammatory Effects of Scopoletin and Underlying Mechanisms.* Pharmaceutical Biology, 2008. **46**(12): p. 854-860.
84. Geyid, A., et al., *Screening of some medicinal plants of Ethiopia for their anti-microbial properties and chemical profiles.* Journal of Ethnopharmacology, 2005. **97**(3): p. 421-427.
85. Landi Librandi, A.P., et al., *Effect of the extract of the tamarind (Tamarindus indica) fruit on the complement system: Studies in vitro and in hamsters submitted to a cholesterol-enriched diet.* Food and Chemical Toxicology, 2007. **45**(8): p. 1487-1495.
86. Kim, H., et al., *Enhanced wound healing by an epigallocatechin gallate-incorporated collagen sponge in diabetic mice.* Wound Repair and Regeneration, 2008. **16**(5): p. 714-720.
87. Masaki, H., T. Atsumi, and H. Sakurai, *Protective activity of hamamelitannin on cell damage of murine skin fibroblasts induced by UVB irradiation.* Journal of Dermatological Science, 1995. **10**(1): p. 25-34.
88. Deters, A., et al., *High molecular compounds (polysaccharides and proanthocyanidins) from Hamamelis virginiana bark: influence on human skin keratinocyte proliferation and differentiation and influence on irritated skin.* Phytochemistry, 2001. **58**(6): p. 949-958.
89. Kato, Y., et al., *Inhibition of Myeloperoxidase-catalyzed Tyrosylation by Phenolic Antioxidants in vitro*. Bioscience, Biotechnology, and Biochemistry, 2003. **67**(5): p. 1136-1139.
90. Madhan, B., et al., *Role of green tea polyphenols in the inhibition of collagenolytic activity by collagenase.* International Journal of Biological Macromolecules, 2007. **41**(1): p. 16-22.
91. Haslam, E., *Natural Polyphenols (Vegetable Tannins) as Drugs: Possible Modes of Action.* Journal of Natural Products, 1996. **59**(2): p. 205-215.
92. Muzzarelli, R.A.A., G. Barontini, and R. Rochetti, *Isolation of lysozyme on chitosan.* Biotechnology and Bioengineering, 1978. **20**(1): p. 87-94.
93. Jin, R., et al., *Injectable chitosan-based hydrogels for cartilage tissue engineering.* Biomaterials, 2009. **30**(13): p. 2544-2551.
94. Harish Prashanth, K.V. and R.N. Tharanathan, *Chitin/chitosan: modifications and their unlimited application potential—an overview*. Trends in Food Science & Technology, 2007. **18**(3): p. 117-131.

95. Chen, X.-G., et al., *The effect of carboxymethyl-chitosan on proliferation and collagen secretion of normal and keloid skin fibroblasts.* Biomaterials, 2002. **23**(23): p. 4609-4614.
96. Janvikul, W., et al., *Fibroblast interaction with carboxymethylchitosan-based hydrogels.* Journal of Materials Science: Materials in Medicine, 2007. **18**(5): p. 943-949.
97. Fei Liu, X., et al., *Antibacterial action of chitosan and carboxymethylated chitosan.* Journal of Applied Polymer Science, 2001. **79**(7): p. 1324-1335.
98. Chen, L., Z. Tian, and Y. Du, *Synthesis and pH sensitivity of carboxymethyl chitosan-based polyampholyte hydrogels for protein carrier matrices.* Biomaterials, 2004. **25**(17): p. 3725-3732.
99. Lin, Y.-H., et al., *Physically crosslinked alginate/N,O-carboxymethyl chitosan hydrogels with calcium for oral delivery of protein drugs.* Biomaterials, 2005. **26**(14): p. 2105-2113.
100. Hirano, S., Y. Yamaguchi, and M. Kamiya, *Novel N-saturated-fatty-acyl derivatives of chitosan soluble in water and in aqueous acid and alkaline solutions.* Carbohydrate Polymers, 2002. **48**(2): p. 203-207.
101. Hu, Y., et al., *Self-aggregation and antibacterial activity of N-acylated chitosan.* Polymer, 2007. **48**(11): p. 3098-3106.
102. Mourya, V.K. and N.N. Inamdar, *Chitosan-modifications and applications: Opportunities galore.* Reactive and Functional Polymers, 2008. **68**(6): p. 1013-1051.
103. Hirano, S., *Chitin and chitosan as novel biotechnological materials.* Polymer International, 1999. **48**(8): p. 732-734.
104. Drozd, N.N., et al., *Comparison of Antithrombin Activity of the Polysulphate Chitosan Derivatives in In Vivo and In Vitro System.* Thrombosis Research, 2001. **102**(5): p. 445-455.
105. Amaral, I.F., P.L. Granja, and M.A. Barbosa, *Chemical modification of chitosan by phosphorylation: an XPS, FT-IR and SEM study.* Journal of Biomaterials Science, Polymer Edition, 2005. **16**(12): p. 1575-1593.
106. Lopez-Perez, P.M., et al., *Surface phosphorylation of chitosan significantly improves osteoblast cell viability, attachment and proliferation.* Journal of Materials Chemistry, 2010. **20**(3): p. 483-491.
107. Miyatake, K., et al., *Anti-inflammatory effect of chemically modified chitin.* Carbohydrate Polymers, 2003. **53**(4): p. 417-423.
108. Bernkop-Schnürch, A., M. Hornof, and D. Guggi, *Thiolated chitosans.* European Journal of Pharmaceutics and Biopharmaceutics, 2004. **57**(1): p. 9-17.
109. Bernkop-Schnürch, A., C.E. Kast, and D. Guggi, *Permeation enhancing polymers in oral delivery of hydrophilic macromolecules: thiomer/GSH systems.* Journal of Controlled Release, 2003. **93**(2): p. 95-103.
110. Roldo, M., et al., *Mucoadhesive thiolated chitosans as platforms for oral controlled drug delivery: synthesis and in vitro evaluation.* European Journal of Pharmaceutics and Biopharmaceutics, 2004. **57**(1): p. 115-121.
111. Föger, F., T. Schmitz, and A. Bernkop-Schnürch, *In vivo evaluation of an oral delivery system for P-gp substrates based on thiolated chitosan.* Biomaterials, 2006. **27**(23): p. 4250-4255.
112. Kast, C.E. and A. Bernkop-Schnürch, *Thiolated polymers — thiomers: development and in vitro evaluation of chitosan–thioglycolic acid conjugates.* Biomaterials, 2001. **22**(17): p. 2345-2352.
113. Kast, C.E., et al., *Chitosan-thioglycolic acid conjugate: a new scaffold material for tissue engineering?* International Journal of Pharmaceutics, 2003. **256**(1–2): p. 183-189.
114. Schmidt, R.J., *Modified polysaccharides containing thiol groups*. 2003, Johnson & Johnson Medical.
115. Curti, E., D. de Britto, and S.P. Campana-Filho, *Methylation of Chitosan with Iodomethane: Effect of Reaction Conditions on Chemoselectivity and Degree of Substitution.* Macromolecular bioscience, 2003. **3**(10): p. 571-576.
116. Jia, Z., D. shen, and W. Xu, *Synthesis and antibacterial activities of quaternary ammonium salt of chitosan.* Carbohydrate Research, 2001. **333**(1): p. 1-6.

117. Avadi, M.R., et al., *Diethylmethyl chitosan as an antimicrobial agent: Synthesis, characterization and antibacterial effects.* European Polymer Journal, 2004. **40**(7): p. 1355-1361.
118. Guo, Z., et al., *Antifungal properties of Schiff bases of chitosan, N-substituted chitosan and quaternized chitosan.* Carbohydrate Research, 2007. **342**(10): p. 1329-1332.
119. Guo, Z., et al., *Hydroxyl radicals scavenging activity of N-substituted chitosan and quaternized chitosan.* Bioorganic & Medicinal Chemistry Letters, 2006. **16**(24): p. 6348-6350.
120. Bernkop-Schnürch, A. and M.E. Krajicek, *Mucoadhesive polymers as platforms for peroral peptide delivery and absorption: synthesis and evaluation of different chitosan–EDTA conjugates.* Journal of Controlled Release, 1998. **50**(1–3): p. 215-223.
121. Prabaharan, M. and J.F. Mano, *Chitosan derivatives bearing cyclodextrin cavitiesas novel adsorbent matrices.* Carbohydrate Polymers, 2006. **63**(2): p. 153-166.
122. Krauland, A.H. and M.J. Alonso, *Chitosan/cyclodextrin nanoparticles as macromolecular drug delivery system.* International Journal of Pharmaceutics, 2007. **340**(1–2): p. 134-142.
123. Leung, H.-W., *Ecotoxicology of Glutaraldehyde: Review of Environmental Fate and Effects Studies.* Ecotoxicology and Environmental Safety, 2001. **49**(1): p. 26-39.
124. Muzzarelli, R.A.A., *Genipin-crosslinked chitosan hydrogels as biomedical and pharmaceutical aids.* Carbohydrate Polymers, 2009. **77**(1): p. 1-9.
125. Moura, M.J., M.M. Figueiredo, and M.H. Gil, *Rheological Study of Genipin Cross-Linked Chitosan Hydrogels.* Biomacromolecules, 2007. **8**(12): p. 3823-3829.
126. Mi, F.-L., et al., *In vitro evaluation of a chitosan membrane cross-linked with genipin.* Journal of Biomaterials Science, Polymer Edition, 2001. **12**(8): p. 835-850.
127. Sundararaghavan, H.G., et al., *Genipin-induced changes in collagen gels: Correlation of mechanical properties to fluorescence.* Journal of Biomedical Materials Research Part A, 2008. **87A**(2): p. 308-320.
128. Sung, H.-W., et al., *Mechanical properties of a porcine aortic valve fixed with a naturally occurring crosslinking agent.* Biomaterials, 1999. **20**(19): p. 1759-1772.
129. Sung, H.-W., et al., *Crosslinking characteristics and mechanical properties of a bovine pericardium fixed with a naturally occurring crosslinking agent.* Journal of Biomedical Materials Research, 1999. **47**(2): p. 116-126.
130. Chiono, V., et al., *Genipin-crosslinked chitosan/gelatin blends for biomedical applications.* Journal of Materials Science: Materials in Medicine, 2008. **19**(2): p. 889-898.
131. Ruoslahti, E., *RGD and other recognition sequences for integrins.* Annual review of cell and developmental biology, 1996. **12**: p. 697-715.
132. Thein-Han, W.W., et al., *Chitosan–gelatin scaffolds for tissue engineering: Physico-chemical properties and biological response of buffalo embryonic stem cells and transfectant of GFP–buffalo embryonic stem cells.* Acta Biomaterialia, 2009. **5**(9): p. 3453-3466.
133. Kim, W.-S., et al., *Wound healing effect of adipose-derived stem cells: A critical role of secretory factors on human dermal fibroblasts.* Journal of Dermatological Science, 2007. **48**(1): p. 15-24.
134. Altman, A.M., et al., *Dermal matrix as a carrier for in vivo delivery of human adipose-derived stem cells.* Biomaterials, 2008. **29**(10): p. 1431-1442.
135. Chen, K.-Y., et al., *Asymmetric Chitosan Membrane Containing Collagen I Nanospheres for Skin Tissue Engineering.* Biomacromolecules, 2009. **10**(6): p. 1642-1649.
136. Williams, A. and I.T. Ibrahim, *Carbodiimide chemistry: recent advances.* Chemical Reviews, 1981. **81**(6): p. 589-636.
137. Everaerts, F., et al., *Biomechanical properties of carbodiimide crosslinked collagen: Influence of the formation of ester crosslinks.* Journal of Biomedical Materials Research Part A, 2008. **85A**(2): p. 547-555.
138. Wang, X.H., et al., *Preparation and Characterization of Collagen/Chitosan Matrices As Potential Biomaterials.* Journal of Bioactive and Compatible Polymers, 2003. **18**(6): p. 453-467.
139. Gübitz, G.M. and A.C. Paulo, *New substrates for reliable enzymes: enzymatic modification of polymers.* Current Opinion in Biotechnology, 2003. **14**(6): p. 577-582.

140. Kumar, G., P.J. Smith, and G.F. Payne, *Enzymatic grafting of a natural product onto chitosan to confer water solubility under basic conditions.* Biotechnology and Bioengineering, 1999. **63**(2): p. 154-165.
141. Yamada, K., et al., *Chitosan based water-resistant adhesive. Analogy to mussel glue.* Biomacromolecules, 2000. **1**(2): p. 252-258.
142. Kumar, G., et al., *Enzymatic gelation of the natural polymer chitosan.* Polymer, 2000. **41**(6): p. 2157-2168.
143. Shao, L., et al., *Enzymatic modification of the synthetic polymer polyhydroxystyrene.* Enzyme and Microbial Technology, 1999. **25**(8–9): p. 660-668.
144. Anghileri, A., et al., *Tyrosinase-catalyzed grafting of sericin peptides onto chitosan and production of protein–polysaccharide bioconjugates.* Journal of Biotechnology, 2007. **127**(3): p. 508-519.
145. Sampaio, S., et al., *Enzymatic grafting of chitosan onto Bombyx mori silk fibroin: kinetic and IR vibrational studies.* Journal of Biotechnology, 2005. **116**(1): p. 21-33.
146. Chen, T., et al., *Enzyme-catalyzed gel formation of gelatin and chitosan: potential for in situ applications.* Biomaterials, 2003. **24**(17): p. 2831-2841.
147. Kurisawa, M., et al., *Injectable biodegradable hydrogels composed of hyaluronic acid-tyramine conjugates for drug delivery and tissue engineering.* Chemical Communications, 2005(34): p. 4312-4314.
148. Sakai, S. and K. Kawakami, *Synthesis and characterization of both ionically and enzymatically cross-linkable alginate.* Acta Biomaterialia, 2007. **3**(4): p. 495-501.
149. Jin, R., et al., *Enzyme-mediated fast in situ formation of hydrogels from dextran–tyramine conjugates.* Biomaterials, 2007. **28**(18): p. 2791-2800.
150. Ogushi, Y., S. Sakai, and K. Kawakami, *Synthesis of enzymatically-gellable carboxymethylcellulose for biomedical applications.* Journal of Bioscience and Bioengineering, 2007. **104**(1): p. 30-33.
151. Sakai, S., et al., *Novel chitosan derivative soluble at neutral pH and in-situ gellable via peroxidase-catalyzed enzymatic reaction.* Journal of Materials Chemistry, 2009. **19**(2): p. 230-235.
152. Sakai, S., et al., *An injectable, in situ enzymatically gellable, gelatin derivative for drug delivery and tissue engineering.* Biomaterials, 2009. **30**(20): p. 3371-3377.
153. Sakai, S., et al., *In Situ Simultaneous Protein−Polysaccharide Bioconjugation and Hydrogelation Using Horseradish Peroxidase.* Biomacromolecules, 2010. **11**(5): p. 1370-1375.
154. Fu, J.-Y., et al., *Characterization of Three Chitosanase Isozymes Isolated from a Commercial Crude Porcine Pepsin Preparation.* Journal of Agricultural and Food Chemistry, 2003. **51**(4): p. 1042-1048.
155. Minagawa, T., et al., *Effects of molecular weight and deacetylation degree of chitin/chitosan on wound healing.* Carbohydrate Polymers, 2007. **67**(4): p. 640-644.
156. Huang, R.-L., et al., *Dietary oligochitosan supplementation enhances immune status of broilers.* Journal of the Science of Food and Agriculture, 2007. **87**(1): p. 153-159.
157. Cullen, B., et al., *Mechanism of action of PROMOGRAN, a protease modulating matrix, for the treatment of diabetic foot ulcers.* Wound Repair Regen, 2002. **10**(1): p. 16-25.
158. Jarman-Smith, M., et al., *Porcine collagen crosslinking, degradation and its capability for fibroblast adhesion and proliferation.* J Mater Sci Mater Med, 2004. **15**(8): p. 925-932.
159. Harley, B.A., et al., *Mechanical characterization of collagen–glycosaminoglycan scaffolds.* Acta Biomater, 2007. **3**(4): p. 463-474.
160. Lin, Y.-C., et al., *Synthesis and characterization of collagen/hyaluronan/chitosan composite sponges for potential biomedical applications.* Acta Biomater, 2009. **5**(7): p. 2591-2600.
161. Pachence, J.M., *Collagen-based devices for soft tissue repair.* Journal of Biomedical Materials Research, 1996. **33**(1): p. 35-40.
162. Mi, F.-L., et al., *In vivo biocompatibility and degradability of a novel injectable-chitosan-based implant.* Biomaterials, 2002. **23**(1): p. 181-191.
163. Silva, S.S., et al., *Novel Genipin-Cross-Linked Chitosan/Silk Fibroin Sponges for Cartilage Engineering Strategies.* Biomacromolecules, 2008. **9**(10): p. 2764-2774.

164. Kesava Reddy, G. and C.S. Enwemeka, *A simplified method for the analysis of hydroxyproline in biological tissues.* Clin Biochem, 1996. **29**(3): p. 225-229.
165. Edwards, C.A. and W.D. O'Brien Jr, *Modified assay for determination of hydroxyproline in a tissue hydrolyzate.* Clin Chim Acta, 1980. **104**(2): p. 161-167.
166. Davidenko, N., et al., *Collagen–hyaluronic acid scaffolds for adipose tissue engineering.* Acta Biomater, 2010. **6**(10): p. 3957-3968.
167. Mi, F.-L., S.-S. Shyu, and C.-K. Peng, *Characterization of ring-opening polymerization of genipin and pH-dependent cross-linking reactions between chitosan and genipin.* Journal of Polymer Science Part A: Polymer Chemistry, 2005. **43**(10): p. 1985-2000.
168. Butler, M.F., Y.-F. Ng, and P.D.A. Pudney, *Mechanism and kinetics of the crosslinking reaction between biopolymers containing primary amine groups and genipin.* Journal of Polymer Science Part A: Polymer Chemistry, 2003. **41**(24): p. 3941-3953.
169. Yan, L.-P., et al., *Genipin-cross-linked collagen/chitosan biomimetic scaffolds for articular cartilage tissue engineering applications.* J Biomed Mater Res A, 2010. **95A**(2): p. 465-475.
170. Lien, S.-M., L.-Y. Ko, and T.-J. Huang, *Effect of pore size on ECM secretion and cell growth in gelatin scaffold for articular cartilage tissue engineering.* Acta Biomaterialia, 2009. **5**(2): p. 670-679.
171. Ma, L., et al., *Collagen/chitosan porous scaffolds with improved biostability for skin tissue engineering.* Biomaterials, 2003. **24**(26): p. 4833-4841.
172. Madhavan, K., et al., *Evaluation of composition and crosslinking effects on collagen-based composite constructs.* Acta Biomater, 2010. **6**(4): p. 1413-1422.
173. Avila, M.Y. and J.L. Navia, *Effect of genipin collagen crosslinking on porcine corneas.* Journal of cataract and refractive surgery, 2010. **36**(4): p. 659-664.
174. Adekogbe, I. and A. Ghanem, *Fabrication and characterization of DTBP-crosslinked chitosan scaffolds for skin tissue engineering.* Biomaterials, 2005. **26**(35): p. 7241-7250.
175. Park, S.-N., et al., *Characterization of porous collagen/hyaluronic acid scaffold modified by 1-ethyl-3-(3-dimethylaminopropyl)carbodiimide cross-linking.* Biomaterials, 2002. **23**(4): p. 1205-1212.
176. Edwards, J.V. and P.S. Howley, *Human neutrophil elastase and collagenase sequestration with phosphorylated cotton wound dressings.* J Biomed Mater Res A, 2007. **83A**(2): p. 446-454.
177. Metzmacher, I., et al., *In vitro binding of matrix metalloproteinase-2 (MMP-2), MMP-9, and bacterial collagenase on collagenous wound dressings.* Wound Repair Regen, 2007. **15**(4): p. 549-555.
178. Rojkind, M., et al., *Role of hydrogen peroxide and oxidative stress in healing responses.* Cellular and Molecular Life Sciences, 2002. **59**(11): p. 1872-1891.
179. Ovington, L., *Advances in wound dressings.* Clin Dermatol, 2007. **25**(1): p. 33-38.
180. Haslam, E., *Natural Polyphenols (Vegetable Tannins) as Drugs: Possible Modes of Action.* J Nat Prod, 1996. **59**(2): p. 205-215.
181. Kapoor, M., et al., *Effects of Epicatechin Gallate on Wound Healing and Scar Formation in a Full Thickness Incisional Wound Healing Model in Rats.* The American Journal of Pathology, 2004. **165**(1): p. 299-307.
182. Kim, H., et al., *Enhanced wound healing by an epigallocatechin gallate-incorporated collagen sponge in diabetic mice.* Wound Repair Regen, 2008. **16**(5): p. 714-720.
183. Amaral, S., et al., *Plant extracts with anti-inflammatory properties—A new approach for characterization of their bioactive compounds and establishment of structure–antioxidant activity relationships.* Bioorganic & Medicinal Chemistry, 2009. **17**(5): p. 1876-1883.
184. Díaz-GonzáLez, M., et al., *Inhibition of deleterious chronic wound enzymes with plant polyphenols.* Biocatal Biotransform, 2012. **30**(1): p. 102-110.
185. Madhan, B., et al., *Stabilization of collagen using plant polyphenol: Role of catechin.* Int J Biol Macromol, 2005. **37**(1–2): p. 47-53.
186. Touriño, S., et al., *Highly Galloylated Tannin Fractions from Witch Hazel (Hamamelis virginiana) Bark: Electron Transfer Capacity, In Vitro Antioxidant Activity, and Effects on Skin-Related Cells.* Chemical Research in Toxicology, 2008. **21**(3): p. 696-704.

187. Madhan, B., et al., *Role of green tea polyphenols in the inhibition of collagenolytic activity by collagenase.* Int J Biol Macromol, 2007. **41**(1): p. 16-22.
188. Singleton, V.L., R. Orthofer, and R.M. Lamuela-Raventós, *[14] Analysis of total phenols and other oxidation substrates and antioxidants by means of folin-ciocalteu reagent*, in *Methods in Enzymology*, P. Lester, Editor. 1999, Academic Press. p. 152-178.
189. Van Wart, H.E. and D.R. Steinbrink, *A continuous spectrophotometric assay for Clostridium histolyticum collagenase.* Anal Biochem, 1981. **113**(2): p. 356-365.
190. Nicholls, S.J. and S.L. Hazen, *Myeloperoxidase and Cardiovascular Disease.* Arterioscler Thromb Vasc Biol, 2005. **25**(6): p. 1102-1111.
191. Fu, X., et al., *Hypochlorous Acid Oxygenates the Cysteine Switch Domain of Pro-matrilysin (MMP-7).* J Biol Chem, 2001. **276**(44): p. 41279-41287.
192. Jackson, J., et al., *The inhibition of collagenase induced degradation of collagen by the galloyl-containing polyphenols tannic acid, epigallocatechin gallate and epicatechin gallate.* Journal of Materials Science: Materials in Medicine, 2010. **21**(5): p. 1435-1443.
193. Kumar, M.S., et al., *Triphala Incorporated Collagen Sponge—A Smart Biomaterial for Infected Dermal Wound Healing.* Journal of Surgical Research, 2010. **158**(1): p. 162-170.
194. Poon, V.K.M. and A. Burd, *In vitro cytotoxity of silver: implication for clinical wound care.* Burns, 2004. **30**(2): p. 140-147.
195. Babich, H. and F. Visioli, *In vitro cytotoxicity to human cells in culture of some phenolics from olive oil.* Il Farmaco, 2003. **58**(5): p. 403-407.
196. Han, B., et al., *Proanthocyanidin: A natural crosslinking reagent for stabilizing collagen matrices.* Journal of Biomedical Materials Research Part A, 2003. **65A**(1): p. 118-124.
197. Popa, M.-I., et al., *Study of the interactions between polyphenolic compounds and chitosan.* React Funct Polym, 2000. **45**(1): p. 35-43.
198. Wang, Y.-W., Q. Wu, and G.-Q. Chen, *Reduced mouse fibroblast cell growth by increased hydrophilicity of microbial polyhydroxyalkanoates via hyaluronan coating.* Biomaterials, 2003. **24**(25): p. 4621-4629.
199. Maharjan, A.S., D. Pilling, and R.H. Gomer, *High and Low Molecular Weight Hyaluronic Acid Differentially Regulate Human Fibrocyte Differentiation.* PLoS ONE, 2011. **6**(10): p. e26078.
200. Deed, R., et al., *Early-response gene signalling is induced by angiogenic oligosaccharides of hyaluronan in endothelial cells. Inhibition by non-angiogenic, high-molecular-weight hyaluronan.* International Journal of Cancer, 1997. **71**(2): p. 251-256.
201. Schramm, H.J. and T. Dülffer, *Synthesis and application of cleavable and hydrophilic crosslinking reagents.* Advances in experimental medicine and biology, 1977. **86A**: p. 197-206.
202. Jue, R., et al., *Addition of sulfhydryl groups of Escherichia coli ribosomes by protein modification with 2-iminothiolane (methyl 4-mercaptobutyrimidate).* Biochemistry, 1978. **17**(25): p. 5399-5406.
203. Hand, E.S. and W.P. Jencks, *Mechanism of the Reaction of Imido Esters with Amines.* Journal of the American Chemical Society, 1962. **84**(18): p. 3505-3514.
204. Charulatha, V. and A. Rajaram, *Dimethyl 3,3'-dithiobispropionimidate: A novel crosslinking reagent for collagen.* Journal of Biomedical Materials Research, 2001. **54**(1): p. 122-128.
205. Mattson, G., et al., *A practical approach to crosslinking.* Molecular Biology Reports, 1993. **17**(3): p. 167-183.
206. Yager, D.R., R.A. Kulina, and L.A. Gilman, *Wound Fluids: A Window Into the Wound Environment?* The International Journal of Lower Extremity Wounds, 2007. **6**(4): p. 262-272.
207. Nicholls, S.J. and S.L. Hazen, *Myeloperoxidase, modified lipoproteins, and atherogenesis.* Journal of Lipid Research, 2009. **50**(Supplement): p. S346-S351.
208. Fisher, J. and S. Mobashery, *Recent advances in MMP inhibitor design.* Cancer and Metastasis Reviews, 2006. **25**(1): p. 115-136.
209. Bernkop-Schnürch, A., H. Zarti, and G.F. Walker, *Thiolation of polycarbophil enhances its inhibition of intestinal brush border membrane bound aminopeptidase N.* Journal of pharmaceutical sciences, 2001. **90**(11): p. 1907-1914.

210. Bravo-Osuna, I., et al., *Effect of chitosan and thiolated chitosan coating on the inhibition behaviour of PIBCA nanoparticles against intestinal metallopeptidases.* Journal of Nanoparticle Research, 2008. **10**(8): p. 1293-1301.
211. Morin, R.J. and N.L. Tomaselli, *Interactive Dressings and Topical Agents.* Clinics in Plastic Surgery, 2007. **34**(4): p. 643-658.
212. Falconnet, D., et al., *Surface engineering approaches to micropattern surfaces for cell-based assays.* Biomaterials, 2006. **27**(16): p. 3044-3063.
213. Hong, R., et al., *Control of Protein Structure and Function through Surface Recognition by Tailored Nanoparticle Scaffolds.* Journal of the American Chemical Society, 2004. **126**(3): p. 739-743.
214. Orelma, H., et al., *Modification of Cellulose Films by Adsorption of CMC and Chitosan for Controlled Attachment of Biomolecules.* Biomacromolecules, 2011. **12**(12): p. 4311-4318.
215. Kommireddy, D.S., et al., *Stem cell attachment to layer-by-layer assembled TiO2 nanoparticle thin films.* Biomaterials, 2006. **27**(24): p. 4296-4303.
216. Ariga, K., J.P. Hill, and Q. Ji, *Layer-by-layer assembly as a versatile bottom-up nanofabrication technique for exploratory research and realistic application.* Physical Chemistry Chemical Physics, 2007. **9**(19): p. 2319-2340.
217. Detzel, C.J., A.L. Larkin, and P. Rajagopalan, *Polyelectrolyte multilayers in tissue engineering.* Tissue engineering. Part B, Reviews, 2011. **17**(2): p. 101-113.
218. Martins, G.V., et al., *Crosslink effect and albumin adsorption onto chitosan/alginate multilayered systems: an in situ QCM-D study.* Macromolecular bioscience, 2010. **10**(12): p. 1444-1455.
219. Brown, M.B. and S.A. Jones, *Hyaluronic acid: a unique topical vehicle for the localized delivery of drugs to the skin.* Journal of the European Academy of Dermatology and Venereology, 2005. **19**(3): p. 308-318.
220. Scordilis-Kelley, C. and J.G. Osteryoung, *Voltammetric Studies of Counterion Transport in Solutions of Chondroitin Sulfate.* The Journal of Physical Chemistry, 1996. **100**(2): p. 797-804.
221. Domard, A., *pH and c.d. measurements on a fully deacetylated chitosan: application to CuII—polymer interactions.* Int J Biol Macromol, 1987. **9**(2): p. 98-104.
222. Castner, D.G., K. Hinds, and D.W. Grainger, *X-ray Photoelectron Spectroscopy Sulfur 2p Study of Organic Thiol and Disulfide Binding Interactions with Gold Surfaces.* Langmuir, 1996. **12**(21): p. 5083-5086.
223. Picart, C., et al., *Molecular basis for the explanation of the exponential growth of polyelectrolyte multilayers.* Proceedings of the National Academy of Sciences of the United States of America, 2002. **99**(20): p. 12531-12535.
224. Zhang, H., A. Qadeer, and W. Chen, *In Situ Gelable Interpenetrating Double Network Hydrogel Formulated from Binary Components: Thiolated Chitosan and Oxidized Dextran.* Biomacromolecules, 2011. **12**(5): p. 1428-1437.
225. Croll, T.I., et al., *A Blank Slate? Layer-by-Layer Deposition of Hyaluronic Acid and Chitosan onto Various Surfaces.* Biomacromolecules, 2006. **7**(5): p. 1610-1622.
226. Richert, L., et al., *Elasticity of Native and Cross-Linked Polyelectrolyte Multilayer Films.* Biomacromolecules, 2004. **5**(5): p. 1908-1916.
227. Paulson, J.C., O. Blixt, and B.E. Collins, *Sweet spots in functional glycomics.* Nat Chem Biol, 2006. **2**(5): p. 238-248.
228. Fukui, S., et al., *Oligosaccharide microarrays for high-throughput detection and specificity assignments of carbohydrate-protein interactions.* Nat Biotech, 2002. **20**(10): p. 1011-1017.
229. Ko, K.-S., F.A. Jaipuri, and N.L. Pohl, *Fluorous-Based Carbohydrate Microarrays.* Journal of the American Chemical Society, 2005. **127**(38): p. 13162-13163.
230. Porcel, C., et al., *Influence of the Polyelectrolyte Molecular Weight on Exponentially Growing Multilayer Films in the Linear Regime.* Langmuir, 2007. **23**(4): p. 1898-1904.
231. Lisboa, P., et al., *Thiolated polyethylene oxide as a non-fouling element for nano-patterned bio-devices.* Applied Surface Science, 2007. **253**(10): p. 4796-4804.
232. Genorio, B.t., et al., *Synthesis and Self-Assembly of Thio Derivatives of Calix[4]arene on Noble Metal Surfaces.* Langmuir, 2008. **24**(20): p. 11523-11532.

233. Salloum, D.S. and J.B. Schlenoff, *Protein Adsorption Modalities on Polyelectrolyte Multilayers.* Biomacromolecules, 2004. **5**(3): p. 1089-1096.
234. Reisch, A., et al., *Polyelectrolyte Multilayers Capped with Polyelectrolytes Bearing Phosphorylcholine and Triethylene Glycol Groups: Parameters Influencing Antifouling Properties.* Langmuir, 2009. **25**(6): p. 3610-3617.
235. Edwards, J.V. and P.S. Howley, *Human neutrophil elastase and collagenase sequestration with phosphorylated cotton wound dressings.* Journal of Biomedical Materials Research Part A, 2007. **83A**(2): p. 446-454.
236. Cullen, B., et al., *Mechanism of action of PROMOGRAN, a protease modulating matrix, for the treatment of diabetic foot ulcers.* Wound Repair and Regeneration, 2002. **10**(1): p. 16-25.
237. Bond, M.D. and H.E. Van Wart, *Characterization of the individual collagenases from Clostridium histolyticum.* Biochemistry, 1984. **23**(13): p. 3085-3091.
238. Bajpai, A.K., *Blood protein adsorption onto macroporous semi-interpenetrating polymer networks (IPNs) of poly(ethylene glycol) (PEG) and poly(2-hydroxyethyl methacrylate) (PHEMA) and assessment of in vitro blood compatibility.* Polymer International, 2007. **56**(2): p. 231-244.
239. Bernsmann, F., et al., *Protein adsorption on dopamine–melanin films: Role of electrostatic interactions inferred from ζ-potential measurements versus chemisorption.* Journal of Colloid and Interface Science, 2010. **344**(1): p. 54-60.
240. Bravo-Osuna, I., et al., *Characterization of chitosan thiolation and application to thiol quantification onto nanoparticle surface.* International Journal of Pharmaceutics, 2007. **340**(1–2): p. 173-181.
241. Hileman, R.E., et al., *Glycosaminoglycan-protein interactions: definition of consensus sites in glycosaminoglycan binding proteins.* BioEssays, 1998. **20**(2): p. 156-167.
242. Pashkuleva, I. and R.L. Reis, *Sugars: burden or biomaterials of the future?* J Mater Chem, 2010. **20**(40): p. 8803-8818.
243. Valle-Delgado, J.J., et al., *Modulation of Aβ42 fibrillogenesis by glycosaminoglycan structure.* The FASEB Journal, 2010. **24**(11): p. 4250-4261.
244. Roach, P., D. Farrar, and C.C. Perry, *Interpretation of Protein Adsorption: Surface-Induced Conformational Changes.* Journal of the American Chemical Society, 2005. **127**(22): p. 8168-8173.
245. Huang, G.-S., et al., *Spheroid formation of mesenchymal stem cells on chitosan and chitosan-hyaluronan membranes.* Biomaterials, 2011. **32**(29): p. 6929-6945.
246. Förster, M., et al., *Topical delivery of cosmetics and drugs. Molecular aspects of percutaneous absorption and delivery.* European journal of dermatology : EJD, 2009. **19**(4): p. 309-323.
247. Elhassan Imam, M. and A. Bernkop-Schnürch, *Controlled Drug Delivery Systems Based on Thiolated Chitosan Microspheres.* Drug Development and Industrial Pharmacy, 2005. **31**(6): p. 557-565.
248. Albrecht, K., et al., *Preparation of Thiomer Microparticles and In Vitro Evaluation of Parameters Influencing Their Mucoadhesive Properties.* Drug Development and Industrial Pharmacy, 2006. **32**(10): p. 1149-1157.
249. Hoyer, H., et al., *Preparation and evaluation of microparticles from thiolated polymers via air jet milling.* European Journal of Pharmaceutics and Biopharmaceutics, 2008. **69**(2): p. 476-485.
250. Lee, D.-W., et al., *Thiolated chitosan nanoparticles enhance anti-inflammatory effects of intranasally delivered theophylline.* Respiratory research, 2006. **7**: p. 112-122.
251. Greindl, M. and A. Bernkop-Schnürch, *Development of a Novel Method for the Preparation of Thiolated Polyacrylic Acid Nanoparticles.* Pharmaceutical Research, 2006. **23**(9): p. 2183-2189.
252. Skirtenko, N., et al., *One-Step Preparation of Multifunctional Chitosan Microspheres by a Simple Sonochemical Method.* Chemistry – A European Journal, 2010. **16**(2): p. 562-567.
253. Fernandes, M.M., et al., *Protein disulphide isomerase-induced refolding of sonochemically prepared Ribonuclease A microspheres.* Journal of Biotechnology, 2012. **159**(1–2): p. 78-82.

254. Grinstaff Mark, W. and S. Suslick Kenneth, *Proteinaceous Microspheres*, in *Macromolecular Assemblies in Polymeric Systems*. 1992, American Chemical Society. p. 218-226.
255. Suslick K. S., E., *Ultrasound: Its chemical, physical and biological effects.* VCH Publishers Inc., New York, 1988.
256. Flint, E.B. and K.S. Suslick, *Sonoluminescence from nonaqueous liquids: emission from small molecules.* Journal of the American Chemical Society, 1989. **111**(18): p. 6987-6992.
257. Avivi, S. and A. Gedanken, *S-S bonds are not required for the sonochemical formation of proteinaceous microspheres: the case of streptavidin.* The Biochemical journal, 2002. **366**(Pt 3): p. 705-707.
258. Prabaharan, M. and J.F. Mano, *Chitosan-Based Particles as Controlled Drug Delivery Systems.* Drug Delivery, 2004. **12**(1): p. 41-57.
259. Clausen, A.E., C.E. Kast, and A. Bernkop-Schnürch, *The Role of Glutathione in the Permeation Enhancing Effect of Thiolated Polymers.* Pharmaceutical Research, 2002. **19**(5): p. 602-608.
260. Martien, R., et al., *Thiolated chitosan nanoparticles: transfection study in the Caco-2 differentiated cell culture.* Nanotechnology, 2008. **19**(4): p. 045101.
261. Schmitz, T., et al., *Synthesis and characterization of a chitosan-N-acetyl cysteine conjugate.* International Journal of Pharmaceutics, 2008. **347**(1–2): p. 79-85.
262. Bernkop-Schnürch, A., A. Heinrich, and A. Greimel, *Development of a novel method for the preparation of submicron particles based on thiolated chitosan.* European Journal of Pharmaceutics and Biopharmaceutics, 2006. **63**(2): p. 166-172.
263. Nasti, A., et al., *Chitosan/TPP and Chitosan/TPP-hyaluronic Acid Nanoparticles: Systematic Optimisation of the Preparative Process and Preliminary Biological Evaluation.* Pharmaceutical Research, 2009. **26**(8): p. 1918-1930.
264. Hankiewicz, J. and E. Swierczek, *Lysozyme in human body fluids.* Clinica Chimica Acta, 1974. **57**(3): p. 205-209.
265. Papini, M., et al., *Lysozyme distribution in healthy human skin.* Archives of Dermatological Research, 1981. **272**(1): p. 167-170.